FINAL REPORT ~ FHWA-OK-12-07

EFFECT OF Y-CRACKING ON CRCP PERFORMANCE

M. TYLER LEY
SPENCER WOESTMAN
KYLE RIDING
WESLEY NYBERG
DUNJA PERIC
AMIR FARID MOMENI

OKLAHOMA STATE UNIVERSITY
CIVIL AND ENVIRONMENTAL ENGINEERING
KANSAS STATE UNIVERSITY
CIVIL AND ENVIRONMENTAL ENGINEERING

PLANNING & RESEARCH DIVISION
ENGINEERING SERVICES BRANCH
RESEARCH SECTION

spr@odot.org, office: (405)522-3795

ODOT SPR ITEM NUMBER 2230

OKLAHOMA DEPARTMENT OF TRANSPORTATION
200 NE 21ST STREET, OKLAHOMA CITY, OK 73105-3204

EFFECT OF Y-CRACKING ON CRCP PERFORMANCE

FINAL REPORT ~ FHWA-OK-12-07

ODOT SP&R ITEM NUMBER 2230

Submitted to:

John R. Bowman, P.E.
Planning & Research Division Engineer
Oklahoma Department of Transportation

Submitted by:

M. Tyler Ley
Spencer Woestman
Kyle Riding
Wesley Nyberg
Dunja Peric
Amir Farid Momeni
Oklahoma State University
Civil and Environmental Engineering
Kansas State University
Civil and Environmental Engineering

October 2012

TECHNICAL REPORT DOCUMENTATION PAGE

1. REPORT NO.	2. GOVERNMENT ACCESSION NO.	3. RECIPIENT'S CATALOG NO.
FHWA-OK- 12-07		

4. TITLE AND SUBTITLE	5. REPORT DATE
Effect of Y-cracking on CRCP Performance	Oct 2012
	6. PERFORMING ORGANIZATION CODE

7. AUTHOR(S)	8. PERFORMING ORGANIZATION REPORT
M. Tyler Ley, Spencer Woestman, Kyle Riding, Wesley Nyberg, Dunja Peric, and Amir Farid Momeni	Click here to enter text.

9. PERFORMING ORGANIZATION NAME AND ADDRESS	10. WORK UNIT NO.
Oklahoma State University Civil & Environmental Engineering 207 Engineering South Stillwater, Oklahoma 74078	11. CONTRACT OR GRANT NO. ODOT SP&R Item Number 2230

12. SPONSORING AGENCY NAME AND ADDRESS	13. TYPE OF REPORT AND PERIOD COVERED
Oklahoma Department of Transportation Planning and Research Division 200 N.E. 21st Street, Room 3A7 Oklahoma City, OK 73105	Final Report Oct 2011 - Dec 2012
	14. SPONSORING AGENCY CODE

15. SUPPLEMENTARY NOTES
Click here to enter text.

16. ABSTRACT

This report covers the investigation of the impact of Y-cracking on concrete pavements in Oklahoma. This study used field and analytical investigations to determine the impact of Y-cracking on the long term performance of continuous concrete pavements.

The research found that Y-cracking in concrete pavements does lead to an increase in the number of punch outs. Of all of the variables investigated the base type and the shoulder type had the largest impact on the amount of Y-cracking that occurred in continuous concrete pavements. The analytical studies confirmed that these variables can lead to increases in pavement stresses and so therefore cracking.

17. KEY WORDS	18. DISTRIBUTION STATEMENT
Concrete Pavements, Punch outs, Y cracking	No restrictions. This publication is available from the Planning & Research Div., Oklahoma DOT.

19. SECURITY CLASSIF. (OF THIS REPORT)	20. SECURITY CLASSIF. (OF THIS PAGE)	21. NO. OF PAGES	22. PRICE
Unclassified	Unclassified	250	N/A

The contents of this report reflect the views of the authors responsible for the facts and the accuracy of the data presented herein. The contents do not necessarily reflect the views of the Oklahoma Department of Transportation or the Federal Highway Administration. This report does not constitute a standard, specification, or regulation. While trade names may be used in this report, it is not intended as an endorsement of any machine, contractor, process or product.

SI* (MODERN METRIC) CONVERSION FACTORS

APPROXIMATE CONVERSIONS TO SI UNITS				
SYMBOL	**WHEN YOU KNOW**	**MULTIPLY BY**	**TO FIND**	**SYMBOL**
LENGTH				
in	Inches	25.4	Millimeters	mm
ft	Feet	0.305	Meters	M
yd	Yards	0.914	Meters	M
mi	Miles	1.61	Kilometers	Km
AREA				
in^2	square inches	645.2	square millimeters	mm^2
ft^2	square feet	0.093	square meters	m^2
yd^2	square yard	0.836	square meters	m^2
ac	Acres	0.405	Hectares	Ha
mi^2	square miles	2.59	square kilometers	km^2
VOLUME				
fl oz	fluid ounces	29.57	Milliliters	mL
gal	Gallons	3.785	Liters	L
ft^3	cubic feet	0.028	cubic meters	m^3
yd^3	cubic yards	0.765	cubic meters	m^3
NOTE: volumes greater than 1000 L shall be shown in m^3				
MASS				
oz	Ounces	28.35	Grams	G
lb	Pounds	0.454	Kilograms	kg
T	short tons (2000 lb)	0.907	megagrams (or "metric ton")	Mg (or "t")
TEMPERATURE (exact degrees)				
^oF	Fahrenheit	5 (F-32)/9 or (F-32)/1.8	Celsius	^oC
ILLUMINATION				
fc	foot-candles	10.76	Lux	lx
fl	foot-Lamberts	3.426	$candela/m^2$	cd/m^2
FORCE and PRESSURE or STRESS				
lbf	Poundforce	4.45	Newtons	N
lbf/in^2	poundforce per square inch	6.89	Kilopascals	kPa

APPROXIMATE CONVERSIONS FROM SI UNITS				
SYMBOL	**WHEN YOU KNOW**	**MULTIPLY BY**	**TO FIND**	**SYMBOL**
LENGTH				
mm	millimeters	0.039	inches	in
m	meters	3.28	feet	ft
m	meters	1.09	yards	yd
km	kilometers	0.621	miles	mi
AREA				
mm^2	square millimeters	0.0016	square inches	in^2
m^2	square meters	10.764	square feet	ft^2
m^2	square meters	1.195	square yards	yd^2
ha	hectares	2.47	acres	ac
km^2	square kilometers	0.386	square miles	mi^2
VOLUME				
mL	milliliters	0.034	fluid ounces	fl oz
L	liters	0.264	gallons	gal
m^3	cubic meters	35.314	cubic feet	ft^3
m^3	cubic meters	1.307	cubic yards	yd^3
MASS				
g	grams	0.035	ounces	oz
kg	kilograms	2.202	pounds	lb
Mg (or "t")	megagrams (or "metric ton")	1.103	short tons (2000 lb)	T
TEMPERATURE (exact degrees)				
^oC	Celsius	1.8C+32	Fahrenheit	^oF
ILLUMINATION				
lx	lux	0.0929	foot-candles	fc
cd/m^2	candela/m^2	0.2919	foot-Lamberts	fl
FORCE and PRESSURE or STRESS				
N	newtons	0.225	poundforce	lbf
kPa	kilopascals	0.145	poundforce per square inch	lbf/in^2

*SI is the symbol for the International System of Units. Appropriate rounding should be made to comply with Section 4 of ASTM E380.
(Revised March 2003)

Acknowledgements:

The researchers would like to thank Chris Westlund, Bryan Hurst, Jeff Dean, Chris Clarke, and Ginger McGovern for their help and guidance on this project. This work would not have been possible without them.

TABLE OF CONTENTS

LIST OF TABLES

LIST OF FIGURES

INTRODUCTION

1.1 Overview

This is the final report for ODOT project 2230 “Effect of Y-cracking on CRCP Performance (PS-14)”. This report summarizes the work that was completed at Oklahoma State University and Kansas State University between October 1st, 2010 and September 30th, 2012. The focus of this project is to determine if a correlation exists between Y-cracking and the subsequent performance of continuously reinforced concrete pavements (CRCP) in Oklahoma. Work was done to correlate the Y-cracking and design and construction variables. It was decided to best organize this work in the following sections:

A. Literature review of both previous national reports and papers and ODOT reports to determine previous experience with Y-cracking, mitigation methods used, and potential future cost-effective solutions to prevent Y-cracking (OSU and KSU).
B. Update the ODOT CRCP project database. In this task the investigators updated the ODOT CRCP database for projects constructed since 2003 (McGovern Personal Communication, 2010). The type of information added included year constructed, percentage of longitudinal and transverse steel, location, type of shoulder, type of base and subbase, edge drain presence, ODOT standards (OSU).
C. Perform visual inspections of ODOT CRCP projects. A number of projects of different ages and construction variables were investigated to determine the prevalence of Y-cracking and the subsequent damage (OSU).
D. Modeling of early age stress development and cracking with HIPERPAV III and Concrete Works (KSU).
E. Modeling of early age stress development and cracking with finite element models (KSU).
F. Suggested modifications to CRCP construction practice to minimize Y-cracking (OSU and KSU).

LITERATURE REVIEW

2.1 Introduction

Y-cracking in CRCPs has been observed on several Oklahoma pavements. Y-cracking has been associated with spalling and punchouts, increasing maintenance costs, and decreasing ride quality (Kohler & Roesler, 2004). Some have suggested that CRCP Y-crack patterns are formed during the early age period, and are influenced by the materials used, percentage of steel, base type and preparation, and curing conditions (Johnston & Surdahl, 2008). This chapter will provide an overview of CRCP and the past work completed on Y-cracking.

2.2 Continuously Reinforced Concrete Pavement Overview

Continuously reinforced concrete pavement (CRCP) is a type of rigid pavement that is designed shrinkage stresses. The cracks are held tight by reinforcing steel. By varying the amount of steel, designers can change the spacing and width of the cracks.

2.2.1 History of CRCP

The first experimental CRCP was built in 1921 on the Columbia Pike near Washington, D.C. Rigid pavements were thought to be weakest at the joints; therefore, there was an interest in using CRCPs because there were no joints (Huang, 2004). Another advantage was that the pavement thickness could be decreased and no joints had to be saw cut. This helps offset some of the costs associated with the reinforcing steel. Although during the 1940s and 1950s many states began performing studies on CRCPs, they were not widely used until the 1960s. As of 2005, there are CRCPs in over 35 states covering more than 28,000 lane miles (Choi & Chen, 2005). The states with the highest number of lane-miles of CRCPs are Illinois, Oklahoma, Oregon, South Dakota, Texas, and Virginia (ERES Consultants, Inc., 2001).

2.2.2 Texas History

For more than fifty years Texas has been the leader in the number of lane-miles and also in designing and monitoring the performance of CRCPs. The Texas Highway Department, which later became the Texas Department of Transportation (TxDOT) in 1951, saw the performance other states were receiving from their CRCPs and decided to try two CRCP projects around Fort Worth, Texas. Both CRCP sections provided 40

years of excellent performance with the only maintenance being surface texturing for safety reasons (The Transtec Group, Inc., 2004). After the excellent performance of these CRCPs, TxDOT built many more miles of CRCPs. Texas has the most lane miles of CRCPs in the world and designs all high-volume heavy-traffic roads as CRCPs (The Transtec Group, Inc., 2004). A major reason Texas has become a leader in the design of CRCPs is because of their extensive monitoring of their CRCPs.

2.2.3 Oklahoma History

Oklahoma Department of Transportation (ODOT) first started building CRCPs in the early to mid-1970s. As of 1996, there were over 686 lane miles of CRCPs in the state of Oklahoma, with most of these miles being in the eastern half of the state. Roughly 75 percent of these CRCPs were built from 1986 to 1996 (McGovern, Ooten, & Senkowski, 1996).

2.3 CRCP Design

The reason CRCPs have become so popular to construct is because, unlike jointed plain concrete pavements (JPCP) or jointed reinforced concrete pavements (JRCP), the joints do not have to be sawed into the concrete, which then needs to be sealed and maintained. If designed correctly, the crack widths will be small and will keep incompressibles out. The American Association of State Highway Transportation Officials (AASHTO) recommends a minimum transverse crack spacing of 3.5 feet and a maximum of 8 feet. The maximum transverse crack spacing is set to reduce the potential for crack spalling because of excessively wide cracks, while the minimum spacing is set to reduce the chance of punchouts (American Association of State Highway and Transportation Officials, 1993). Most transverse cracks develop early in the life of the concrete, usually within the first few months, with incidences of cracking diminishing after about one or two years.

Unlike jointed pavements, CRCP's transverse crack widths are designed to be very small. The increase in longitudinal reinforcing steel causes the transverse cracks to be held together tightly. These tight transverse cracks not only provide a smooth ride to users, but also allows for load transfer by aggregate interlock and protects from water infiltration. These tight transverse cracks do not allow a clear path for the water to infiltrate into the base, which prevents pumping of the base. The crack spacing can be

controlled by changing the percent of longitudinal reinforcing steel; the more steel, the smaller the crack widths and crack spacing (McGovern, Ooten, & Senkowski, 1996). Furthermore, with CRCPs, the thickness of the concrete can usually be reduced by 20 to 30 percent as compared to other pavement thicknesses. This usually translates to a pavement that is 1 to 2 inches thinner than a jointed pavement (Huang, 2004).

2.4 Cracks Associated with CRCP

There are four general types of cracks that have been classified pertaining to CRCPs, as seen in Figure 2.1, all of which correspond to the designed mean transverse cracks. Cluster cracks happen when the mean crack spacing of the CRCP is reduced and more than three cracks happen in a close spacing of each other. Several studies have indicated possible causes of cluster cracking, “Cluster cracking has been associated with variation in subgrade support, poor concrete consolidation, inadequate drainage, high base friction, and high ambient temperature at time of construction” (McGovern, Ooten, & Senkowski, 1996). The next crack type that happens is Y-cracking. Y-cracking is identified by a single crack that splits off into two other cracks that spread apart. The third type, a meandering crack, is just a transverse crack that does not stay perpendicular to the edge of the pavement and wanders one way or another. The final crack type that can form is the divided crack. Divided cracks are two cracks that do not crack the full width of the pavement and usually meet around an area and may or may not touch each other. Cluster cracks, Y-cracks, and divided cracks have been suspected to lead to early-age spalling and later punchout distresses (Kohler and Roesler 2004).

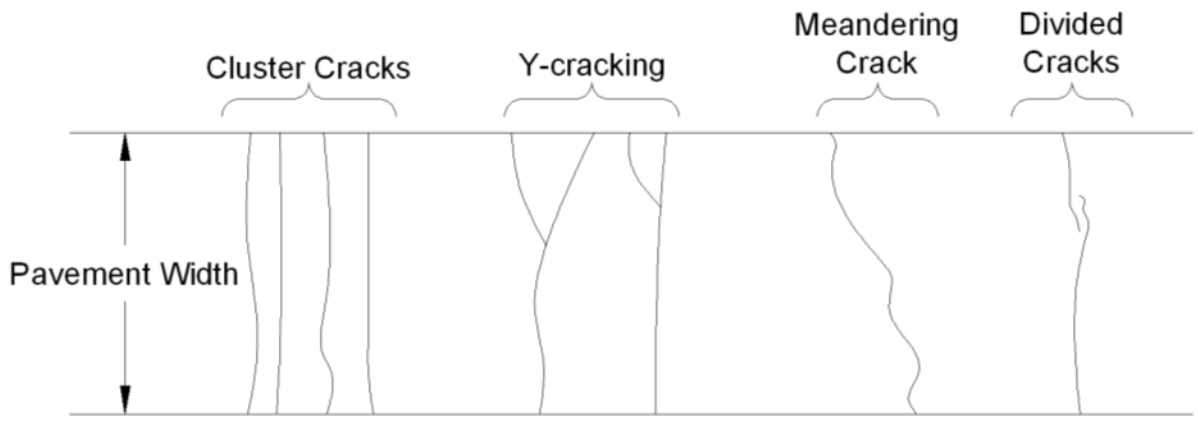

Figure 2.1 Crack shapes and patterns associated with defective passive cracks. After (Kohler and Roesler 2004)

2.4.1 Y-Cracking

These types of cracks could severely decrease the performance and life of the CRCPs. Figure 2.2 is a picture of Y-cracking in an Oklahoma CRCP. Y-cracking is easily categorized by its very unique shape. There is a single crack, or "trunk" crack, which splits into two other cracks, called the "branch" cracks. It is not known how the crack propagates, whether the braches form and converge into one crack or the trunk forms and branches into the other two cracks.

Figure 2.2 Y-cracking example

2.5 Problems Associated with Y-Cracking

Y-cracking has been speculated to cause punchouts and spalling to occur because the section of the pavement at the location of the crack bifurcation can become a cantilevered section when aggregate interlock is degraded (Kohler & Roesler, 2004). These distresses are used to gauge the performance of the CRCP throughout its service life.

2.5.1 Spalling

Spalling is defined as “the cracking, breaking, or chipping of the slab edges within 2 feet of the crack” (Choi & Chen, 2005). Normal CRCPs are designed with tight cracks that help resist spalling. Transverse crack spacing and crack width have been associated with controlling the resistance to spalling in CRCPs (Kohler & Roesler, 2004). Spalling can be caused by excessive crack widths, which causes excessive stresses at the cracks. These stresses are from water infiltration, expansion of slabs, and traffic loading (Choi & Chen, 2005). An example of spalling in Oklahoma can be seen in Figure 2.3.

Figure 2.3 Example of spalling

2.5.2 Punchouts

The most common major distress associated with CRCPs and its performance life is punchouts. A punchout is defined as “an isolated piece of concrete that settles

into depression or void at the edge of the concrete slab" (Beyer & Roesler, 2009). An example of a punchout between two closely spaced transverse cracks can be seen in Figure 2.4.

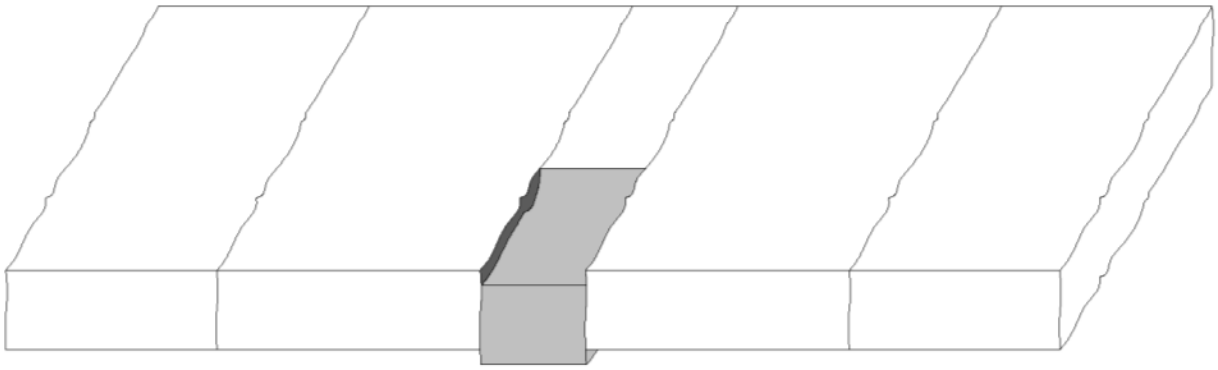

Figure 2.4 Example of punchout between two closely spaced transverse cracks. After (Kohler 2005)

A punchout can develop between two transverse cracks or at the branches of a Y-crack. The primary reason for punchouts has been found to be erosion of the subbase and loss of support under the slab (Zollinger & Barenberg, 1990). For this reason, the control of spalling is a key factor in preventing punchouts from happening. When spalling occurs, that means the crack width is wide enough to allow infiltration of water into the subbase of the CRCP. If the subbase is not made of non-erodible material, and there is enough heavy traffic, then pumping of the subbase will occur. Pumping will remove water and soil from the base through the crack and cause loss of support under the slab.

Punchouts usually happen where two transverse cracks are close. This is because the cross sectional area of the concrete to resist the stress is less than when the crack spacing is at its designed interval and uniform. Transverse crack spacing and crack width have been associated with punchouts in CRCPs (Kohler & Roesler, 2004).

2.6 Possible Causes of Y-Cracking

There have been several research projects studying the effects of various factors on the transverse crack spacing of CRCPs. However, there have been few that have tried to correlate the effect of these variables on Y-cracking.

2.6.1 Transverse Crack Spacing

Transverse crack spacing is believed to have a major effect on the possibility of Y-cracking in CRCPs. The transverse crack spacing is affected by many factors; the key variables are percent longitudinal steel, depth of steel placement, and climatic condition at time of construction (Zollinger & Barenberg, 1990). Typical desired transverse crack spacing is from 3.5 to 8 feet (Huang, 2004). More closely spaced cracks are believed to increase the probability of cluster cracking and Y-cracking (Johnston, 2008). ***One reason for the increased possibility of cluster and Y-cracking is that the closeness of these cracks lessens the distance for a crack to form, making it easier for variations in the subgrade restraint and support to cause cluster cracking and for cracks that meander slightly from their normal direction to intersect another crack and form a Y-crack.*** Large variability in crack spacing increases the probability for punchouts, which could be caused by the formation of Y-cracks or cluster cracks (Kohler & Roesler, 2004). A large variability in the crack spacing could also be a sign of poor subgrade and concrete uniformity and poor overall quality control in construction.

2.6.2 Crack Width

A factor that is directly related to the transverse crack spacing is the crack width. It has been seen that the smaller the transverse crack spacing the smaller the crack width, principally because both factors are affected by the amount of steel bridging the crack (The Transtec Group, Inc., 2004). A maximum crack width of 0.04 inches is recommended (Huang, 2004). One reason for this is that as the crack width increases the infiltration of water into the base material also increases. When more water is allowed into the subbase the probability of pumping can increase, which can lead to punchouts of the CRCPs. Another reason for the maximum crack width is that as the crack width increases the load transferred by aggregate interlock decreases. Crack widths are significantly affected by the following factors: time of crack occurrence,

ambient temperature, type of coarse aggregate, depth of reinforcement, and percent of longitudinal steel. Cracks that form early in the life of the CRCP have been seen to be wider and meander more than cracks that form later. This increase in meandering increases the probability of cracks to intersect and cause Y-cracking (McGovern, Ooten, & Senkowski, 1996).

2.6.3 Percent of Longitudinal Steel

The percent of longitudinal steel is a major factor on the transverse crack spacing and crack width. As the percent of longitudinal steel increases the crack width decreases because the stresses and corresponding strains in each bar decrease, holding the cracks tightly together. It should also be noted that even though percent of longitudinal steel has a significant effect on cracking patterns, it cannot be completely controlled if there are other factors (Huang, 2004). An example of this relationship can be seen in a study done by Suh and McCullough, shown in Figure 2.5. In this figure the medium amount of steel refers to the Texas design standard. The high and low refer to about 0.1 percent more and less of the medium amount of steel, respectively (Suh & McCullough, 1994).

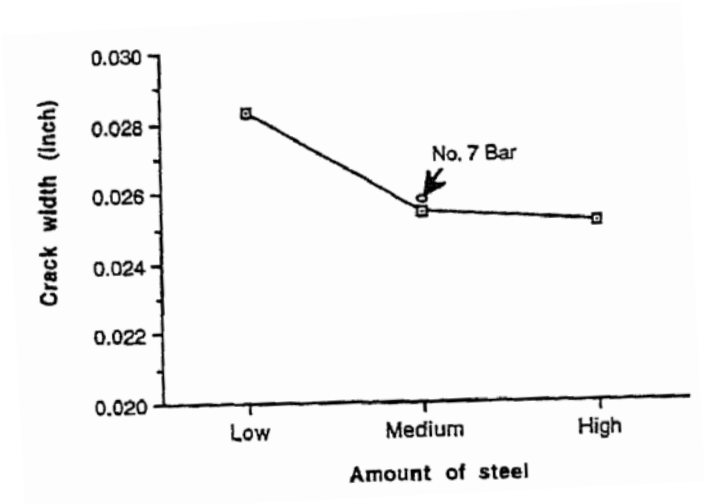

Figure 2.5 Effect of longitudinal steel design on crack width. From Young-Chan, S., and B. McCullough. Factors Affecting Crack Width of Continuously

Reinforced Concrete Pavement. In Transportation Research Record 1449, Figures 8 and 9, p.138. Copyright, National Academy of Sciences, Washington, D.C., 1994. Reproduced with permission of the Transportation Research Board. None of this material may be presented to imply endorsement by TRB of a product, method, practice, or policy.

2.6.4 Percent of Transverse Steel

Much less research has focused on the effect of the percent of transverse steel in CRCPs than the effect of longitudinal steel. In a study done by Al-Qadi and Elseifi, field test data showed that transverse cracks occurred mostly in the vicinity above transverse bars (60% of transverse cracks within 0.4 inches of transverse bars). But they also noted that transverse cracks did occur away from transverse bars, which led them to conclude that there was a possibly correlation between the transverse bars and the location of transverse cracks. Next they did a thermal stress analysis by creating a Finite Element Model (FEM) and it showed that high longitudinal tensile stress could build up in the concrete above the transverse bars. The model also showed how uniformly distributed compressive longitudinal stresses can build up at the pavement surface in between the transverse bars. This could explain the occurrence of cracks that did not occur over the transverse bars. Since the stress was uniform the crack would probably occur at a weak spot in the concrete, not necessarily at the midpoint between transverse bars (Al-Qadi & Elseifi, 2006).

2.6.5 Depth of Reinforcement

Tayabji et. al. (1998) showed that as the depth of reinforcement increases, the percent of Y-cracking decreases. Figure 2.6 shows the relationship between steel cover depth and Y-cracking, while Figure 2.7 shows the relationship between the steel cover depth and cluster cracking. Tayabji et al. provided a trendline showing a relationship between cluster cracking and steel cover depth, however it appears from Figure 2.7 that this trend is very weak and somewhat suspect.

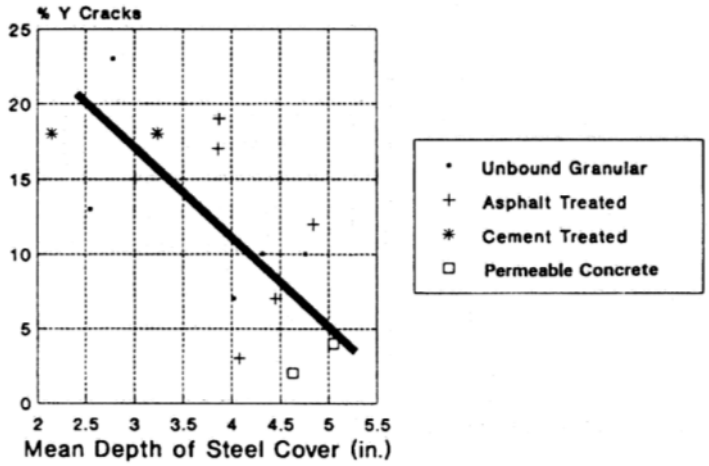

Figure 2.6 Y-cracking versus the mean depth of steel cover. (Tayabji, Zollinger, Vederey, & Gagnon, 1998)

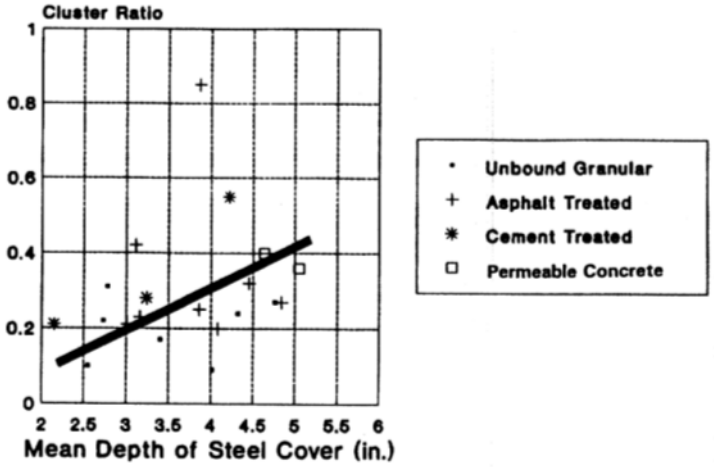

Figure 2.7 Cluster ratio versus the mean depth of steel cover. (Tayabji, Zollinger, Vederey, & Gagnon, 1998)

2.6.6 Base Type

The effect of base type on cracking patterns is not as clear as other factors. It can be seen in Figure 2.6 and Figure 2.7 that the relationship between the type of subbase and cluster and Y-cracking is still not clear (Tayabji, Zollinger, Vederey, & Gagnon, 1998). Other studies have shown that the base type matters because the amount of restraint provided by the base affects how many cracks occur, the transverse crack spacing, and when the cracks develop.

Early cracking can lead to spalling, wide cracks, and meandering because the concrete strength is not high enough at the early ages to resist these stresses (Johnston 2008). TxDOT has made it mandatory that bases be stabilized with either cement or asphalt. They did this to help prevent pumping and also to help with high stresses if support was lost at pavement edges in order to prevent punchouts (The Transtec Group, Inc., 2004). It was later discovered by Texas that the cement-stabilized bases, while providing more support, started excessively cracking. The stiffer bases provide more restraint for the concrete pavement. Cement-stabilized bases are also vulnerable to shrinkage cracking. The cracks in the base can reflect through in the pavement, giving more cracking. Currently in Texas, if a cement-stabilized base is used, a bond-breaker is required to reduce the subbase restraint and reduce excessive cracking in the CRCP (McGovern, Ooten, & Senkowski, 1996).

2.6.7 Coarse Aggregate

One material parameter that may be important with CRCPs is the concrete coefficient of thermal expansion (CoTE). The CoTE of the concrete is dependent on the water-cement ratio, concrete age, richness of the mixture, relative humidity, and type of aggregate in the concrete mixture. However, the most important of these parameters is the type of coarse aggregate used because of the high volume of aggregates used in concrete (Huang, 2004). Suh and McCullough studied the difference in crack width between siliceous river gravel and limestone at various slab temperatures at the time of measurements. Their results can be seen in Figure 2.8. From this figure it can be seen that the siliceous river gravel led to greater crack widths at all slab temperatures. This greater crack width is caused by the siliceous river gravel having a higher CoTE than the limestone aggregates studied, and hence more thermal movement. It also can be seen that at lower temperatures the difference in crack width is greater than at higher temperatures (Suh & McCullough, 1994).

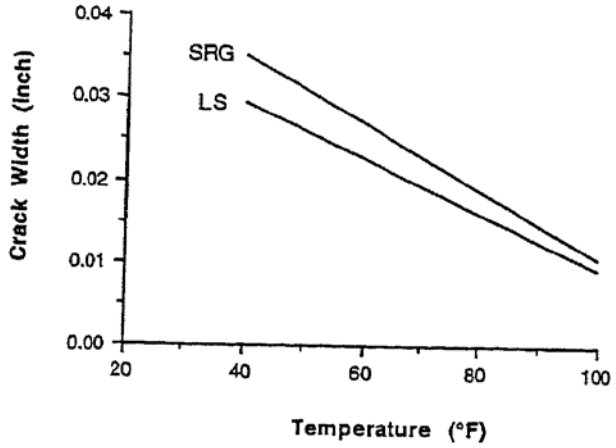

Figure 2.8 The effect of coarse aggregate type and slab temperature on crack width. From Young-Chan, S., and B. McCullough. Factors Affecting Crack Width of Continuously Reinforced Concrete Pavement. In Transportation Research Record 1449, Figures 8 and 9, p. 138. Copyright, National Academy of Sciences, Washington, D.C., 1994. Reproduced with permission of the Transportation Research Board. None of this material may be presented to imply endorsement by TRB of a product, method, practice, or policy.

TxDOT has studied the effects of coarse aggregate type on CRCP performance. Those studies have shown that CRCPs constructed with siliceous river gravel do not last as long as those constructed with limestone. The limestone CRCPs have, on average, lasted 10 years longer than siliceous river gravel CRCPs. The reason for this is the effect that the coarse aggregate type has on the transverse crack spacing. The crack spacing for siliceous river gravel and limestone were 2 to 3 feet and 6 feet, respectively. The higher CoTE of siliceous river gravel causes more thermal stresses in the concrete compared to the lower CoTE of limestone. This results in more cracking of the concrete and lower mean crack spacing. The frequency distribution of cracks can be seen in Figure 2.9. The closer crack spacing, such as seen with the siliceous river gravel, can lead to more punchouts in CRCPs.

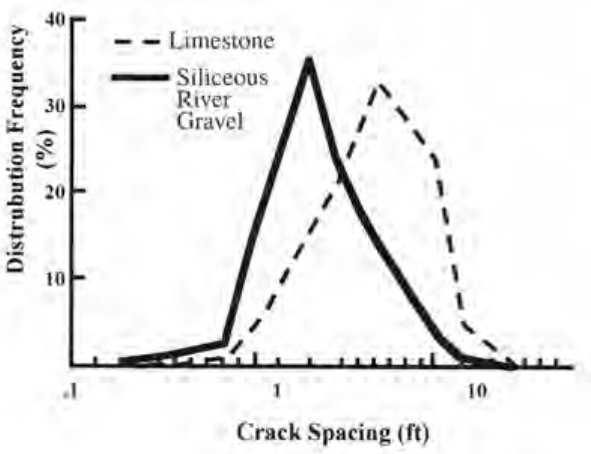

Figure 2.9 Influence of aggregate type on crack spacing. (The Transtec Group, Inc. 2004)

The coarse aggregate is also believed to affect the amount of cracks that meander. Studies have shown that pavements with limestone and lightweight aggregates tend to have cracks that are straighter with less meandering than pavements with siliceous river gravel. The lightweight and limestone aggregates are a weaker aggregate and have a stronger bond with the paste than siliceous river gravel. This causes the cracks to be able to propagate through the lightweight and limestone aggregates but not through the siliceous river gravel. Since it is difficult for the cracks to propagate through the siliceous river gravel, they will meander through the paste because it is weaker at early ages (Du & Lukefahr, 2007).

Another factor of coarse aggregate that has been shown to affect the performance of CRCPs is the aggregate size. In a study in South Dakota, a maximum coarse aggregate size of 1 inch and 1½ inches were used with no other factors adjusted. The crack spacing was on average 3.09 feet and 2.19 feet for the 1½ inches and 1 inch aggregate, respectively. Further inspection showed that the cracks from the larger aggregate were more uniform and tighter. Also, the larger aggregate reduced the amount of cluster cracks and Y-cracking. The increase in aggregate size causes an increase in steel bond strength and concrete fracture resistance (Johnston, 2008).

2.6.8 Construction Environment

The two main construction environment factors that affect the performance of CRCPs are the concrete temperature and air temperature at the time of curing.

Thermal stresses are driven by the concrete pavement temperature change. Figure 2.10 shows this relationship between the ambient temperature and cracking for an example pavement. At point A, the concrete sets and is in compression as the temperature of the concrete increases from the heat of hydration. At point B, the maximum temperature and compression of the concrete is achieved. At point C, the concrete temperature decreased which leads to a decrease in concrete compression until temperature decreases and autogenous shrinkage changes the compression in the concrete to tension. After this point, the stresses vary as the temperature difference in the concrete and air change. At point D, the tensile stresses have exceeded the tensile strength of the concrete and cracking occurs (Schindler & McCullough, 2002).

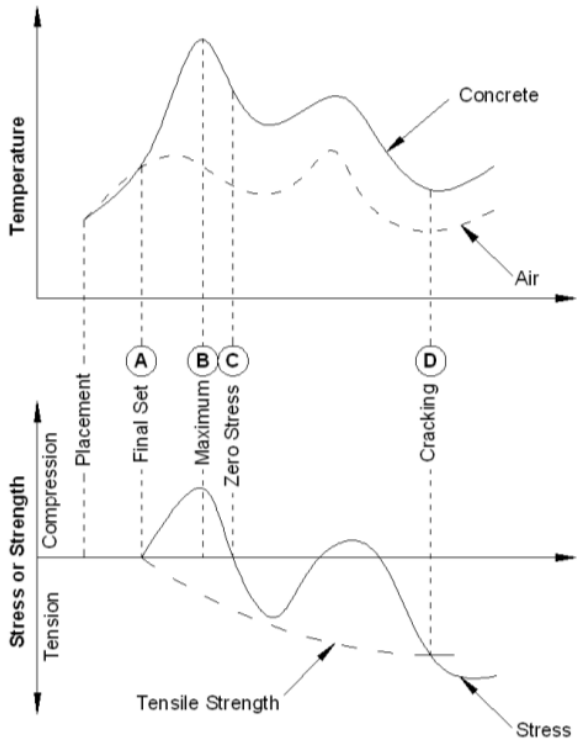

Figure 2.10 Relationship between temperature and concrete cracking. After (Schindler & McCullough, 2002)

Because of the relationship between the difference in concrete temperature and air temperature and the subsequent temperature decrease of the concrete with time, there have been many problems with construction of CRCPs in hot weather. In Texas,

CRCPs placed in hot weather have exhibited non-uniform crack spacing and Y-cracking. Because of this, TxDOT has determined the air temperature and concrete temperature must be monitored during construction (The Transtec Group, Inc., 2004). Texas currently has a maximum concrete temperature at placement of 95°F to help reduce this risk (Texas Department of Transportation, 2004).

A major factor that affects the air temperature and concrete temperature is the placement season. Crack widths have been seen to be more than two times greater in CRCPs placed in the summer months than CRCPs placed in the winter months (Suh & McCullough, 1994). The crack spacing has been found to be narrower for CRCPs placed in warmer weather because the higher the concrete second zero stress temperature, the more total temperature decrease and strain that will result during the cold winter months (The Transtec Group, Inc., 2004). This decrease in crack spacing caused by placement and curing in warm weather could increase the potential for punchouts in CRCPs.

2.6.9 Shrinkage

Tayabji et. al. showed that as the total shrinkage strain in the concrete increases, Y-cracking increases and the cluster ratio decreases, as seen in Figure 2.11 and Figure 2.12. There appears to be more of a trend between the shrinkage strain and cluster cracking, than with the shrinkage strain and the Y-cracking (Tayabji, Zollinger, Vederey, & Gagnon, 1998).

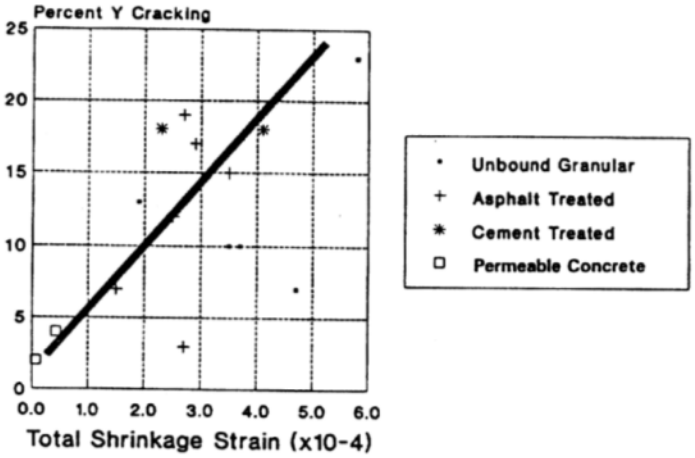

Figure 2.11 Y-cracking versus total shrinkage strain for different subbase types. (Tayabji, Zollinger, Vederey, & Gagnon, 1998)

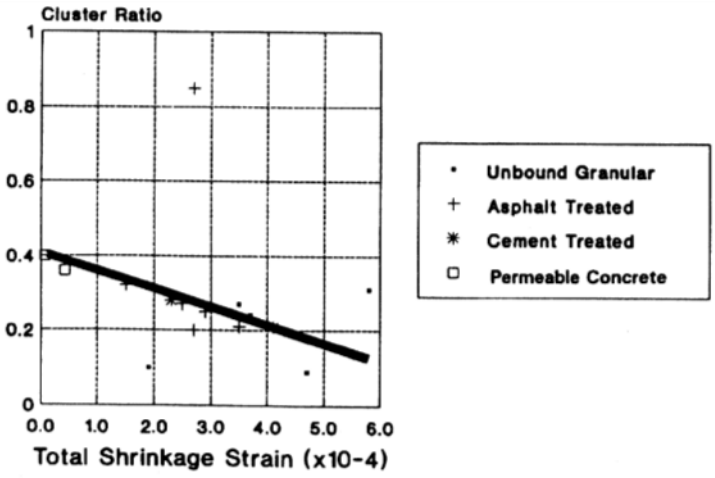

Figure 2.12 Cluster ratio versus total shrinkage for different subbase types. (Tayabji, Zollinger, Vederey, & Gagnon, 1998)

Shrinkage strain is one of the key factors that affect the development of early-age cracking in CRCPs (Kohler & Roesler, 2006). When cracks develop in the first few days, they have a higher tendency to meander. This increases the probability of cracks that can result in Y-cracking (McGovern, Ooten, & Senkowski, 1996). To control the amount of total shrinkage in concrete, the correct actions must be taken in design and construction to control autogenous and drying shrinkage. This can be accomplished by not using excessive amounts of cement and using a moderate water-to-cement ratio.

2.7 Historical Issues with Y-Cracking

No studies have previously been performed exclusively focusing on Y-cracking. However, a study by Tayabji et al. was completed in October 1998 to update the design, construction, maintenance, and rehabilitation of CRCP for better performance. The study was funded by the states of Arizona, Arkansas, Connecticut, Delaware, Illinois, Louisiana, Oklahoma, Oregon, Pennsylvania, South Dakota, and Texas. One of the focuses of the study was to conduct field and laboratory testing on existing CRCPs. The field studies were all conducted in the fall of 1991 (Tayabji, Zollinger, Vederey, & Gagnon, 1998). A total of 23 CRCP sites were selected; five from Illinois, three from

Iowa, five from Oklahoma, three from Oregon, two from Pennsylvania, and five from Wisconsin. Sites were selected to include a wide variety of design and construction attributes of the CRCPs. Field investigations at each site included the performance of a representative 1000 foot length section by the following: visual condition surveys, profile measurements, falling weight deflectometer, and corrosion testing. Laboratory testing included: concrete core testing for strength, stiffness, and CoTE, base, subbase, and subgrade material characterization. The study also gathered design, construction, maintenance, performance, and traffic data. The authors attempted to correlate the actual crack spacing to the performance of the CRCPs. The performance was judged by the extent of different types of structural distresses such as Y-cracking and cluster cracking observed in the pavement. The results have been discussed in previous sections (Tayabji, Zollinger, Vederey, & Gagnon, 1998).

2.8 Previous work by ODOT

The second study, "Performance of Continuously Reinforced Concrete Pavements in Oklahoma - 1996" by McGovern et al. (1996), was completed in August 1996 under the direction of the Oklahoma Department of Transportation (ODOT). The purpose of this study was to inspect the performance of Oklahoma CRCPs and concentrate on crack spacing, cluster cracking, Y-cracking, and overall condition. The report also compares the CRCP design and construction methods between ODOT and TxDOT. ODOT summarizes various studies that have been conducted on their CRCPs since 1988, including the study by Tayabji et al. Based on these previous surveys, ODOT conducted field surveys of 44 projects in June of 1996 and investigated the number of punchouts per mile. After this, ODOT did a CRCP tour in July and August of 1996, performed by ODOT Pavement Engineer Mr. Tim Borg. The CRCP tour focused on cracking patterns such as cluster cracking, Y-cracking, and crack spacing (McGovern, Ooten, & Senkowski, 1996).

Based on previous studies, the 1996 ODOT field studies and CRCP tour, and comparisons between ODOT and TxDOT design and construction methods, ODOT made recommendations for future design and construction of CRCPs in Oklahoma. Although the study was not inclusive of all CRCPs in Oklahoma, the data from the CRCPs studied showed that Oklahoma had fewer punchouts per mile than the average

for all of the sites in the Tayabji study. The major concern for the Oklahoma CRCPs was the large crack spacing and cluster cracking. The following recommendations were made:

- Continue to investigate the projects with 0.61 percent longitudinal steel
- Use an asphalt bond breaker between the CRCP and cement treated base
- Decrease the amount of cement used in cement treated base
- Longitudinal construction joints should be sealed and sawed between the outside lane and PCC shoulder

ODOT also decided to keep investigating the effect that ambient conditions during construction, depth of steel, swelling potential of soil, coarse aggregate type, and rate of strength gain had on the performance of CRCPs (McGovern, Ooten, & Senkowski, 1996).

ODOT CRCP DATABASE

3.1 Overview

The CRCP database contains information such as year constructed, percentage of longitudinal and transverse steel, location, type of shoulder, type of base and subbase, edge drain presence, and ODOT standards. The database contains this information for all of the CRCPs in the state of Oklahoma. It was a goal of this project to completely update this database.

3.2 CRCP Database Update

Updating the CRCP database consisted of three main steps. Step one was to complete all entries contained in the original database. The next step was to locate and add all CRCP projects not in the original database. The final step was to complete all the new entries in the database.

Steps one and three were completed using standards, plan sets, and other information obtained through requests from ODOT. Step two was completed using historical research sites list, 2009 Interstate Highway Pavement History, Interstates Database, and Appendix B of McGovern et al. 1996. Once these steps were completed the database was formatted and finalized. Due to size and clarity constraints the CRCP database has been included as a separate Access database file.

FIELD INSPECTION

4.1 Overview

4.1.1 Visual Inspection

For this project a visual inspection was conducted by slowly driving the shoulder of the roadway of a number of CRCP sections chosen by the research oversight committee. For a few of the sites, mainly the ones studied in previous inspections, measurements were taken so that mean spacing, standard deviation, coefficient of variation, and extent of Y-cracks could be determined. These sites are noted in the following sections.

A summary of each visual inspection location and findings is included in the appendix. These sites were chosen to get a diverse section of CRCP with different years of service, construction type, and amount of distress. More details about the methods of inspection are given followed by the analysis of the data.

4.2 Field Inspection Methodology

The field inspection of CRCP consisted of gathering three main pieces of information at every project visited. This information included counting Y-cracks, patches, and photographing all subjects of interest. Only the outside lane of traffic was considered during this investigation. Each piece of information was recorded onto a separate data form depending on the information type and direction of traffic where the data was gathered. In addition to gathering the previously mentioned data, crack spacing measurements were taken at a few projects.

Y-cracks, patches, and photographs were all recorded while traveling the shoulder of the roadway in a vehicle at a slow speed. While traveling the shoulder, extreme caution was used to avoid self-endangerment while inspecting the pavement. Stretches of roadway where there was either no shoulder to traverse or the danger were not inspected. A handheld Global Positioning System (GPS) was zeroed at the beginning joint of the pavement. The location of each photograph and patch was measured with the GPS to the one hundredth of a mile (0.01 mile). Y-cracks were counted using a handheld mechanical counter. Y-crack counts were totaled in one-mile

increments except when short segments or the CRCP was intersected by bridges or ramps.

During the inspection many different Y-crack patterns were seen. A consistent counting method was used to total the Y-cracks. Figure 4.1 shows common Y-crack patterns and also how they were counted. Each “Y” or branch of a transverse crack was counted as one Y-crack. Multiple Y-cracks were counted when transverse cracks rejoined the same transverse crack. Y-cracks were only counted in the outside lane of traffic.

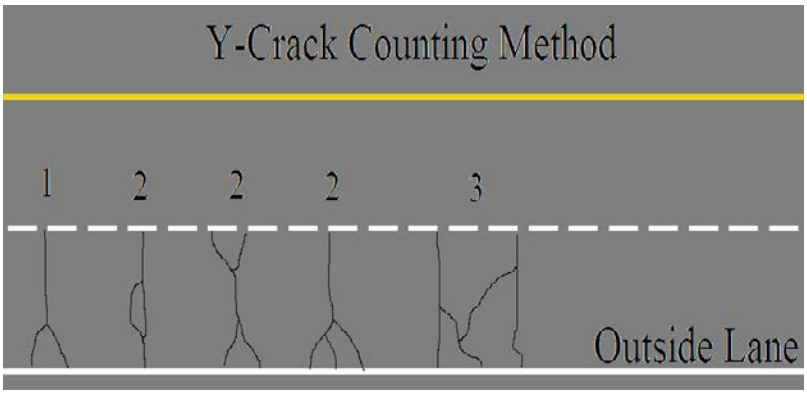

Figure 4.1 Visual summary of Y-crack counting method

When a patch was found the vehicle was stopped and the type (AC – asphalt concrete or PC = Portland cement) and location of each patch from the beginning of the project was recorded. Every area where a material had been added to the CRCP was recorded as a patch, despite its size. If two small patches occurred side by side in the roadway they were recorded as two patches, despite having the same location corresponding to the GPS. As with Y-cracks, the number of patches was recorded within each length of inspection (typically one mile increments).

Photographs were taken at all subjects of interest which included developing punchouts, asphalt patches were the cause of failure could be seen, deteriorated patches, exposed steel, and deteriorated pavement joints. The location of each of these pictures was recorded. Crack spacing measurements were also taken at a few locations. These measurements were performed from the shoulder of the pavement by

using a rolling measuring wheel accurate to one tenth of a foot (0.1 ft). The distance to each crack from the starting point was recorded. The crack spacing was measured at the intersection of the main lane and the shoulder.

4.3 Data Analysis

The data was analyzed and the following information about the Y-cracks were found per mile: average number, standard deviation, median number, maximum number, minimum number, mean spacing, standard deviation, and coefficient of variation for each project and each direction. Similar numbers were also found for the patches. This data was then used to correlate project details to Y-cracks and patch measurements. The summary of these findings can be found in the tables below. The summary tables include the field-inspected information and calculation as well as project information obtained from the project plan-sets and specifications. A number of plots comparing the characteristics of the projects to the Y-crack and patch information were created using the information found in the tables. Table 4.1 contains the county, ODOT project number, route, date opened, direction of traffic, length observed, contractor, pavement, thickness and shoulder type for the field-inspected projects. Table 4.2 shows the base types and thicknesses for each project studied along with the percent of longitudinal and transverse steel contained within the roadway (where Base-1 is base directly beneath CRCP, Base-2 is base beneath Base-1, and subbase is the base directly beneath Base-2; 1-depth, 2-depth and S-depth refer to the thickness of each layer). Tables 4.3 and 4.4 contain the Y-crack and patch statistics calculated from the collected field data.

Table 0.1 CRCP project data taken from ODOT plan-sets and ODOT databases

County	Project	Route	Date Opened	Direction	Total Length Observed	Contractor	Thickness	Shoulder Type
Logan	IR-35-4(115)147	35	1988	South Bound	5.2	Koss	10	JPCP
Logan	IR-35-4(115)147	35	1988	North Bound	5.36	Koss	10	JPCP
Oklahoma	IR-35-3(073)123	35	2001	North Bound	0.73	Neilson Inc	10	CRCP
Oklahoma	IR-35-3(073)123	35	2001	South Bound	1.01	Neilson Inc	10	CRCP
Cleveland	IM-NHIY-35-2(221)(247)120	35	2002	South Bound	0.9	Haskell Lemon	10	CRCP
Cleveland	IM-NHIY-35-2(221)(247)120	35	2002	North Bound	0.86	Haskell Lemon	10	CRCP
Cleveland	IM-NHIY-35-3(108)119	35	2005	South Bound	0.62	Haskell Lemon	10	CRCP
Cleveland	IM-NHIY-35-3(108)119	35	2005	North Bound	0.94	Haskell Lemon	10	CRCP
Carter	IMY-35-1(127)024	35	2007	North Bound	4.6	Koss	12	JPCP
Carter	IMY-35-1(127)024	35	2007	South Bound	4.66	Koss	12	JPCP
Okfuskee	IR-40-5(169)226	40	1985	East Bound	4.71	Koss	9	JPCP
Okfuskee	IR-40-5(169)226	40	1985	West Bound	4.69	Koss	9	JPCP
Atoka	F-299(99)	69	1989	North Bound	1.25	Wittwer	10	JPCP
Atoka	F-299(99)	69	1989	South Bound	1.37	Wittwer	10	JPCP
Atoka	F-299(45)	69	1986	North Bound	1.37	Koss	9	JPCP
Atoka	F-299(35)	69	1986	North Bound	1.08	Northern Improv.	9	JPCP
Atoka	F-299(35)	69	1986	South Bound	3.15	Northern Improv.	9	JPCP
Pittsburg	MAF-186(183)	69	1991	North Bound	3.98	Koss	10	JPCP
Pittsburg	MAF-186(185)	69	1989	North Bound	6.04	Koss	10	JPCP
Pittsburg	DPIY-204(001)	69	1994	North Bound	3.66	Koss	10	JPCP
Pittsburg	DPIY-204(001)	69	1994	South Bound	3.62	Koss	10	JPCP
Pittsburg	MAF-186(185)	69	1989	South Bound	6	Koss	10	JPCP
Pittsburg	MAF-186(183)	69	1991	South Bound	2.98	Koss	10	JPCP
Noble	MAIR-35-4(111)192	35	1988	North Bound	5.47	Northern Improv.	10	JPCP
Noble	MAIR-35-4(111)192	35	1988	South Bound	5.46	Northern Improv.	10	JPCP
Washita	IM-40-2-2(119)040	40	1992	West Bound	3.08	Koss	10	JPCP
Washita	IM-40-2-2(119)040	40	1992	East Bound	3.03	Koss	10	JPCP

Table 0.2 Continued CRCP project data taken from ODOT plan-sets and ODOT databases (see section 4.3 for title descriptions)

County	Project	Base 1	1-Depth (in)	Base 2	2-Depth (in)	Sub Base	S-Depth (in)	% Long.	% Trns.
Logan	IR-35-4(115)147	Type A AC	3	N/A	N/A	Select	8	0.51%	0.11%
Logan	IR-35-4(115)147	Type A AC	3	N/A	N/A	Select	8	0.51%	0.11%
Oklahoma	IR-35-3(073)123	OGBB	4	Agg. Base	12	N/A	N/A	0.61%	0.07%
Oklahoma	IR-35-3(073)123	OGBB	4	Agg. Base	12	N/A	N/A	0.61%	0.07%
Cleveland	IM-NHIY-35-2(221)(247)120	OGBB	4	Agg. Base	12	N/A	N/A	0.61%	0.07%
Cleveland	IM-NHIY-35-2(221)(247)120	OGBB	4	Agg. Base	12	N/A	N/A	0.61%	0.07%
Cleveland	IM-NHIY-35-3(108)119	OGBB	4	Agg. Base	12	N/A	N/A	0.71%	0.07%
Cleveland	IM-NHIY-35-3(108)119	OGBB	4	Agg. Base	12	N/A	N/A	0.71%	0.07%
Carter	IMY-35-1(127)024	OGBB	4	Agg. Base	8	Lime Treated	8	0.73%	0.06%
Carter	IMY-35-1(127)024	OGBB	4	Agg. Base	8	Lime Treated	8	0.73%	0.06%
Okfuskee	IR-40-5(169)226	CABB	4	N/A	N/A	Method B	12	0.50%	0.08%
Okfuskee	IR-40-5(169)226	CABB	4	N/A	N/A	Method B	12	0.50%	0.00%
Atoka	F-299(99)	Type A AC	3	Agg. Base	12	N/A	N/A	0.61%	0.07%
Atoka	F-299(99)	Type A AC	3	Agg. Base	12	N/A	N/A	0.61%	0.07%
Atoka	F-299(45)	Type C AC	3	N/A	N/A	N/A	N/A	0.50%	0.08%
Atoka	F-299(35)	Type C AC	3	N/A	N/A	N/A	N/A	0.50%	0.08%
Atoka	F-299(35)	Type C AC	3	N/A	N/A	N/A	N/A	0.50%	0.08%
Pittsburg	MAF-186(183)	OGPC	4	Stab Agg	12	N/A	N/A	0.61%	0.07%
Pittsburg	MAF-186(185)	OGPC	4	Stab Agg	12	N/A	N/A	0.61%	0.07%
Pittsburg	DPIY-204(001)	OGPC	4	Stab Agg	12	Method B	N/A	0.61%	0.07%
Pittsburg	DPIY-204(001)	OGPC	4	Stab Agg	12	Method B	N/A	0.61%	0.07%
Pittsburg	MAF-186(185)	OGPC	4	Stab Agg	12	N/A	N/A	0.61%	0.07%
Pittsburg	MAF-186(183)	OGPC	4	Stab Agg	12	N/A	N/A	0.61%	0.07%
Noble	MAIR-35-4(111)192	Econocrete	4	N/A	N/A	Method B	N/A	0.61%	0.11%
Noble	MAIR-35-4(111)192	Econocrete	4	N/A	N/A	Method B	N/A	0.61%	0.11%
Washita	IM-40-2-2(119)040	OGPC	4	Aggr Base	4	N/A	N/A	0.61%	0.07%
Washita	IM-40-2-2(119)040	OGPC	4	Aggr Base	4	N/A	N/A	0.61%	0.07%

Table 0.3 CRCP project field collected data

County	Project	Route	Direction	AVG Y-crack/mile	STD Y-crack/mile	median Y-crack/mile	Max Y-crack/mile	Min. Y-crack/mile
Logan	IR-35-4(115)147	35	South Bound	124	30	114	167	97
Logan	IR-35-4(115)147	35	North Bound	95	13	94	111	78
Oklahoma	IR-35-3(073)123	35	North Bound	45	N/A	45	45	45
Oklahoma	IR-35-3(073)123	35	South Bound	73	28	73	93	54
Cleveland	IM-NHIY-35-2(221)(247)120	35	South Bound	35	13	35	44	26
Cleveland	IM-NHIY-35-2(221)(247)120	35	North Bound	127	N/A	127	127	127
Cleveland	IM-NHIY-35-3(108)119	35	South Bound	85	N/A	85	85	85
Cleveland	IM-NHIY-35-3(108)119	35	North Bound	60	N/A	60	60	60
Carter	IMY-35-1(127)024	35	North Bound	72	40	56	133	33
Carter	IMY-35-1(127)024	35	South Bound	58	28	64	86	21
Okfuskee	IR-40-5(169)226	40	East Bound	102	19	98	133	87
Okfuskee	IR-40-5(169)226	40	West Bound	100	12	104	109	83
Atoka	F-299(99)	69	North Bound	87	53	68	147	47
Atoka	F-299(99)	69	South Bound	150	52	122	210	118
Atoka	F-299(45)	69	North Bound	101	24	101	118	84
Atoka	F-299(35)	69	North Bound	90	N/A	90	90	90
Atoka	F-299(35)	69	South Bound	73	N/A	73	73	73
Pittsburg	MAF-186(183)	69	North Bound	127	22	138	150	99
Pittsburg	MAF-186(185)	69	North Bound	109	23	109	143	75
Pittsburg	DPIY-204(001)	69	North Bound	96	21	94	129	77
Pittsburg	DPIY-204(001)	69	South Bound	74	18	77	92	51
Pittsburg	MAF-186(185)	69	South Bound	171	32	171	213	125
Pittsburg	MAF-186(183)	69	South Bound	132	16	130	149	111
Noble	MAIR-35-4(111)192	35	North Bound	157	29	154	205	127
Noble	MAIR-35-4(111)192	35	South Bound	153	14	154	168	128
Washita	IM-40-2-2(119)040	40	West Bound	117	20	126	131	94
Washita	IM-40-2-2(119)040	40	East Bound	129	39	131	167	89

Table 0.4 Continued CRCP project field collected data

County	Project	Route	Direction	AVG patch/mile	STD patch/mile	median patch/mile	Max patch/mile	Min. patch/mile
Logan	IR-35-4(115)147	35	South Bound	5	8	2	21	0
Logan	IR-35-4(115)147	35	North Bound	0	1	0	2	0
Oklahoma	IR-35-3(073)123	35	North Bound	0	N/A	0	0	0
Oklahoma	IR-35-3(073)123	35	South Bound	1	N/A	1	1	1
Cleveland	IM-NHIY-35-2(221)(247)120	35	South Bound	0	N/A	0	0	0
Cleveland	IM-NHIY-35-2(221)(247)120	35	North Bound	0	N/A	0	0	0
Cleveland	IM-NHIY-35-3(108)119	35	South Bound	0	N/A	0	0	0
Cleveland	IM-NHIY-35-3(108)119	35	North Bound	0	N/A	0	0	0
Carter	IMY-35-1(127)024	35	North Bound	0	0	0	0	0
Carter	IMY-35-1(127)024	35	South Bound	0	0	0	0	0
Okfuskee	IR-40-5(169)226	40	East Bound	7	5	6	13	2
Okfuskee	IR-40-5(169)226	40	West Bound	58	28	59	101	32
Atoka	F-299(99)	69	North Bound	4	4	4	7	2
Atoka	F-299(99)	69	South Bound	11	19	1	33	0
Atoka	F-299(45)	69	North Bound	3	1	3	4	3
Atoka	F-299(35)	69	North Bound	20	N/A	20	20	20
Atoka	F-299(35)	69	South Bound	32	6	31	40	26
Pittsburg	MAF-186(183)	69	North Bound	1	1	0	2	0
Pittsburg	MAF-186(185)	69	North Bound	0	1	0	2	0
Pittsburg	DPIY-204(001)	69	North Bound	0	0	0	0	0
Pittsburg	DPIY-204(001)	69	South Bound	1	1	1	2	0
Pittsburg	MAF-186(185)	69	South Bound	1	1	1	4	0
Pittsburg	MAF-186(183)	69	South Bound	1	2	0	4	0
Noble	MAIR-35-4(111)192	35	North Bound	5.1	5	2.6	13	1.1
Noble	MAIR-35-4(111)192	35	South Bound	3	1	3.1	3.9	1.1
Washita	IM-40-2-2(119)040	40	West Bound	6.4	10.3	1	18.3	0
Washita	IM-40-2-2(119)040	40	East Bound	3.6	1.5	4	5	2

4.4 ADT Data Procedure

Once the field inspection plots had been produced it was decided to correlate the average patches per mile and average Y-cracks per mile to the amount of traffic that a pavement had seen over its lifetime. ODOT provided annual daily traffic (ADT) data from 1995 to 2010 for all of the project sites. The traffic counts provided were in vehicles per day from 1995 to 2010, with the 2010 data including both dump/concrete trucks and semi-trucks with trailer counts. To produce the amount of traffic the pavement had endured over its lifetime the vehicles per day data was converted to equivalent single axel loads (ESALs) and summed up over each year of the pavements existence.

Since many of the projects were older than 1995 the data provided had to be back-casted in order to estimate the vehicles per day values for years prior to 1995. A linear trend line was used as it fit the data well. This line was used to produce values for each year of missing data.

Since ODOT only began calculating truck counts in 2010 an assumption had to be made in order to estimate the percent trucks that each pavement had seen. It was assumed that the 2010 reported percent trucks, both dump/concrete trucks and semi-truck with trailers, held constant over the life of the pavement. Therefore all ESAL calculations were made using the percent trucks from 2010. The semi-trucks with trailers were considered class nine vehicles, the dump/concrete trucks were considered class six vehicles, and all remaining vehicles were considered class three vehicles. The vehicles classes were taken from the Federal Highway Administration (FHWA) vehicle classification chart. These vehicles on a CRCP have an ESAL equivalency of 4.016 ESALs, 0.298 ESALs and 0.0004 ESALs respectively.

Once the vehicles per day had been determined for each year of the entire life of the pavement and the percent trucks had been assumed the ESALs per year were calculated. To perform the ESALs per year calculation a 50-50 directional split was assumed, since the vehicle per day data was for both directions, along with that all of the traffic was assumed to be carried by the outside lane, since most of the roadways were two lane routes. Using these assumptions the ESALs were calculated by converting vehicles per day to ESALs per year. Once the ESALs for each year had

been determined they were added up for each year of service so that the total ESALs for a pavements life was found.

Again these assumptions were made because of the lack of heavy traffic data. These assumptions may impact the ESAL based observations but should not impact any of the other analysis.

4.5 Comparison of Field Observations to the PMS Database

As part of the project the research team had hoped to compare their field data to the data contained in the PMS database. This was done so as the research team had hoped to use the PMS Database to extend the findings to all CRCP in the state and to also use this historic data to quantify how damage occurred over time.

The PMS Database is an Access Database that contains pavement management condition data. The data contained within the database was collected from downward facing images, taken by driving a vehicle equipped with multiple downward facing cameras over the roadway at highway speeds. All of the images were taken in the outside lane of traffic. The raw data is stored at $1/100^{th}$ – mile intervals (52.8 ft.), and organized by control section, direction, and beginning/ending milepost (chainage). The data has been collected, by an outside contractor working for ODOT, on Oklahoma's Highways since 2001, on a 2-year collection cycle.

Different data fields are collected for different pavement types. The CRCP-specific distress fields include longitudinal cracks, punchouts, AC patches, PC patches. These distress fields are described and defined by the *Oklahoma Department of Transportation Pavement Management Distress Rating Guide*. These descriptions can be seen in the following Table 4.5.

Table 4.5 Tabular summary of ODOT Pavement Management Distress Ratings for CRC pavements

Distress type	Recorded Measurement	Description	Rating Procedure
Longitudinal Cracks	Length	A crack that projects within 45 degrees of parallel to the pavements longitudinal centerline	A Level 1 has a mean width less than 0.25 inches with no spalling; likewise, a Level 2 crack has a mean width greater than or equal to 0.25 inches, or contains spalling. Sealed longitudinal joints are considered Level 2, unless it is apparent their width is less than 0.25 inches
Punchouts	Amount	areas of distressed pavement separated from normal pavement by wide or spalled cracks and often exhibiting spalling, breakup, and/or faulting	Level 1 punchouts have mean crack widths less than 0.125 inches and spalling up to 3 inches wide, Level 2 punchouts have mean crack widths between 0.125 and 0.25 inches and spalling width between 3 and 6 inches, Level 3 punchouts have crack widths greater than 0.25 inches, spalling greater than 6 inches. All patches are recorded as level 3 punchouts.
AC Patch	Area	asphalt patching on CRCP	Only the quantity is recorded
PC Patch	Area	A Portland cement concrete patch replacement of the originally continuously reinforced concrete pavement	Only the quantity is recorded

4.6 PMS Database Comparison Procedure

The focus of the PMS database comparison was to analyze three different databases to determine how patches increase over time and observe areas prior to becoming patches, and see how the data aligned with the patches recorded in the field investigation portion of this research project. In doing this comparison the consistency and accuracy of the database collections could also be observed. The 2001, 2006, and 2008 PMS databases were all obtained for the stretches of pavements studied in the field investigation portion of this research project. These pavements were selected through the direction of ODOT. The county, route, and length of each section of pavement studied in the field investigation, and analyzed in the database comparisons, can be seen in the following Table.

Table 4.6 Pavements for PMS Database Comparison

County	Route	Length Observed
Logan	35	10.56
Oklahoma	35	01.74
Cleveland	35	03.32
Carter	35	09.26
Okfuskee	40	09.4
Atoka	69	08.22
Pittsburg	69	26.28

To compare the location of patches between the three databases a graphical approach was used. To produce patch comparison graphs the AC and PC patches were copied from the 2001, 2006, and 2008 databases and put into an Excel spreadsheet. Level 3 punchout data was also incorporated into the graphs. The reasoning behind this being that some AC patches, depending on their size, could be recorded as a level 3 punchout one year and an AC patch the next depending on interpretation. Therefore by including level 3 punchouts, patches occurring in 2001 or 2006 should appear again in 2008. Thus by including AC patches, PC patches, and

level 3 punchouts all of the patches would be accounted for, and theoretically the 2001, 2006 and 2008 PMS databases would align. As a comparison the data collected during the field measurements was compared to the data contained in the provided database.

During the data compilation process it was noticed that the PMS databases did not always begin and end at the exact same chainages from year to year. However, to keep consistency within the data, all of the begin and end points from the PMS database were used, regardless of where the true begin and end points occurred according to the plan sets. This should only have a minor impact on the results.

Once the AC and PC patches were all compiled in the Excel spreadsheet three columns were created, for each year of the database, adding the AC and PC patches together. This formed a total square foot of patch per chainage column for each database.

In order to plot just the location of each patch, and not the actual size of the patch, every chainage showing a recorded square foot of patch was plotted based on the year of the database. Each of the three databases were plotted to be staggered so that the changes in patches over time could be easily compared.

In addition to comparing the data from the three databases to one another, the patch locations observed in the field inspection section of this report were also included. To show a distinction between the data from the downward facing images and the data collected during the OSU field inspection, the patches observed during the OSU inspection were plotted below the x-axis.

The graphs plotted chainage on the x-axis vs. patch and punchout location on the y-axis. Each graph contained four data sets, the 2001, 2006, and 2008 PMS database patch locations, along with the site inspection patch locations. A few of the pavements were constructed either after 2001 or 2006, and therefore contained less than four sets of data.

Each graph displays one direction of the studied roadway within the county. Vertical lines above the x-axis show the location of each patch or punchout collected from the downward facing images. The lines are staggered at different heights based on the year they were observed to make the graphs easier to interpret. The vertical lines below the x-axis mark the location of all of the patches observed during the field

inspection of this research project. Theoretically patches observed in 2001 should be present in both 2006 and 2008, and patches observed in 2006 and should be present in 2008. Therefore, every patch from 2001 and 2006 should have been reported in the later inspection, hence the later years should overlay the earlier years. Because once a patch is made it will remain in the roadway. When the years do not overlay one another an error has occurred. This indicates that either something is wrong with the year-to-year inspections or an error exists between the database and the field inspection.

4.6.1 PMS Database Comparison Graphs

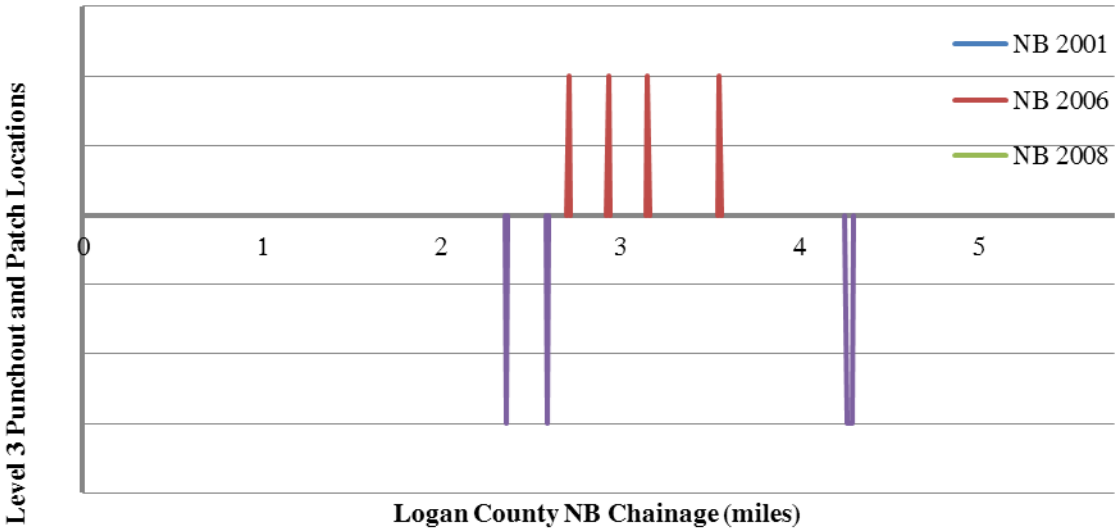

Figure 4.2 Logan County North bound patch locations

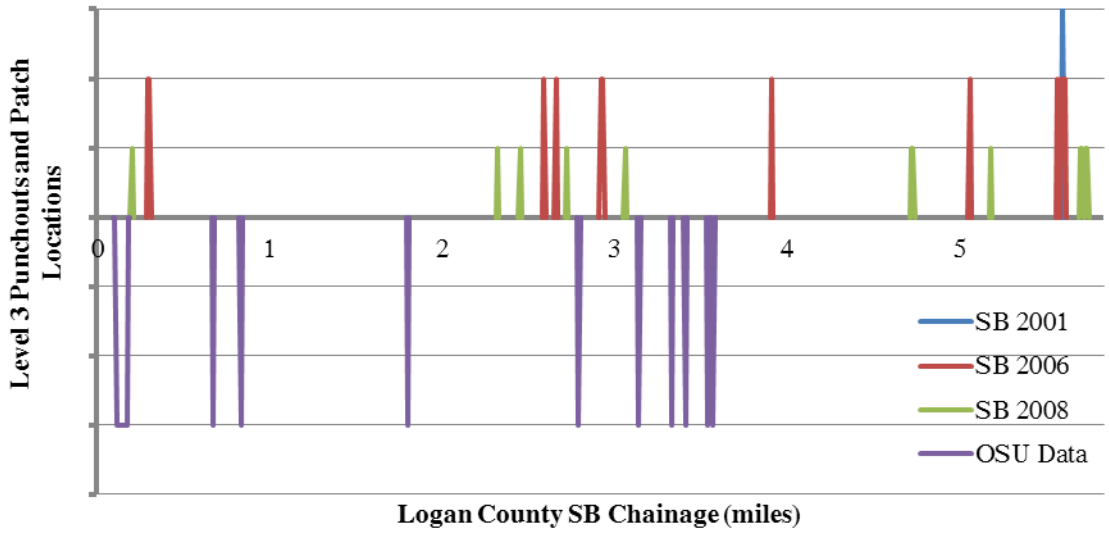

Figure 4.3 Logan County South bound patch locations

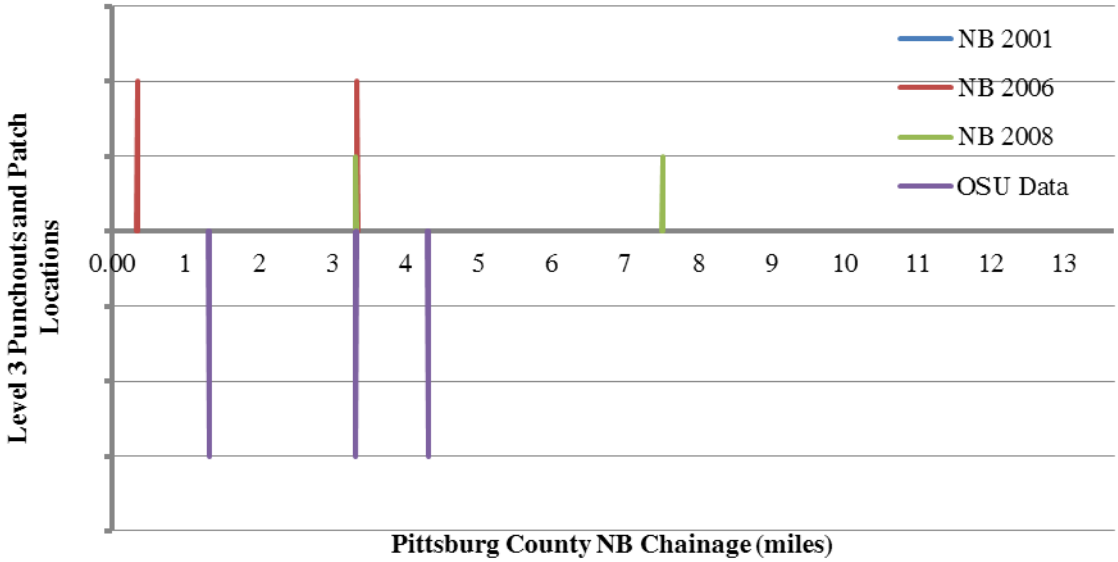

Figure 4.4 Pittsburg County North bound patch locations

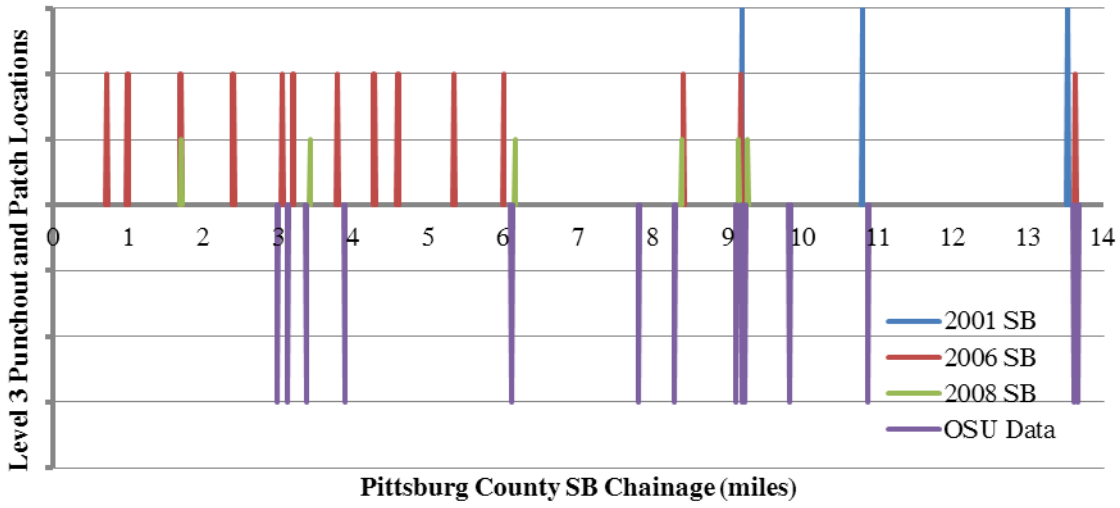

Figure 4.5 Pittsburg County South bound patch locations

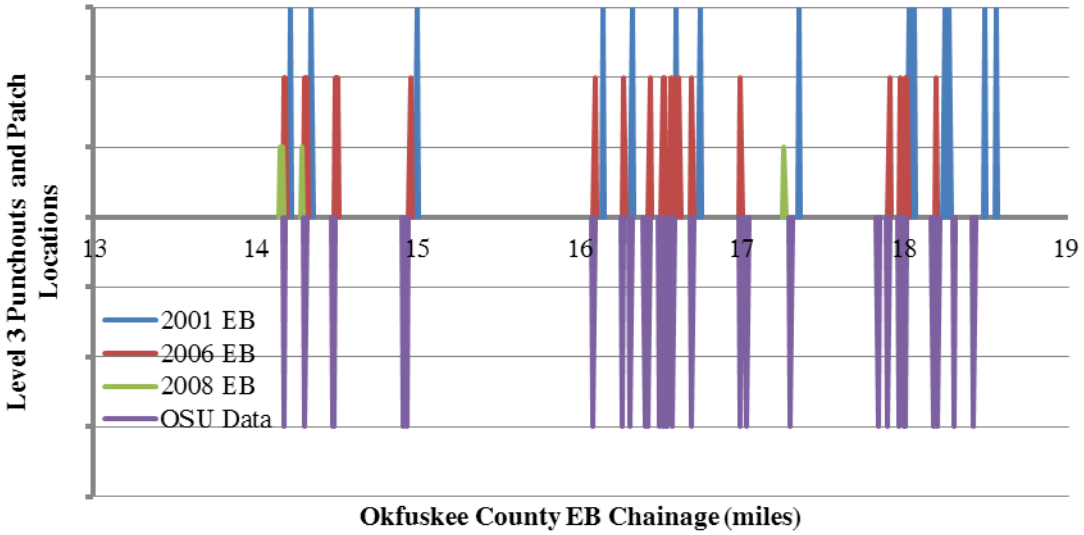

Figure 4.6 Okfuskee County East bound patch locations

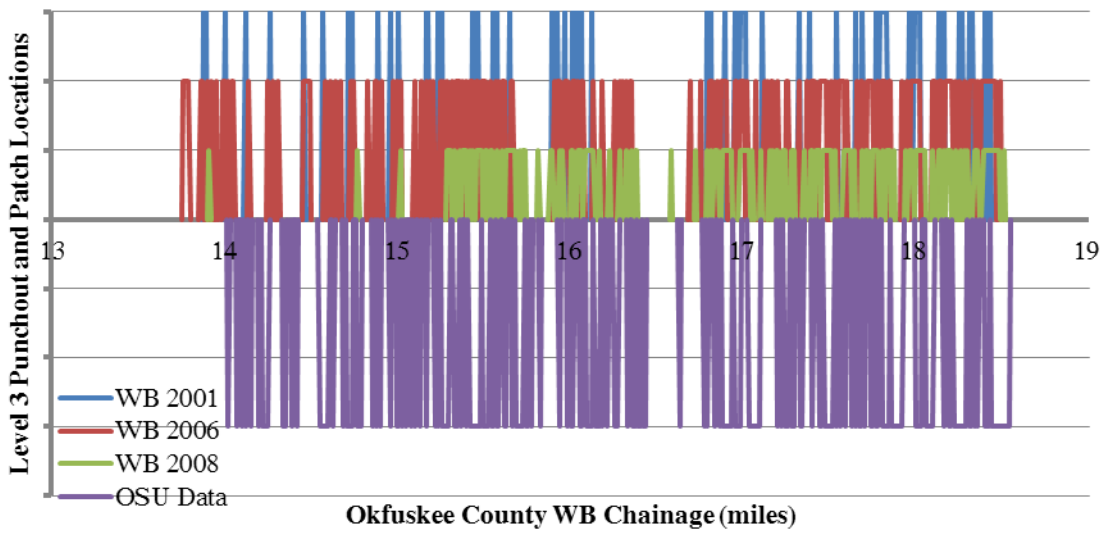

Figure 4.7 Okfuskee County West bound patch locations

4.6.2 Observations from PMS Comparison Graphs

If the three databases perfectly aligned the 2001 markers would be overlaid by the 2006 and 2008 markers. There are few instances when this occurs. Secondly the OSU Data should mirror across the x-axis for every patch that was found and existed as of 2008. This seems to be the case most of the time. There are several instances where patches were recorded in 2001 but they were not recorded in 2006 and/or 2008. The accuracy between each year of the databases and between the OSU collected data can be seen in the comparison table below.

Table 4.7 Punchout plus Patches Comparison Table

			Punchouts and Patches Present				Difference Between Years		
County	Route	Direction	001	006	008	SU	2001-2006	2006-2008	2008-OSU
Logan	35	NB	0	4	0	3	+4	-4	+3
Logan	35	SB	1	2	2	6	+11	0	+4
Pittsburg	69	NB	0	2	0	4	+2	-2	+4
Pittsburg	69	SB	3	3	6	4	+20	-17	+8
Okfuskee	40	EB	4	2	4	3	+8	-18	+29
Okfuskee	40	WB	6	73	50	7	+107	-23	-73

Table 4.7 helps to illustrate the fact that the PMS Databases do not align between years or with the OSU field collected data. The four columns under the "Punchouts and Patches Present" column contain the total number of punchouts and patches reported in the PMS Database and field inspection for the designated year. In a perfect situation the amount of patches and punchouts in a pavement would not decrease from year to year, meaning that once a patch is formed it is counted as a patch every following year. Inspection of the table demonstrates that this is not the case. The second group of three columns titled "difference between years" shows the change, either plus or minus, between the consecutive inspections. In an ideal situation the difference between years would either be zero or positive. Meaning either no new punchouts or patches occurred or punchouts and patches were added between inspections. Negative values represent a decline in the amount of punchouts and patches seen between years, and thus represent some type of error with the collection of the data or input of the data. It is because of these negative values that the PMS Database was determined to be unreliable for this project and was not used.

4.7 Results

Before the field inspection data can be analyzed, it is important to understand how CRCP construction has changed in Oklahoma over time. This is summarized in

section 4.8. After this is better understood then it is easier to correlate both Y-cracking and patches to different pavement parameters. Sections 4.9 and 4.10 provide a more in depth investigation into Y-cracking and patches and how they are influenced by different pavement parameters. Finally, section 4.11 investigates possible correlations between Y-cracks and patches.

4.8 Evolution of Steel Content and Thickness in Oklahoma

The following plots show how the longitudinal steel content and thickness of CRCP has changed over time in Oklahoma. Figure 4.8 provides a graphical presentation as to how longitudinal steel content has increased over time by plotting the year of completion on the x-axis and the longitudinal steel content on the y-axis. The plot shows that steel contents have risen from 0.50% in 1985 to 0.73% in 2007.

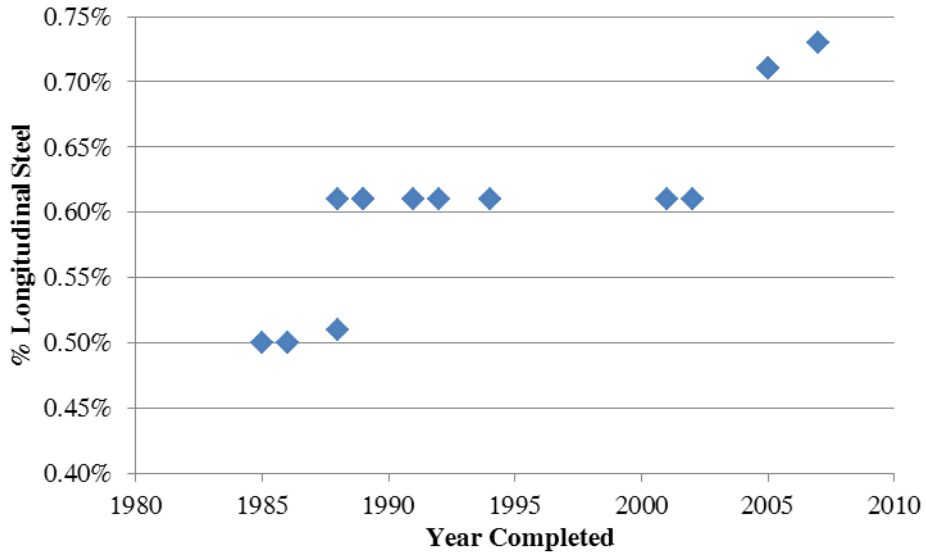

Figure 4.8 Year completed vs. percent longitudinal steel content

Figure 4.9 illustrates how the thickness of pavements has changed over time. As a general rule pavements have increased in thickness from 1985 to 2007; however, there was one modern pavement constructed in 2005 with the same thickness as the pavements constructed in the 1980s. Together the two plots show that pavements have increased in both thickness and steel content from 1985 to 2007, for instance pavements constructed in 1985 were typically nine inches thick and had longitudinal steel contents of 0.50%, while pavements constructed in 2007 had thickness of twelve inches and longitudinal steel contents of 0.73%.

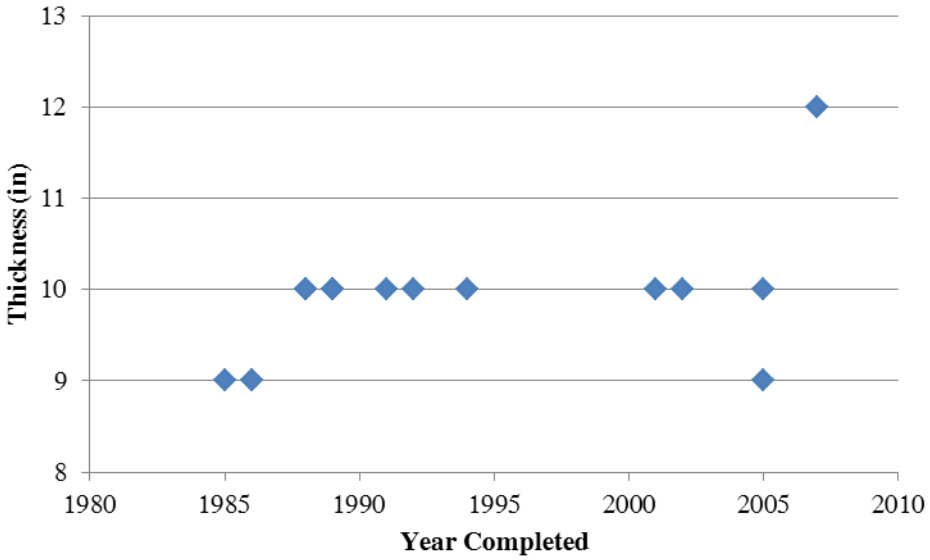

Figure 4.9 Year completed vs. pavement thickness

4.9 Correlation of Y-cracks to Different Pavement Parameters

In order to better understand what leads to the formation of Y-cracks plots were created to compare the average observed Y-cracks per mile to year completed, estimated ESALs, thickness, percent longitudinal steel, percent transverse steel, shoulder type, and base type. Figures 4.10 thru 4.16 graphically present the trends between the different parameters.

Figure 4.10 plots the year the CRCP project was completed on the x-axis and the average Y-cracks per mile on the Y-axis. The plot also contains different symbols that distinguish between the 9, 10, and 12 inch thick pavements that were studied. The graph shows a correlation between year completed and Y-cracking; the graph suggests that more modern pavements are experiencing less Y-cracking.

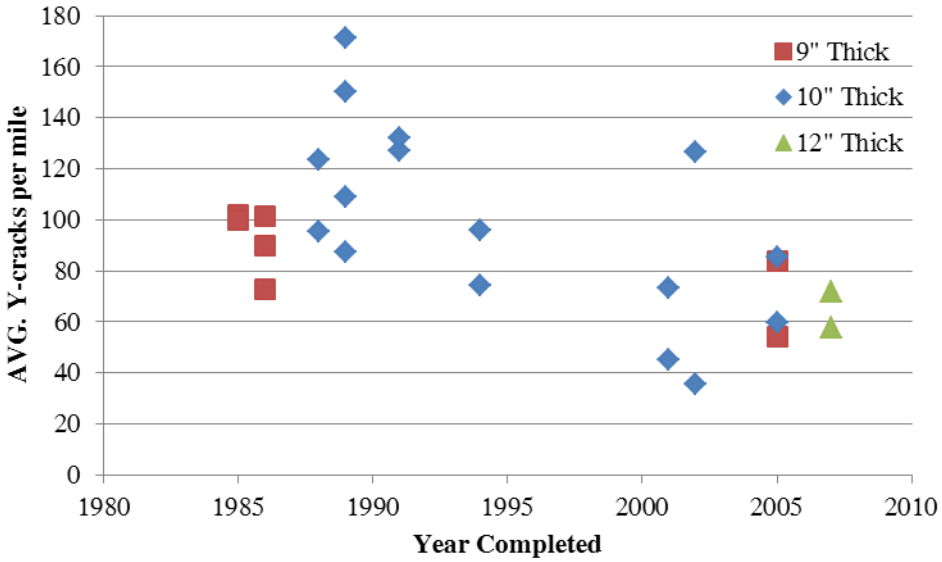

Figure 4.10 Year completed vs. field collected average Y-cracks per mile

Figure 4.11 relates the CRCP thickness to the average Y-cracks per mile. The thickness is plotted on the x-axis and the average Y-cracks per mile is plotted on the y-axis. As the graph shows multiple pavements were studied that had the same thickness; therefore, a round yellow marker was inserted into the graphs marking the average number of Y-cracks for each thickness. The chart seems to show that Y-cracking is not directly controlled by the thickness of the pavement because all of the thicknesses seem to have average Y-crack numbers that are fairly close.

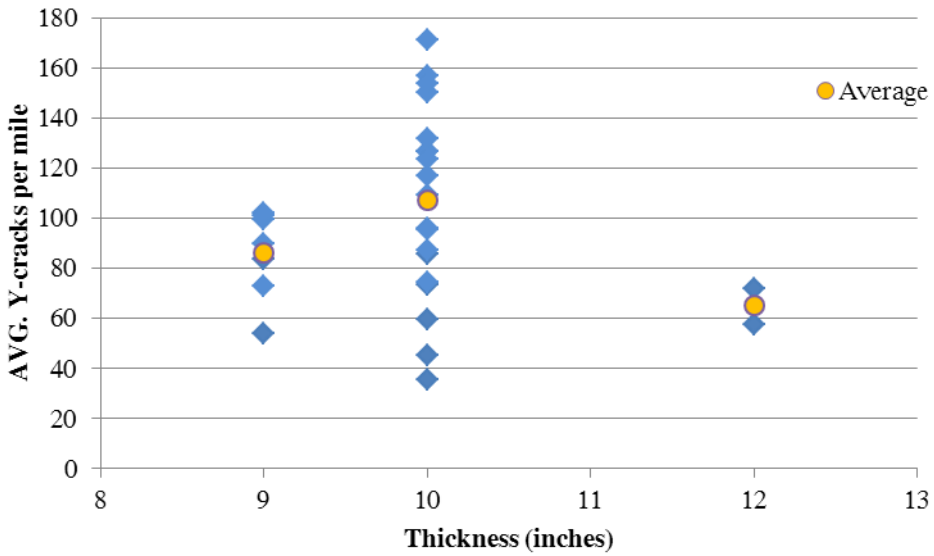

Figure 4.11 Thickness vs. average observed Y-cracks per mile

Figure 4.12 was created to determine if any correlation between the longitudinal steel content and the amount of Y-cracks existed. For this plot the percent of longitudinal steel contained within the pavement was plotted on the x-axis while the average amount of Y-cracks per mile was plotted on the y-axis. Since multiple pavements were studied with the same steel contents a round yellow marker was inserted into the graph to help illustrate where the average amount of Y-cracks per mile was for each steel content. During the investigation steel contents of 0.50%, 0.51%, 0.61%, 0.71% and 0.73% were studied; however average markers were only inserted for the 0.50%, 0.61%, and 0.73% steel content because of the small variability between the other steel content values. From this plot there appears to be no linear trend between the different longitudinal steel contents, however the higher longitudinal steel contents contained less Y-cracks per mile.

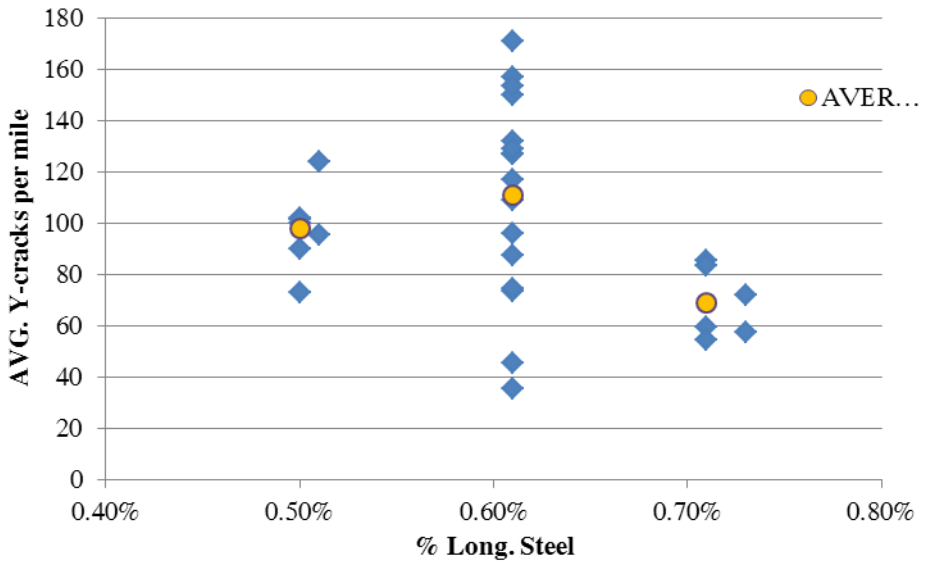

Figure 4.12 Percent longitudinal steel vs. average observed Y-cracks per mile

Figure 4.13 was developed to show possible trends between the amount of transverse steel and the average amount of Y-cracks per mile in a pavement. To do this the amount of transverse steel was plotted on the x-axis and the average amount of Y-cracks per mile was plotted on the y-axis. Since multiple pavements were looked at with the same steel contents, yellow round markers were inserted into the plot to mark the average number of Y-cracks per mile seen at each steel content. Also note that one pavement was inspected where no transverse steel was used. The plot seems to show that as the transverse steel content increases so does the amount of Y-cracks per mile, except when no transverse steel was used.

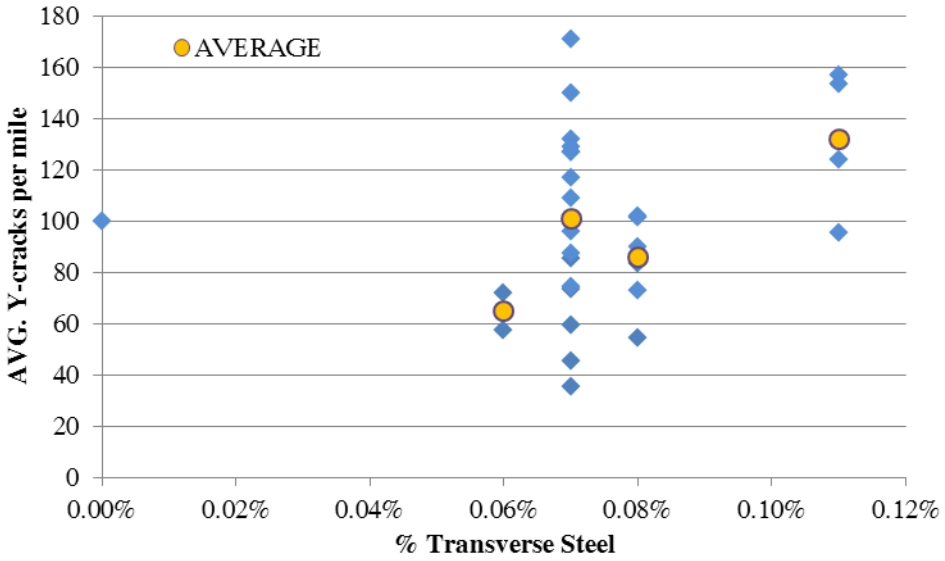

Figure 4.13 Percent transverse steel vs. average observed Y-cracks per mile

Figure 4.14 shows the trend between shoulder type and the amount of Y-cracks per mile. The bar chart plots the average amount of Y-cracks per mile for pavements with CRCP shoulder, jointed plain concrete paved shoulders (JPCP), and the average Y-cracks for all of the pavements studied. From the figure it appears that pavements with CRCP shoulders contained significantly fewer, 35% less, Y-cracks per mile than pavements with JPCP shoulders.

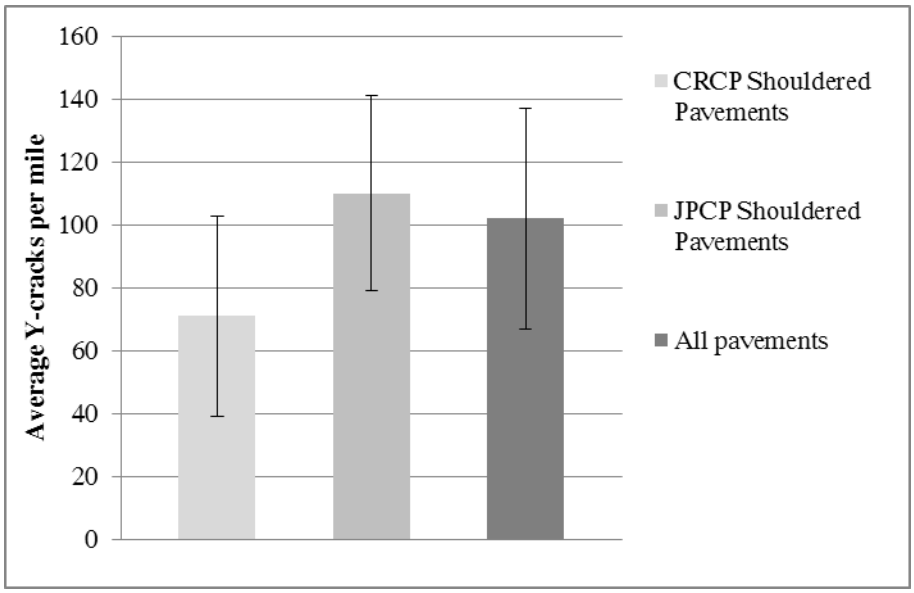

Figure 4.14 Shoulder type vs. average Y-cracks per mile

To compare the effect of base type to the amount of Y-cracks in a pavement the plot in figure 4.15 was created. The figure plots the average amount of Y-cracks per type of pavement base used. From the figure it appears that the pavements contained the least Y-cracks per mile when an open graded bituminous base. However, it is important to state that six of the seven pavements cast on top of a bituminous base had CRC shoulders. This helps to reiterate the difficulty of isolating one pavement variable in order to pinpoint the cause of Y-cracks.

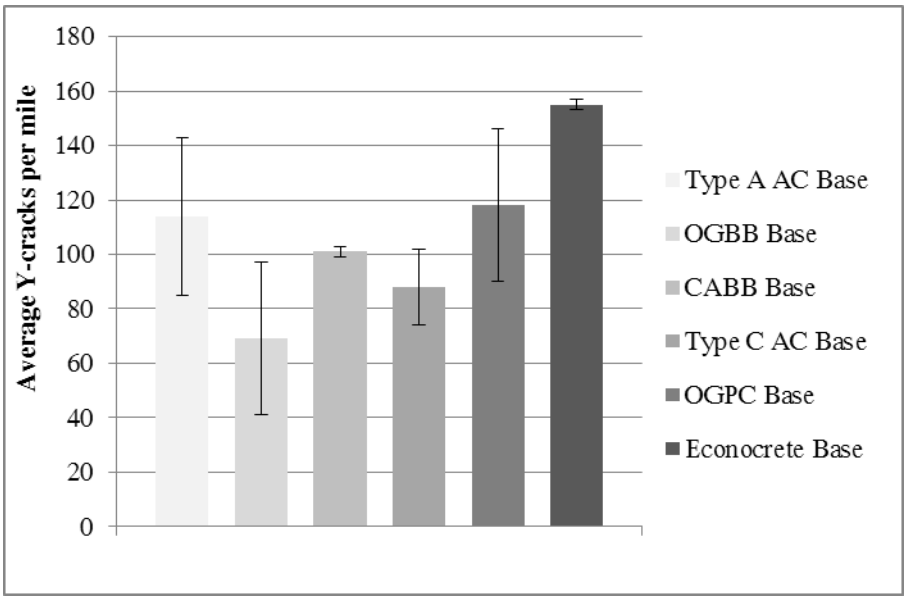

Figure 4.15 Base type vs. average Y-cracks per mile (Type A AC – Superpave Type S3, OGBB – Open Graded Bituminous Base, CABB – Course Aggregate Bituminous Base, Type C AC – Superpave type S5, OGPC – Open Graded Permeable Course) (2009 Interstate Structural History)

4.16 Correlation of Patches to Different Pavement Parameters

In order to better understand what leads to patching, plots were created to compare the average observed patches per mile to year completed, estimated ESALs, thickness, percent longitudinal steel and percent transverse steel. Figures 5.9 thru 5.17 graphically present the trends between the different parameters.

Figure 4.16 was created in order to find a possible trend between the age of pavement and the amount of patches contained within the pavement. To do this the year the CRCP was completed was plotted on the x-axis while the average amount of patches per mile was plotted on the y-axis. The pavements investigated were also broken down by thickness based on the type of marker assigned to each data point. The plot shows that as a pavement increases in age the amount of patches per mile increases as well. This is a strong trend as all pavements with ten years of service have many more patches than the younger pavements. Since nearly all of the newer pavements are thicker than the older pavements it is difficult to determine whether the thickness of a pavement has an effect on the development of patches.

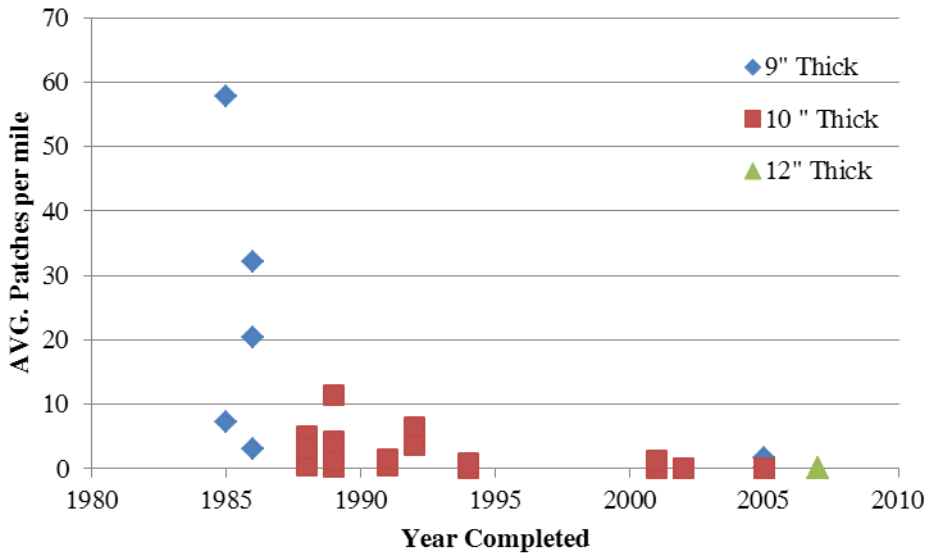

Figure 4.16 Year completed vs. average observed patches per mile

Figure 4.17 was created as a comparison between the age of the pavement and the amount of ESALs a pavement has seen. The purpose was to determine if patches were more closely related to the ESALs a pavement saw or the age of the pavement. To make this comparison estimated cumulative ESALs were plotted on the x-axis along with the average patches per mile on the y-axis and different markers were used to distinguish between the different pavement thicknesses. From the graph it appears that the more ESALs a pavement endures the higher the amount of patches the pavement contains; furthermore, it appears as though thinner pavements with high ESAL counts seemed to have more patches per mile than slightly thicker pavements with similar ESAL counts.

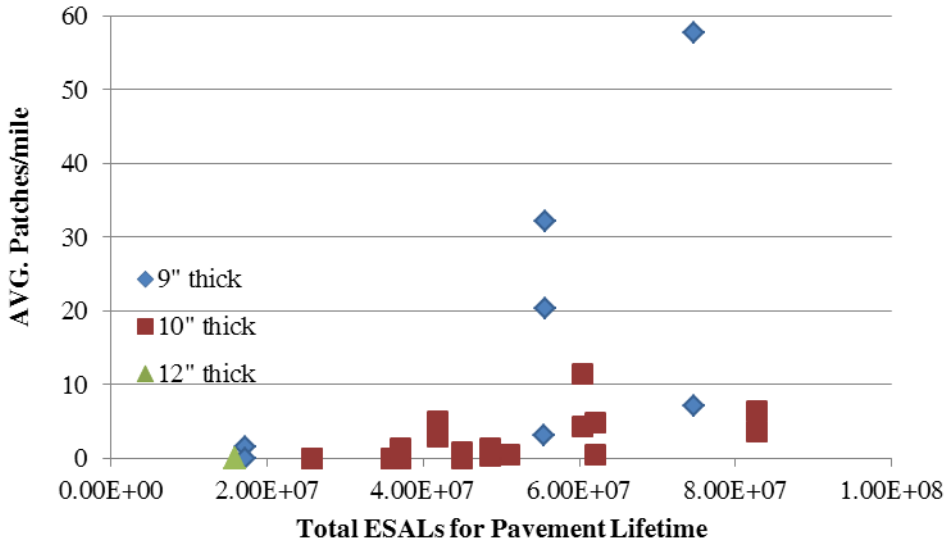

Figure 4.17 Cumulative ESALs vs. average observed patches per mile

Figure 4.18 was created in order to uncover possible trends between pavement thickness and the amount of patches contained within a pavement. To investigate these trends for pavement thickness was plotted on the x-axis and the average number of patches per mile was plotted on the y-axis. Different marker types were also inserted into the graph to declare the age of the pavement. Since multiple pavements of the same thickness were studied average markers were inserted at each pavement thickness to help simplify the graph. From the graph it can be seen that thinner pavements seem to have more patches per mile, however it is also important to realize that most of the older pavement are thin.

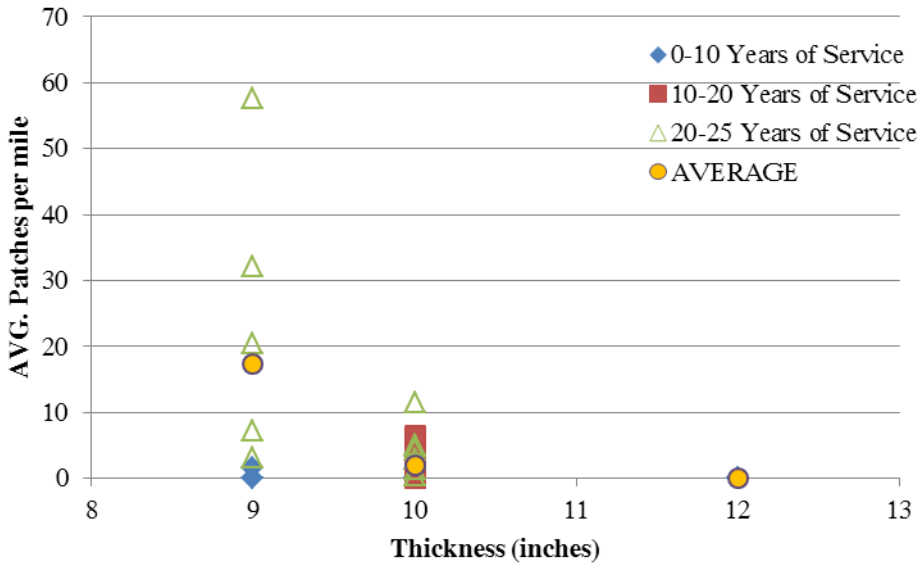

Figure 4.18 Thickness vs. average observed patches per mile

In order to locate any trends between the longitudinal steel content and the amount of patches contained with a pavement, a plot was developed showing the percent longitudinal steel on the x-axis and the average patches per mile on the y-axis, see figure 4.19. Because of the changes of steel content over the years different markers were assigned to each pavement based on the years of service the pavement had endured. Since multiple pavements were observed with the same steel contents yellow average markers were inserted into the plot to assist in the plots interpretation. The plot seems to show that higher steel contents lead to a decrease in the amount of patches, however it must be noted that all of the pavements with higher steel contents are younger than the other pavements.

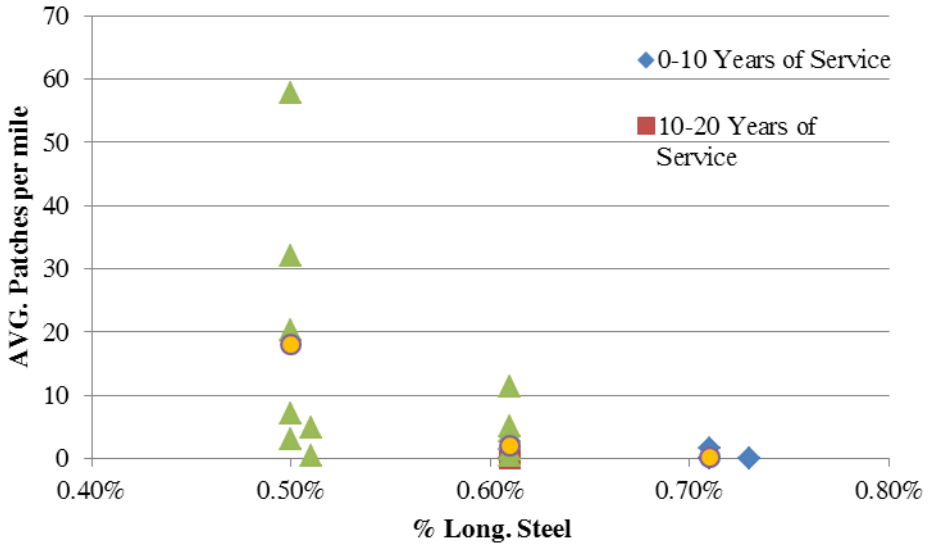

Figure 4.19 Percent longitudinal steel vs. average observed patches per mile

A plot was also created in figure 4.20 to look for correlations between the amount of transverse steel and the amount of patches within a pavement. To make this correlation percent transverse steel was plotted on the x-axis and the average amount of patches per mile was plotted on the y-axis, different markers were also incorporated to distinguish the years of service for each pavement. Finally, round yellow markers were inserted to mark the average number of patches for each steel content studied. From the graph it can be seen that the pavement with no transverse steel contained a very high amount of patches, while the other pavements did not display a clear trend. This suggests that the amount of transverse steel does not significantly impact the amount of patches contained within a pavement, except when no transverse steel is used.

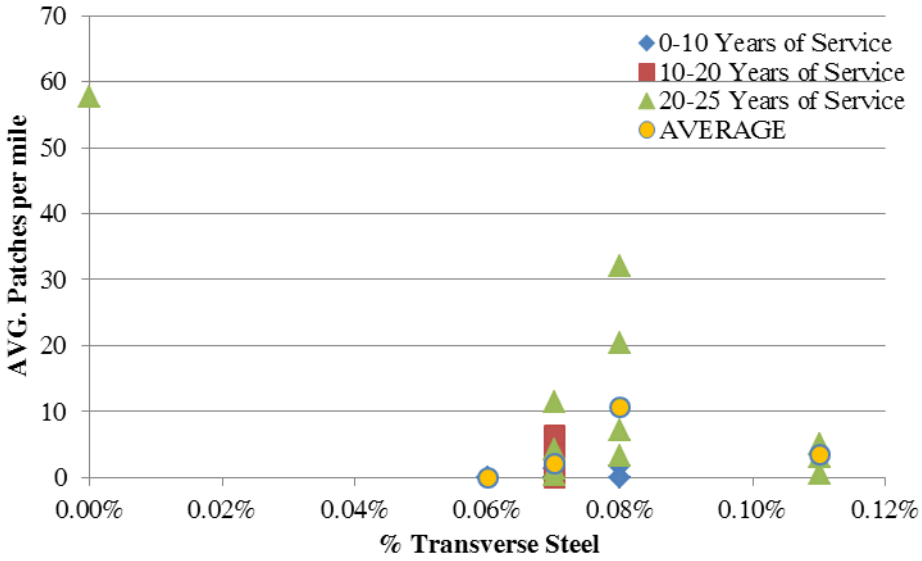

Figure 4.20 Percent transverse steel vs. average observed patches per mile

Figures 4.21 and 4.22 were created to help determine how shoulder type and base type influence patch formation. The three previously mention projects with very high patch contents were omitted from these graphs. From these graphs it appears that CRCP shouldered pavements help to reduce the amount of patches contained within the roadway. The graphs also illustrate that open graded bituminous bases help to reduce the amount of patches seen within the roadway; however, it is important to state that every CRC shouldered pavement contained an open graded bituminous base. Therefore, either one or both could be contributing to the reduction of patches.

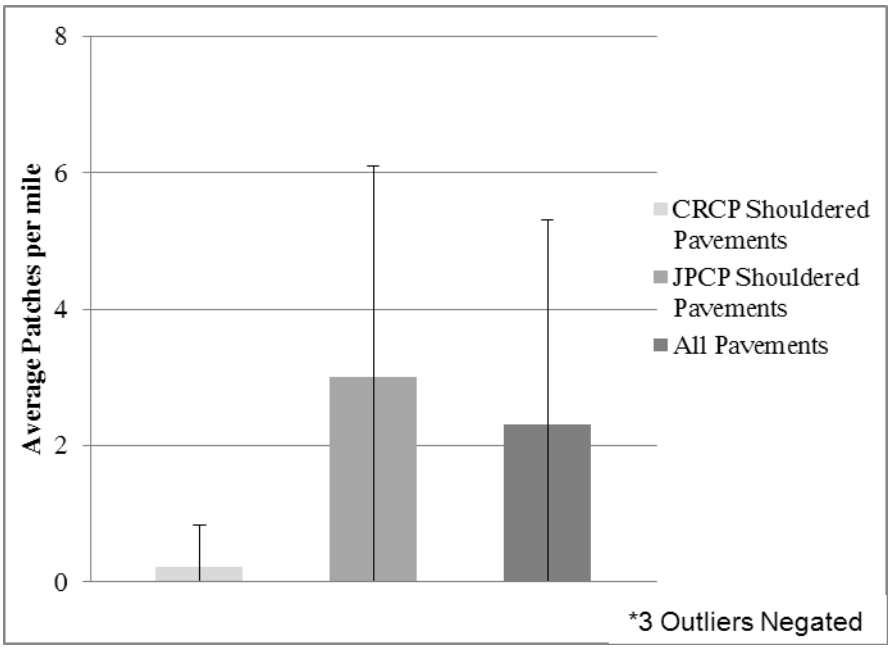

Figure 4.21 Shoulder type vs. average patches per mile

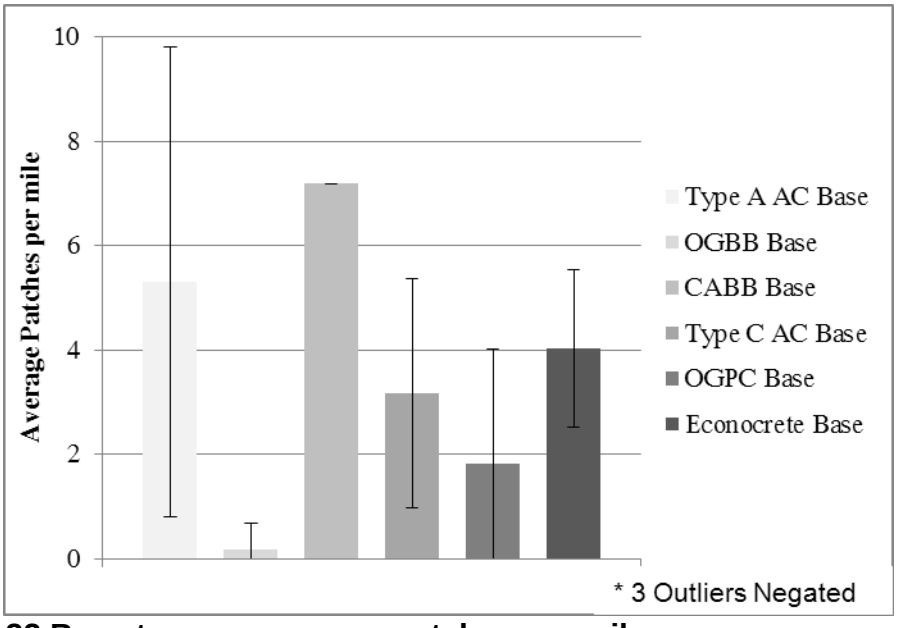

Figure 4.22 Base type vs. average patches per mile

4.11 Correlation Between Y-cracks and Patches

One goal of this study was to determine the effect of Y-cracking on CRCP performance. Since patches are considered pavement failures, which lead to expensive repair costs, and decreases in ride quality, it was important to relate patches to Y-cracking. In order to look for possible trends between Y-cracks and patches a plot was created that plotted average number of Y-cracks per mile on the x-axis and average number of patches per mile on the y-axis, different marker types were also inserted to differentiate between the ages of the pavements. Figure 4.22 shows the plot of Y-cracks vs. patches. The chart contains three distinct outliers. The most extreme outlier, nearly 60 patches per mile, can be accounted for by the fact that no transverse steel was used. The other two outliers were from the same project and can likely be attributed to a local phenomenon.

Figure 4.23 is an enhanced version of figure 4.22. Figure 4.23 removes the outliers of figure 4.22, so that there is a better look at the data. The figure helps to show that as Y-cracks increase to more than 60 Y-cracks per mile there is an increase in patches per mile. A trend line has been added to this graph in order to highlight this.

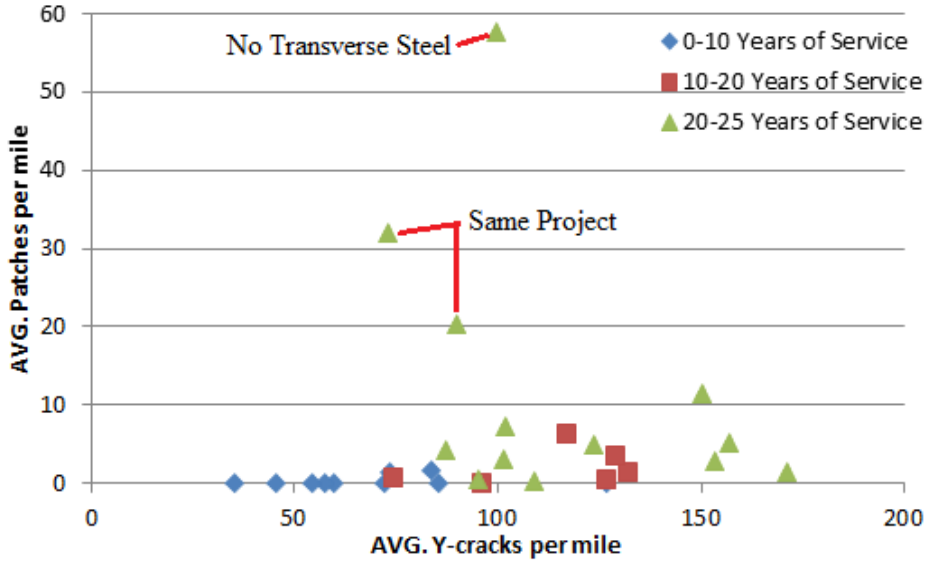

Figure 4.23 Average observed Y-cracks per mile vs. average observed patches per mile

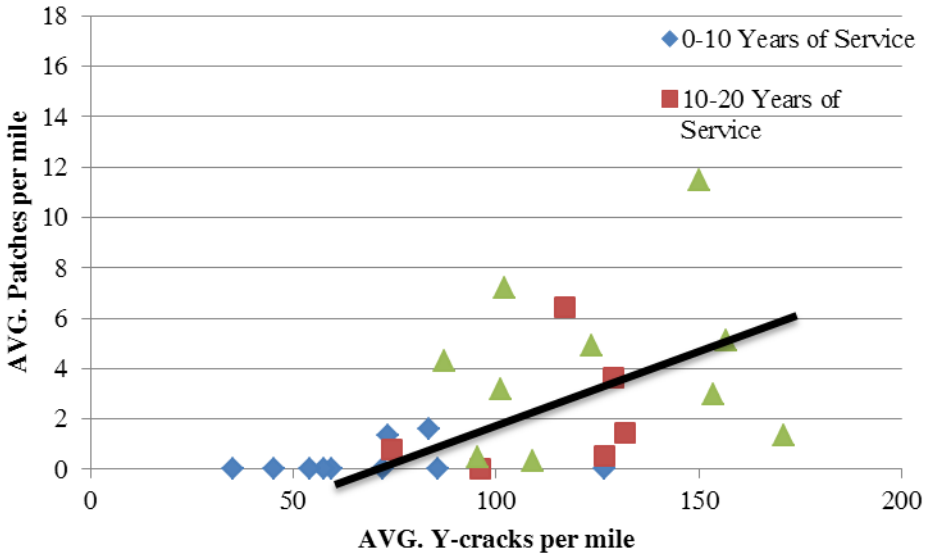

Figure 4.24 Y-cracks vs. patches with an enhanced scale

4.12 Crack Spacing Comparison

Table 4.8 contains mean spacing, standard deviation, coefficient of variation, and extent of Y-cracks information for a couple of sites. These measurements were taken at predetermined sites and locations so that the data could be directly compared to data previously measured by Tayabji et al. (2004). Because of differences in collection techniques these numbers may not exactly match. From these measurements the difference in the mean crack spacing does not seem to have decreased. This means that more cracking has not occurred in the roadway, as this would have decreased the crack spacing. From the table it can also be seen that the amount or extent of Y-cracks has not increased. This supports the observation that after an initial period of service that Y-cracks do not appear to increase with time.

Table 4.8 Table comparing 2011 OSU field collected measurements and 1991 Strategic Highway Research Program Collected Data

				OSU Collected Data				SHRP Study Collected Data			
County	**Route**	Date Completed	Direction	Mean Spacing (ft)	Standard Deviation (ft)	Coefficient of Varation (%)	Extent of Y-cracks (%)	Mean Spacing (ft)	Standard Deviation (ft)	Coefficient of Varation (%)	Extent of Y-cracks (%)
Logan	**35**	1988	North Bound	5.21	2.90	56	11	4.72	2.29	49	12
Okfuskee	**40**	1985	West Bound	5.92	3.06	52	11	2.59	5.78	68	19

4.13 Discussion

Using the graphs, found in the results section, several trends between Y-cracking and patches when comparing to year, thickness, percent longitudinal steel, and percent transverse steel can be observed. However, it is important to realize that no two pavements are alike. Every pavement studied varies from the other pavements in multiple ways. For example, pavements with the same steel content and thickness do not have the same bases, and pavements with the same thickness and base have differing steel contents. Because of the variability between pavement characteristics it becomes very difficult, if not impossible, to isolate the Y-cracking phenomenon to one variable. However the results do provide some insight into the impact of Y-cracking on CRCP performance.

While looking at the plots comparing average observed Y-cracks to the various pavement parameters several trends can be seen:

- The average amount of Y-cracks observed per mile seems to be lower for more recently constructed pavements, Figures 4.10
- The average amount of Y-cracks per mile seems to be fairly constant despite the thickness of the pavement, Figure 4.11
- Longitudinal steel contents do not seem to directly relate to the average amount of Y-cracks observed, Figure 4.12
- Higher amounts of transverse steel do not seem to lower the amount of Y-cracks, in fact higher transverse steel contents seem to increase the amount of Y-cracking. Pavements with 0.06% transverse steel contained 50% less Y-cracks per mile when compared to pavements with 0.11% transverse steel, see Figure 4.13
- Pavements with CRCP shoulders contain less Y-cracks per mile. The average Y-cracks per mile for all of the pavements studied in Oklahoma was 105.5, in contrast the average Y-cracks per mile for pavements with non CRC shoulders was 110 Y-cracks per mile, and the average Y-cracks per mile for pavements with CRC shoulders was 71 Y-cracks per mile. Therefore, it appears that by using CRC shoulders the Y-cracks per mile can be reduced by 35% when compared to non CRC shouldered pavements, see Figure 4.14

- Pavements contained less Y-cracks per mile when cast directly on top of open graded bituminous base; however, six of these seven studied pavements also contained CRC shoulders, see Figure 4.15
- Using the plots created comparing patches to different pavement parameters trends can also be observed:
- Pavements completed after 1990 have 90% less patches per mile values, this could be due to relatively young age of the pavement, low ESAL exposure, thicker pavement, and or higher steel contents, see Figures 4.16 and 4.17
- Higher patches per mile seems to correlate with age and estimated ADT, see Figure 4.17
- Pavements that are thicker and have higher steel contents appear to have less patches per mile, but these pavements are also much younger than the thinner pavements and previous graphs showed patches to be related to age and ADT, see Figures 4.18 and 4.19
- Percent transverse steel does not seem to have an effect on patches; however, if no transverse steel was used high patch counts were seen, see Figure 4.20
- Pavements with CRCP shoulders and open graded bituminous bases appear to contain less patches per mile when compared to other pavements with different shoulder and base types; however, these pavements are also relatively young

The plot of average Y-cracks per mile vs. average patches per mile (Figures 4.23 and 4.24) contains important observations. When first looking at the plot, three data outliers stick out. However, one of the outliers can be attributed to the project containing no transverse steel which is likely the cause for producing the high amount of patches despite its Y-cracks per mile being average (100 per mile). The other two outliers are located on the same project in differing directions; therefore, these two may be due to some localized phenomenon with their construction. When these data points are removed a slight trend can be seen. According to the data, when pavements exhibit 60 Y-cracks per mile the amount of patches within the roadway begin to increase, and according to the trend line, when pavements reach 150 Y-cracks per mile 5 patches per mile typically occur. Despite this trend, more work is needed to verify that the increase

in Y-cracks per mile directly results in more patches per mile. To verify this, pavements with high Y-crack contents need to be monitored over time, and the cause of every future patch needs to be documented.

Table 4.9 was created to summarize the effect of changing different CRCP parameters and their effect on the amount of both Y-cracks and patches contained within the pavement for the projects investigated.

Table 4.9 Summary all of the information pulled from the graphs in chapter 5 affecting both Y-cracking and patch formation

Pavement Parameter	Y-cracks	Patches
Increase in Age	No Effect	Increase
Increase in ESALs	No Effect	Increase
Increase in Thickness	No Effect	Decrease
Increase in Longitudinal	No Effect	Decrease
Increase in Transverse	Increase	No Effect
CRCP Shoulders/Open	Decrease	Possible

Throughout the research 94 miles of Oklahoma CRCP were inspected. During these inspections 9925 total Y-cracks were observed, of these only 19 appeared to be developing punchouts or the cause of an asphalt patch in the roadway. This data suggests that 0.2% of all Y-cracks lead to punchouts; however, it is impossible to tell the cause of many of the existing patches. When all of the data is considered it suggests that high Y-crack counts do lead to a slight increase in patches per mile. Therefore, if Y-crack counts can be reduced to 60 Y-cracks per mile or fewer the amount of patches in the roadway should be minimized.

4.14 Field Inspection Conclusion

In this study 94 miles of CRCP were inspected for patches, punchouts, and Y-cracks. The CRCPs varied in thickness, steel content, age, shoulder type, base, and geographic location. While this provided multiple variables to use to correlate with Y-cracking, it also made the isolation of the Y-cracking phenomenon challenging. Despite the challenges, information was gathered through field inspection and database research in order to determine the effect of Y-cracking on CRCP performance.

During the field inspection the most common cause of punch-out was closely spaced transverse cracks intersected by longitudinal cracks. The database portion of the project also yielded clues to the task of reducing Y-cracks. Using the field inspection data along with the project information contained within the database it was determined that:

- Pavements with CRC shoulders and open graded bituminous bases contained 35% less Y-cracks per mile than pavements with non CRC shoulders.
- Pavements with higher transverse steel contents contained more Y-cracks per mile
- Pavements without transverse steel showed poor performance
- Pavements in this study did not experience a change in Y-cracks per mile when the longitudinal steel content was increased to 0.71% and 0.73%, when compared to steel contents of 0.50% and 0.61%

From the results of this study Y-cracks appear to correlate with patches. As Y-cracks increase beyond 60 Y-cracks per mile, patches tend to increase as well. Therefore, if the amount of Y-cracks contained in a pavement can be minimized with the suggestions above then the overall quality of the roadway can be preserved. Recommendations to reduce the amount of Y-cracks and patches in future CRCP include: pavements should be constructed with 10 to 12 inches in thickness, longitudinal steel content between 0.61% and 0.73%, always use transverse steel with a suggested content of 0.06%, and use CRC shoulders with an open graded bituminous base.

While all of these new observations are important to understanding the effect of Y-cracking in continuously reinforced concrete pavements it is important to realize that Y-cracks are not the only parameter that can lead to the formation of a punch-out. Since many other pavement distress types can lead to punch-out formation much more work is needed in order to better understand the correlation between Y-cracks and punchouts. In order to better understand how Y-cracks are formed CRCPs should be monitored during the early age of the pavement and throughout the pavements life.

PAVEMENT MODELING WITH HIPERPAV III AND CONCRETE WORKS

5.1 Introduction

Closer crack spacing is thought to increase the occurrence of meandering or Y-cracks in CRCP (Johnston & Surdahl, 2008). In order to investigate the effects of construction, material, and design choices on the crack spacing, a sensitivity analysis was performed using the HIPERPAV III software package. HIPERPAV (High Performance Concrete Paving) was developed by the Transtec Group, Inc. under contract by the Federal Highway Administration (FHWA). The first generation of HIPERPAV I was created in 1996 and consisted of a module for early-age behavior for Jointed Plain Concrete Pavements (JPCP). In the second version, modules were created for JPCP Long-Term Pavement Performance (LTPP) and early-age behavior for Continuously Reinforced Concrete Pavements (CRCP). HYPERPAV III, the version used in this study, added an improved model for drying shrinkage (Ruiz et al., 2005).

5.2 CRCP Early-Age Module

HIPERPAV III predicts the crack spacing and width at 72 hours and one year after construction. It is assumed that the concrete experiences the lowest temperature and most of the drying shrinkage during the first year, with little change in the concrete shrinkage and crack spacing afterwards. The one-year crack spacing is given in the software as the long-term crack spacing (Ruiz et al., 2005). A flow chart of the process HIPERPAV III uses in modeling CRCP early-age crack spacing and width is shown in Figure 5.1. First, the software predicts the concrete pavement temperature based on the concrete mixture proportions, construction sequences and timing, and environmetal condition such as temperature, wind speed, humidity, and cloud cover. The strength and the modulus of elasticity are calculated using the predicted temperature and equivalent age maturity method to adjust for the impact of temperature on the hydration rate. The model uses the B3 model for calculating the drying shrinkage strain and the temperature change and concrete coefficient of thermal expansion to calculate the thermal strain (Ruiz et al., 2001). Stresses are predicted using these volumetric changes and the restraint provided by the steel and subbase friction. The crack spacing,

crack width, and steel stress are calculated from the stresses and strength calculated (Ruiz et al., 2005).

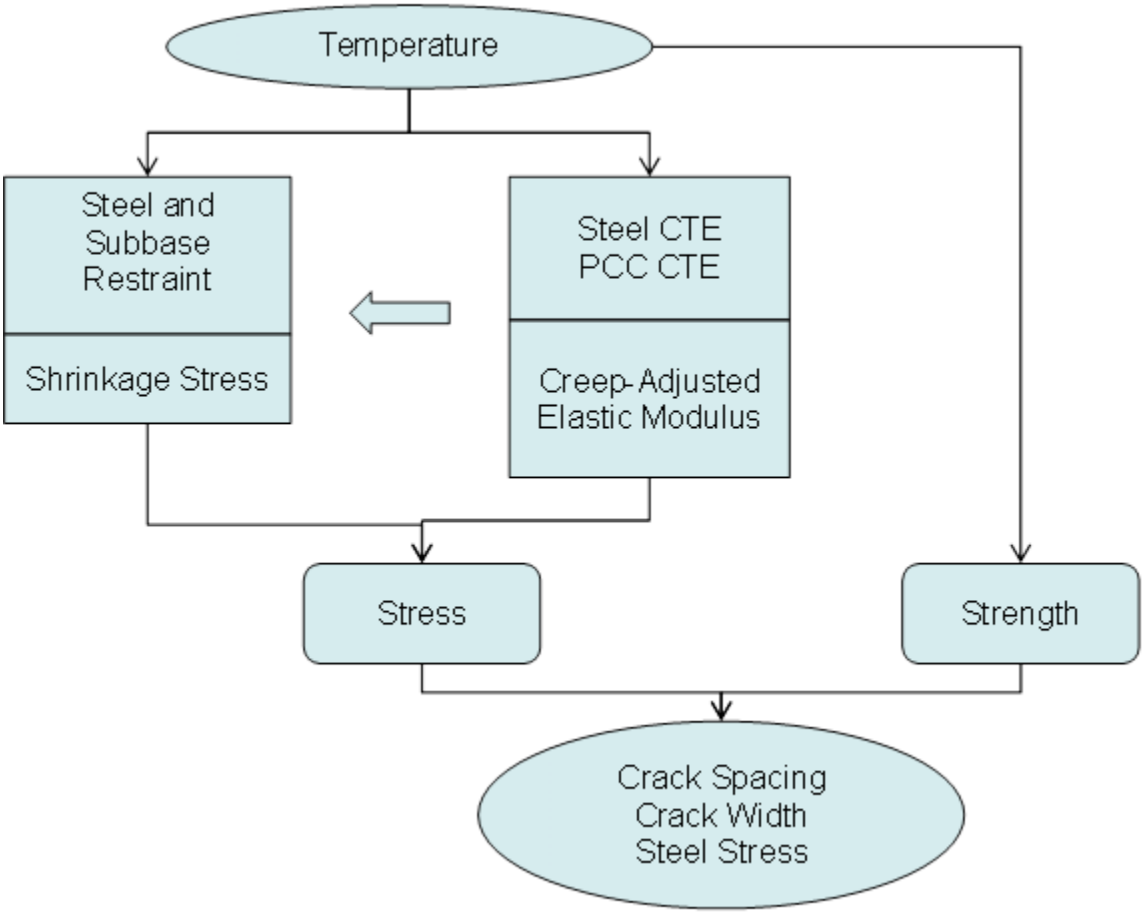

Figure 5.1 CRCP early-age module. After (Ruiz et al., 2005)

5.3 Oklahoma CRCP Modeled

The sensitivity analysis was performed for five Oklahoma sites that were also included in a six-state field investigation of CRCPs conducted in 1991 (Tayabji et al., 1998). Three of these sites (OK-1, OK-2, and OK-3) were also investigated as part of this study. Details about the five pavement sites studied are shown in Table 5.1.

Table 5.1 Pavement Sites Studied in Sensitivity Analysis

Site Designation	Location	Year Construction	Year Opened to

		Began	Traffic
OK-1	I-40 from milepost 226 to 231, approximately 77 miles east of Oklahoma City, OK.	1987	1989
OK-2	US-69, approximately 19 miles northeast of Atoka, OK.	1986	1988
OK-3	I-35, approximately 25 miles north of Oklahoma City, OK.	1988	1989
OK-4	US-69, approximately 23 miles south of Atoka, OK.	1984	1985
OK-5	I-40, approximately 30 miles west of the Oklahoma-Arkansas border.	1989	1990

5.4 Procedure

A sensitivity analysis for possible contributing factors to Y-cracking was completed to understand the relative importance of each factor in creating closely spaced cracks at 72 hours and 1 year after placement. HIPERPAV was used to model the average transverse crack spacing, transverse crack spacing standard deviation, and crack width of CRCP based on the environmental conditions during placement, concrete mixture used, construction conditions, and pavement design.

HIPERPAV needs many project specific inputs to calculate the crack spacing and widths. Table 5.2 shows the input parameters that were constant for all modeled sites (OK-1 through OK-5). These values are assumed from design methods, materials, construction, and testing that are usually used in Oklahoma. Table 5.3 shows the site specific input values used. The input values for the slab thickness, bar spacing, bar diameter, and subbase thickness were reported by Tayabji et al. (1998).

Table 5.2 Constant Input Values for HIPERPAV

Input Parameter	Input Value
Number of Bar Mats	1
Yield Strength	60 ksi
Steel Modulus	29000 ksi
Steel Coefficient of Thermal Expansion	6.5×10^{-6} /°F
ASTM Cement Type Classification	Type I
Strength Type	Compressive
28-Day Strength	3000 psi
Coefficient of Variation	0.167
Age Curing Applied	1 hr
Age Plastic Sheeting Removed	1 day
Consider Construction Traffic	No

Table 5.1 Site Specific Input Values

Site	Slab Thickness	Bar Spacing	Bar Diameter	Subbase Thickness	Maximum Aggregate Size	Site Latitude	Site Longitude
OK-1	9 in.	8.75 in.	0.625 in.	4 in.	2”	35.4°	-96.2°
OK-2	9 in.	6.875 in.	0.625 in.	3 in.	1.5”	34.6°	-96.0°
OK-3	10 in.	6.875 in.	0.625 in.	3 in.	1.5”	35.8°	-97.4°
OK-4	9 in.	6.875 in.	0.625 in.	6 in.	1.5”	34.1°	-96.3°
OK-5	10 in.	7.25 in.	0.750 in.	4 in.	1.5”	35.5°	-94.9°

The variables chosen for the sensitivity analysis were the construction time, construction date, curing method, subbase material, subgrade support, and aggregate type. These inputs were chosen based on either extremes likely used in the pavement construction or variables that were not known. Construction date, subbase material,

and subgrade support were based on information from the Tayabji et al. study (1998), but were not specifically given. For example, the subbase material for the OK-1 site was found to be asphalt concrete. The subbase surface roughness however was not known and was varied in the sensitivity analysis. The subgrade support values were selected based on typical ranges found for the type of subgrade present for the pavement (Huang, 2004). Table 5.4 shows the variables selected for the five sites studied. All six different variables were varied for each site, giving a total of 648 different input combinations used for each site. For every run the transverse crack spacing average, transverse crack spacing standard deviation, and transverse crack width at 72 hours and 1 year were recorded.

Table 5.2 OK-1 Variables and Values Included in Sensitivity Analysis

Variables	Values Included in Analysis				
	OK-1	OK-2	OK-3	OK-4	OK-5
Construction Time	7:00 A.M.	7:00 A.M.	7:00 A.M.	7:00 A.M.	7:00 A.M.
	10:00 A.M.	10:00 A.M.	10:00 A.M.	10:00 A.M.	10:00 A.M.
	3:00 P.M.	3:00 P.M.	3:00 P.M.	3:00 P.M.	3:00 P.M.
Construction Date	1/12/1988	1/12/1987	1/12/1989	1/12/1985	1/12/1990
	7/26/1988	7/26/1987	7/26/1988	7/26/1984	7/26/1989
	10/22/1988	10/22/1987	10/22/1988	10/22/1984	10/22/1989
Curing Method	None	None	None	None	None
	SCLCC	SCLCC	SCLCC	SCLCC	SCLCC
	DCLCC	DCLCC	DCLCC	DCLCC	DCLCC
	PS	PS	PS	PS	PS
Subbase Material	RAC	RAC	RAC	RAC	CSS15
	SAC	SAC	SAC	SAC	CSS10
Subgrade Support	100 psi	100 psi	100 psi	100 psi	200 psi
	150 psi	150 psi	200 psi	150 psi	250 psi
	200 psi	200 psi	300 psi	200 psi	300 psi
Aggregate Type	SG	SG	SG	SG	SG
	GR	GR	GR	GR	GR
	LS	LS	LS	LS	LS

Note: ..... SCLCC = Single Coat Liquid Curing Compound

DCLCC = Double Coat Liquid Curing Compound

RAC = Rough Asphalt Concrete

SAC = Smooth Asphalt Concrete

CSS15 = Cement Stabilized Subbase 15 psi

CSS10 = Cement Stabilized Subbase 10 psi

PS = Plastic Sheeting

SG = Siliceous Gravel

GR = Granite

LS = Limestone

5.5 Data Analysis Procedure

For each of the 18 input values used in the study, a dataset was created that grouped together all results that used that input. For example, the dataset created for the 7:00 a.m. placement time would contain the 216 different combinations of values used for the other 5 input variables used in the study. The average crack spacing, average crack spacing standard deviation, and average crack width of each dataset was calculated.

The next step was to statistically analyze the sorted data for each data group in each site. The statistical method chosen to analyze the data was inferences from matched pairs. This test was used to determine if there is a statistical difference between two samples that have dependent samples, or matching pairs. The data meets all the requirements for this test, which are as follows from Triola (2006):

"1. The sample data consist of matched pairs.

2. The samples are simple random samples.

3. Either or both of these conditions are satisfied: The number of match pairs of sample data is large ($n > 30$) or the pairs of the values have differences that are from a population having a distribution that is approximately normal."

After the averages were calculated the input values were chosen based on the highest and lowest values in that dataset. An example of the process used follows for the construction time at 1 year for OK-1 (Triola, 2006).

"Notation: d = individual difference between two values in a single matched pair

μ_d = mean value of the difference d for the population of all matched pairs

$\bar{d}$ = mean value of the differences d for the paired sample data

s_d = standard deviation of the differences d for the paired sample data

n = number of pairs of data (Triola, 2006)"

Step 1: The claim that the difference between the crack spacing average with a 7:00 A.M. construction time and a 3:00 P.M. construction time can be expressed as $\mu_d \neq 0$, which is the alternative hypothesis.

Step 2: If the claim in Step 1 is not valid, $\mu_d = 0$ which is the null hypothesis.

Step 3: A significance level or probability of $\alpha = 0.01$ is selected.

Step 4: Find the student *t* distribution fromTable 5.5, $t = \pm 2.600$ for $\alpha = 0.01$ (Area in Two Tails) and the $n - 1 = 215$ degrees of freedom.

Table 5.3 *t* Distribution: Critical *t* Values. After (Triola 2006)

Degrees of Freedom	Area in Two Tails (α = 0.01)
100	2.626
200	2.601
300	2.592
400	2.588

Step 5: Calculate $\bar{d} = 0.11$ and $s_d = 0.22$. For $\mu_d = 0$ and n=216, the value of the test statistic can be found.

$$t = \frac{d - \mu_d}{\frac{s_d}{\sqrt{n}}} - \frac{0.11 - 0}{\frac{022}{\sqrt{216}}} = 7.5$$

Step 6: Because the test statistic t falls in the critical region, we can reject the null hypothesis and state that the average crack spacing for a 7:00 A.M. and 3:00 P.M. concrete placement time are significantly different. The evaluation of the t-value can be seen graphically in Figure 5.2.

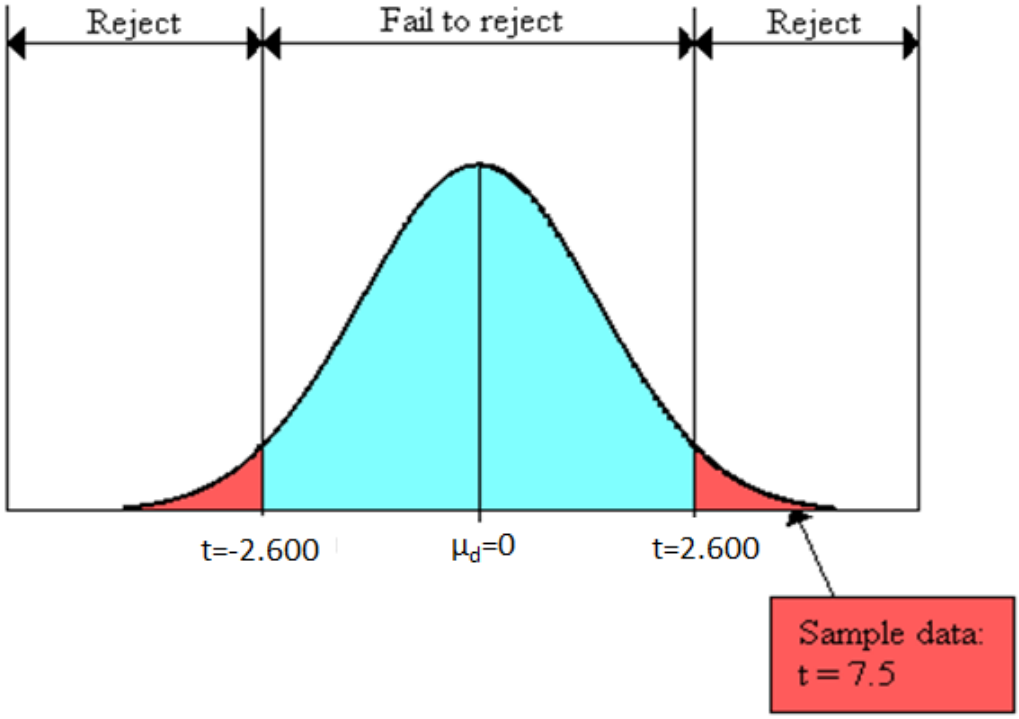

Figure 5.2 Distribution of differences between values in matched pairs. After (Triola 2006)

5.6 Sensitivity Analysis Results

The average crack spacing, average crack spacing standard deviation, and average crack width for each of the 18 datasets for the five sites examined at 72 hours and 1 year are given in Appendix A. The results of the inferences from matched pairs at 72 hours and 1 year are given in Appendix B.

Figures 5.3-5.5 show the percent change seen in the average crack spacing, average crack spacing standard deviation, and average crack width for the five sites. Figures 5.6-5.8 show the absolute t-value for each input variable category at 72 hours and 1 year for each site. The subgrade support was shown to have no significant effect on the crack spacing and width.

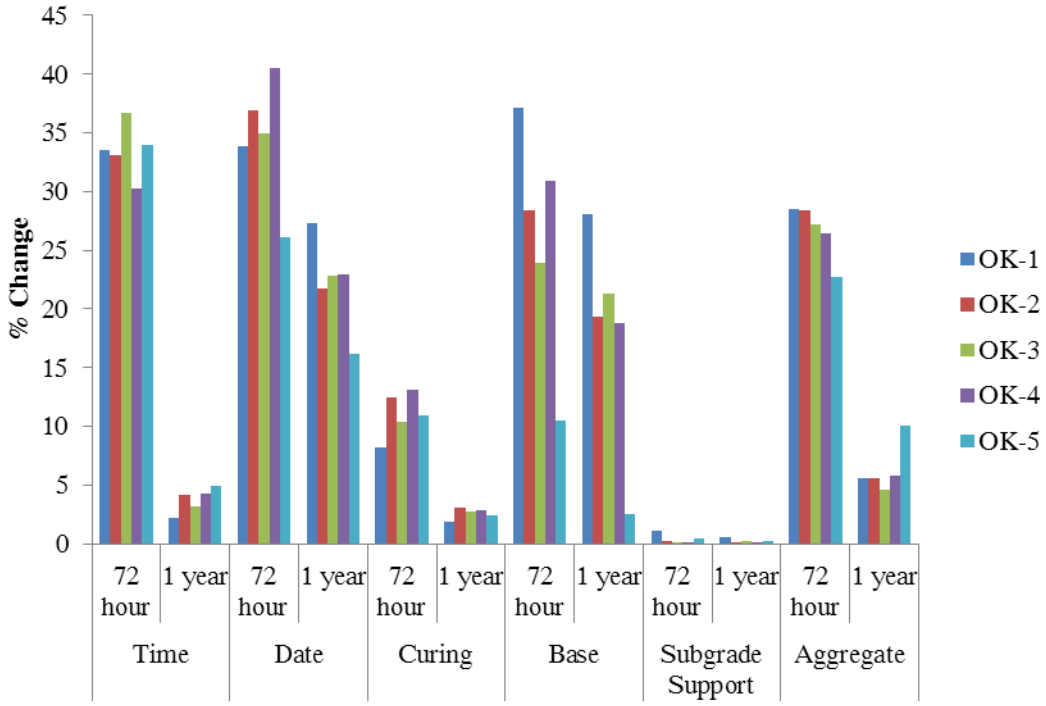

Figure 5.3 % Change for the Average Crack Spacing at 72 Hours and 1 Year

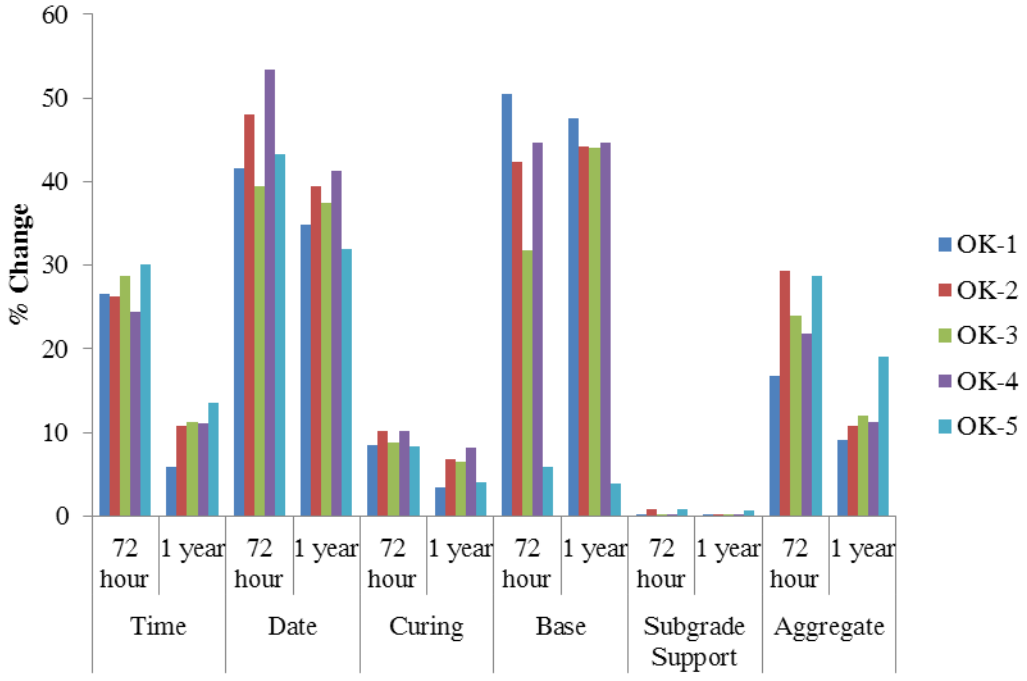

Figure 5.4 % Change for the Average Crack Spacing Standard Deviation at 72 Hours and 1 Year

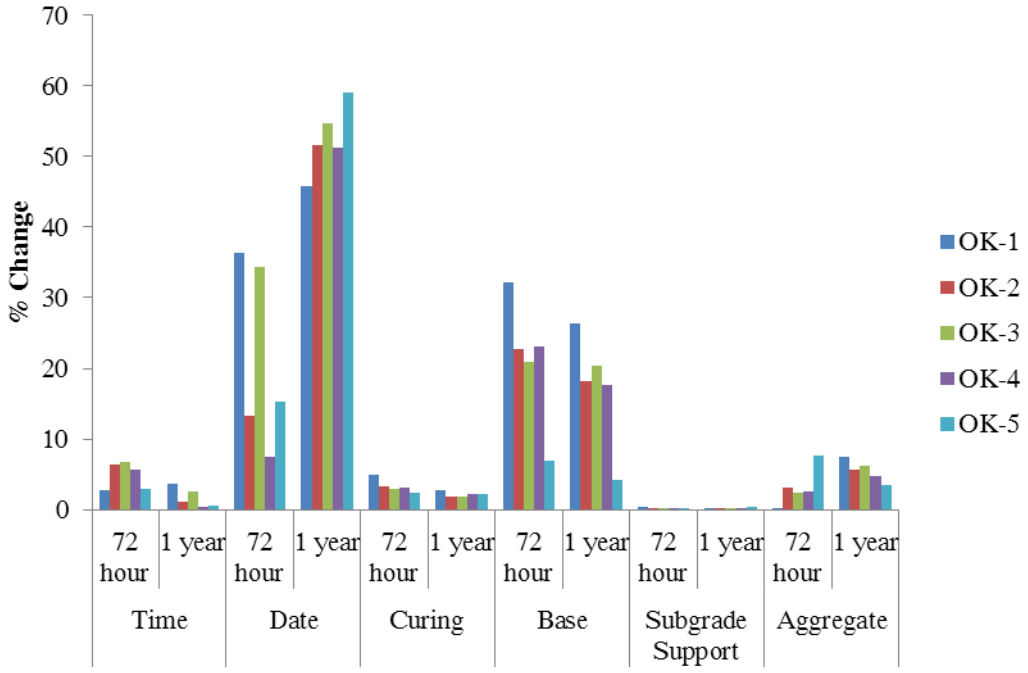

Figure 5.5 % Change for the Average Crack Width at 72 Hours and 1 Year

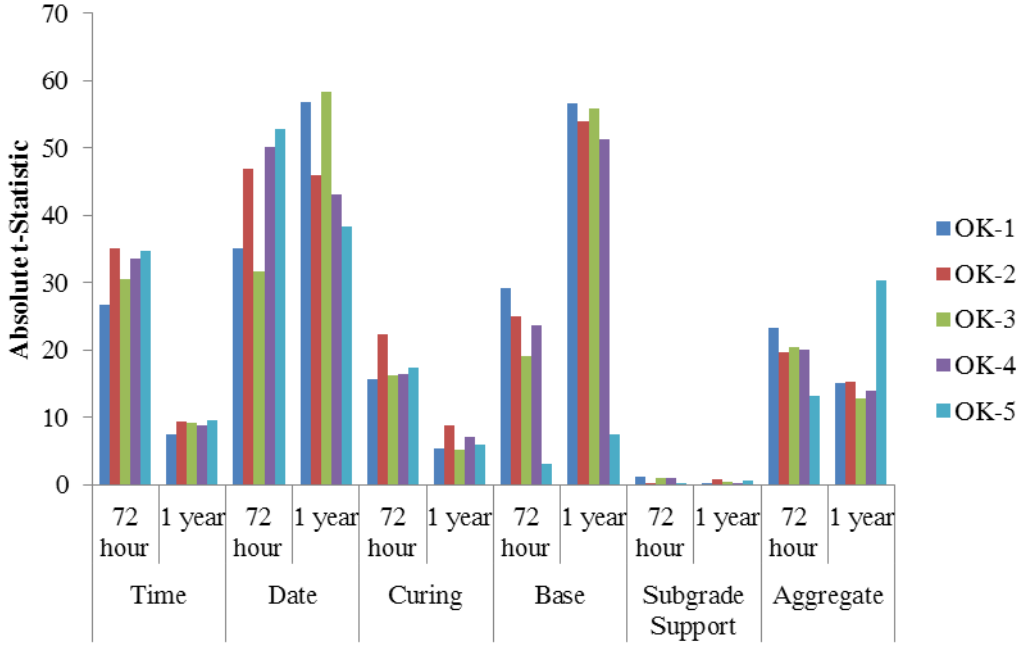

Figure 5.6 Absolute t-Statistic for the Average Crack Spacing at 72 Hours and 1 Year

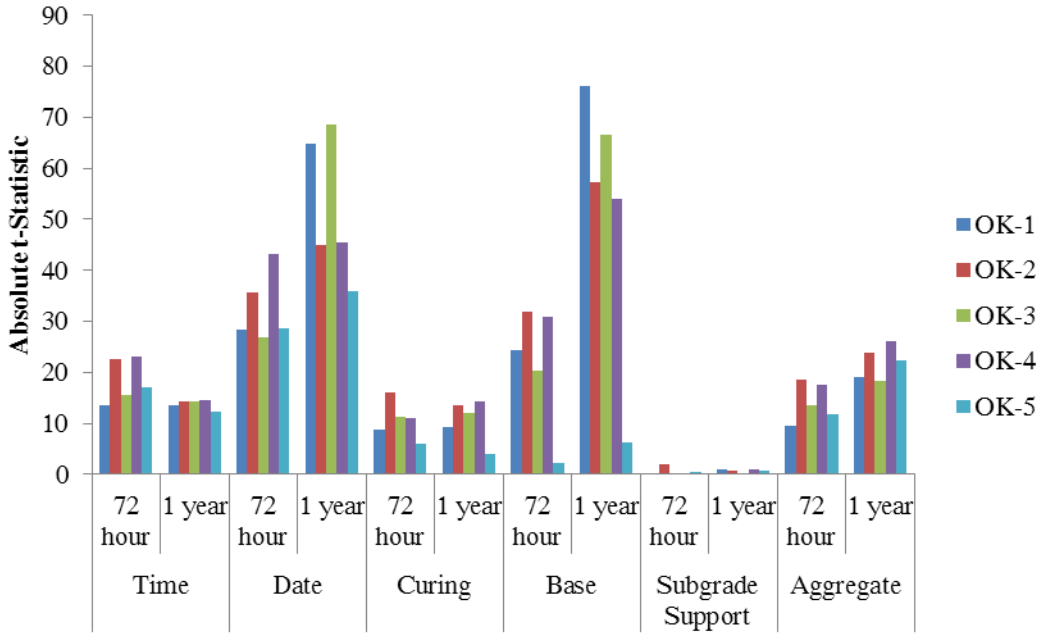

Figure 5.7 Absolute t-Statistic for the Average Crack Spacing Standard Deviation at 72 Hours and 1 Year

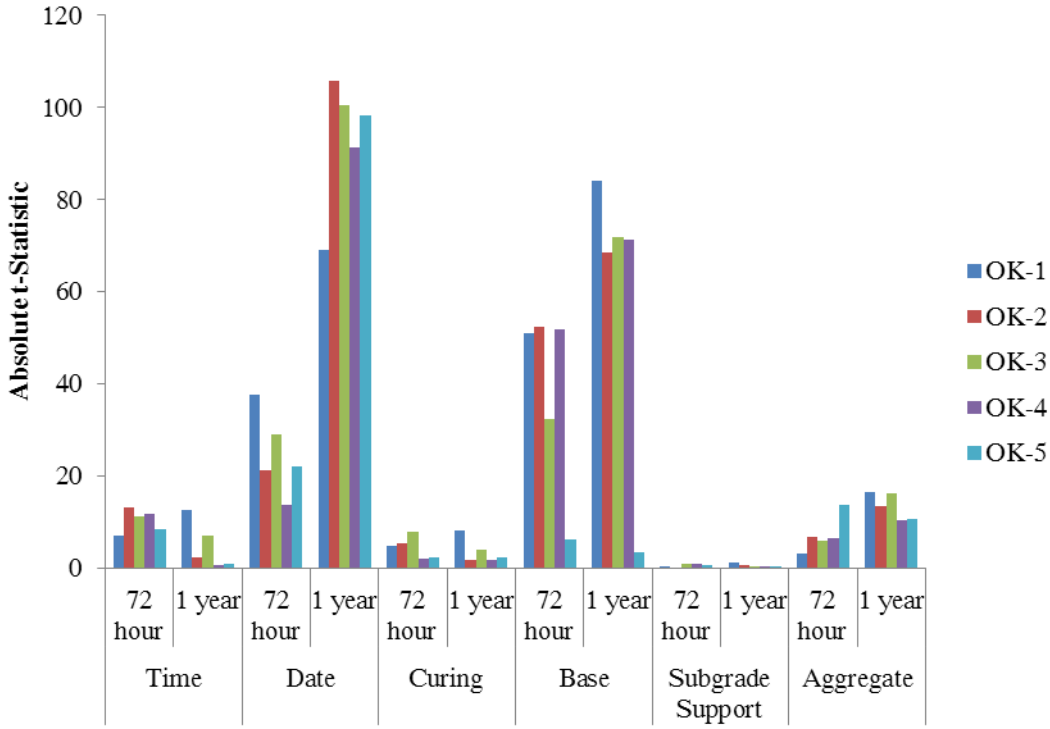

Figure 5.8 Absolute t-Statistic for the Average Crack Width at 72 Hours and 1 Year

The input variables were categorized as either having no effect, moderate effect, or large effect based on the absolute t-statistic value. Input variables were classified as having a moderate effect if the t-value was between the critical t-value for the number of samples considered and 40, and as a large effect if the t-value was above 40. Table 5.6 shows the classifications for each variable at 72 hours, while Table 5.7 shows the classifications for each variable at 1 year. Detailed results are given in Appendix B and C.

Table 5.4 Input Variable Sensitivity Classification at 72 hours. White = Not Statistically Significant Difference, Gray = Moderate Effect, Black = Large Effect.

Output	Variable	OK-1	OK-2	OK-3	OK-4	OK-5
Average Crack Spacing	Construction Time					
	Construction Date					
	Curing Method					
	Subbase Material					
	Subgrade Support					
	Aggregate Type					
Average Crack Spacing Standard Deviation	Construction Time					
	Construction Date					
	Curing Method					
	Subbase Material					
	Subgrade Support					
	Aggregate Type					
Average Crack Width	Construction Time					
	Construction Date					
	Curing Method					
	Subbase Material					
	Subgrade Support					
	Aggregate Type					

Table 5.5 Input Variable Sensitivity Classification at 1 year. White = Not Statistically Significant Difference, Gray = Moderate Effect, Black = Large Effect.

Output	Variable	OK-1	OK-2	OK-3	OK-4	OK-5
Average Crack Spacing	Construction Time					
	Construction Date					
	Curing Method					
	Subbase Material					
	Subgrade Support					
	Aggregate Type					
Average Crack Spacing Standard Deviation	Construction Time					
	Construction Date					
	Curing Method					
	Subbase Material					
	Subgrade Support					
	Aggregate Type					
Average Crack Width	Construction Time					
	Construction Date					
	Curing Method					
	Subbase Material					
	Subgrade Support					
	Aggregate Type					

Several trends were noted in the average crack spacing for the different variables. Changing the placement time from 7:00 a.m. to 3:00 p.m. increased the average crack spacing by 30 to 37%, whereas at 1 year it only increased it by 2-5%. This is because at 72 hours the restraint stresses are much more dominated by the thermal stresses caused by the diurnal temperature change. Whether the concrete sets while the ambient temperature is increasing or decreasing can either amplify or reduce the early age thermal tensile stresses (Riding et al., 2009). At one year, the cracking is

dominated by drying shrinkage and the difference in between the concrete temperature at setting and the lowest concrete temperature reached during the winter, which is the maximum thermal tensile stress. This was seen in the placement date data, where concrete placed in the summer months experienced higher temperatures during curing and much more cracking at 72 hours and 1 year.

Curing was seen to have a modest impact on cracking at 72 hours, with only a small difference seen at 1 year. The subbase material increased the cracking with an increase in the surface roughness, especially at one year, because of the higher amount of friction restraint provided. This shows the value of having a good bond breaker that will not restrain the concrete pavement from shrinking. Subgrade support was seen to have no effect on the early-age or long term cracking for pavements without traffic. This is because the stresses from restrained movement are perpendicular to the subgrade support. ***From the inferences of matched pairs analysis, the concrete placement date was seen to have the largest effect on the 72 hour crack spacing. At 1 year, the construction date and base material friction had the largest impact on the crack spacing and width.***

5.7 Concrete Temperature Development

This was explored by modeling the pavement temperature under different conditions to see how the concrete pavement temperature development. The ConcreteWorks software package was used to understand the variation of temperature along the depth of concrete for concretes with different construction conditions (Riding, 2007). For these sites, four construction parameters were changed to understand their effect on variation of temperature along the depth of concrete pavement. These four parameters were: construction date, construction time, coarse aggregate type and curing method.

For each site, pavements were modeled with placements on Jan 12, July 26, and Oct 22. Construction times modeled were 7 A.M, 10 A.M and 3 P.M. Limestone, granite and siliceous gravel were used as coarse aggregate in the concrete mixtures. The four curing methods used were no curing, Single Coat Liquid Curing Compound (SCLCC), Double Coat Liquid Curing Compound (DCLCC) and Plastic Sheeting (PS). The curing

methods change the surface solar absorptivity and emissivity. Single coat and double coat curing compounds are assumed to have the same surface absorptivity and emissivity properties. This will cause these curing methods to have the same temperature in the simulations, however the concrete cured with a double coat of curing compound should be assumed to have less drying shrinkage during early ages. A total of 540 combinations of inputs were run for these three construction dates, three construction times, three aggregate types, four curing methods, and five sites. Similar trends were seen for the five OK sites.

To see the effect of each factor on variation of temperature with time at the mid-point of the concrete pavement, several graphs were drawn. The concrete placement time did have a significant effect on the temperature after placement, as shown in Figure 1. For the concrete temperatures shown in Figure 5.9, the pavements were modeled using siliceous gravel as the coarse aggregate, no special curing, and placed on July 26. The temperature development during the first 24 hours is the most critical for reducing early cracking and low cracking spaces. High temperatures at time of set mean that the concrete has to change temperature more to return to ambient temperature. This change in the temperature based on placement time confirms the change in cracking distance found in the HIPERPAV modeling.

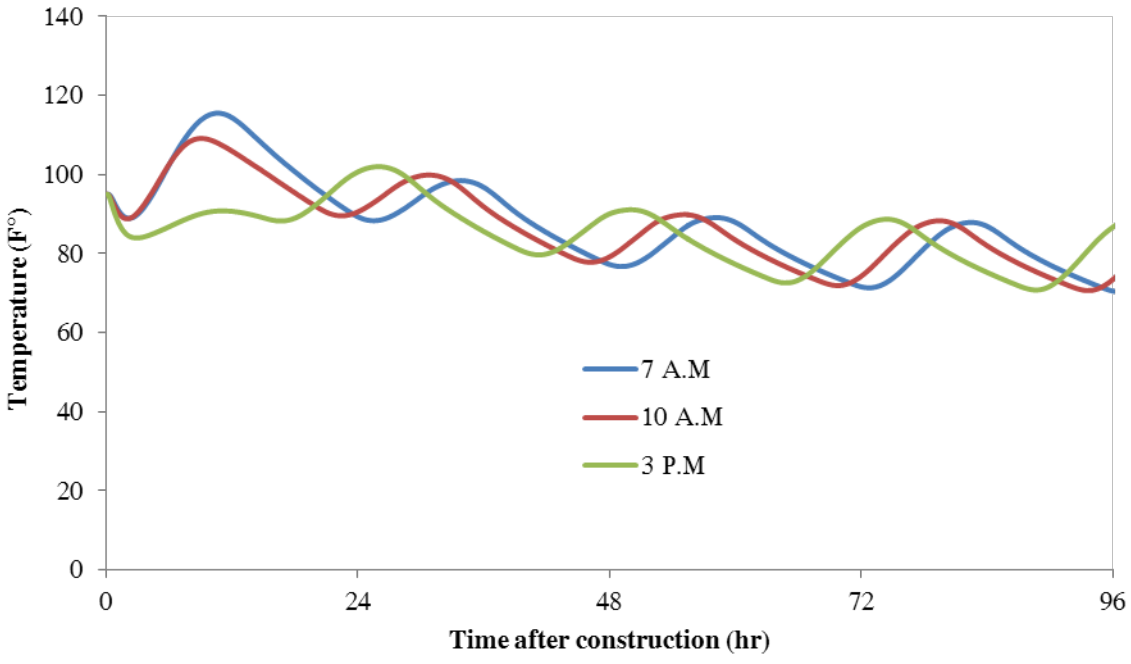

Figure 5.9 Variation of temperature at the mid-point for three different construction times

The time of year the concrete was placed makes a big difference in the temperature development as seen in Figure 5.10. The concrete placed in July showed over 36°F temperature drop between the peak temperature after placement and the end of the first week. The concrete placed in October had a temperature drop from peak after placement had a temperature drop even less than 27°F while the temperature drop for the concrete placed in January was even lower. This confirms the moderate and large differences seen in cracking at 72 hours. The temperature drop from concrete placement at setting seen in July will be much larger than that seen for the January and October placements. Stress development normally begins at the time of set. For time of set occurring at a constant maturity, the July concrete placement, the concrete temperature was approximately 93°F. During the winter, this temperature has to drop to the same freezing temperatures experienced by the pavements placed at other times of the year, resulting in a larger drop in temperature. Assuming that the concrete pavements all reach the same low temperature in the winter for all paving seasons, the pavement placed in July would have to cool 19°F more than the pavement placed in October, and 37°F more than the pavement placed in January. This large and significant difference in crack spacing seen with pavement placement dates can help explain the large temperature differences modeled.

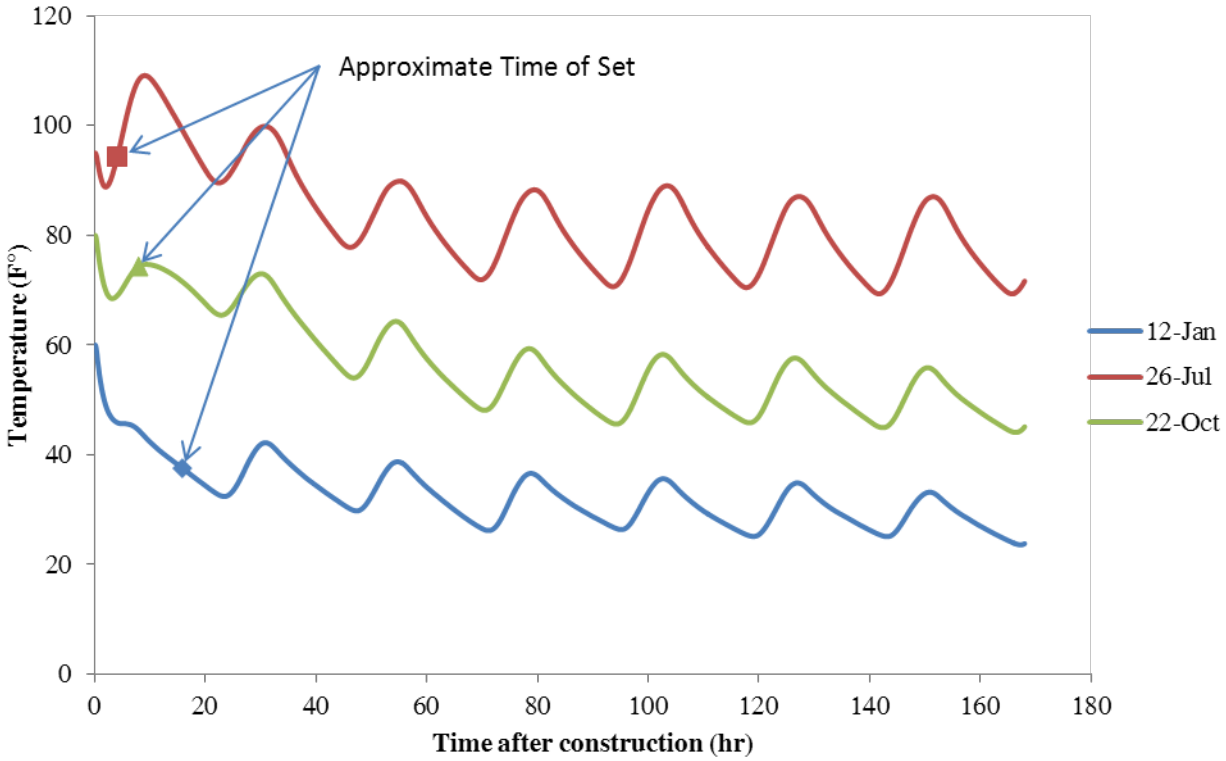

Figure 5.10 Variation of temperature at the mid-point for three different construction dates

Very little temperature difference was seen for the concrete pavement placed using different types of aggregates as seen in Figure 5.11. Although the specific heat and thermal conductivity of the concrete containing the different coarse aggregates was different, the difference did not have a large effect on the temperature development. The difference seen between the pavement cracking based on aggregate is instead because of the difference in the aggregate coefficient of thermal expansion. This higher amount of free shrinkage for every degree in temperature drop translates into higher stresses when the pavement is restrained in a CRCP by the subbase. It is recommended to consider the aggregate coefficient of thermal expansion when selecting concrete materials to make sure that the concrete coefficient of thermal expansion matches that used in the design.

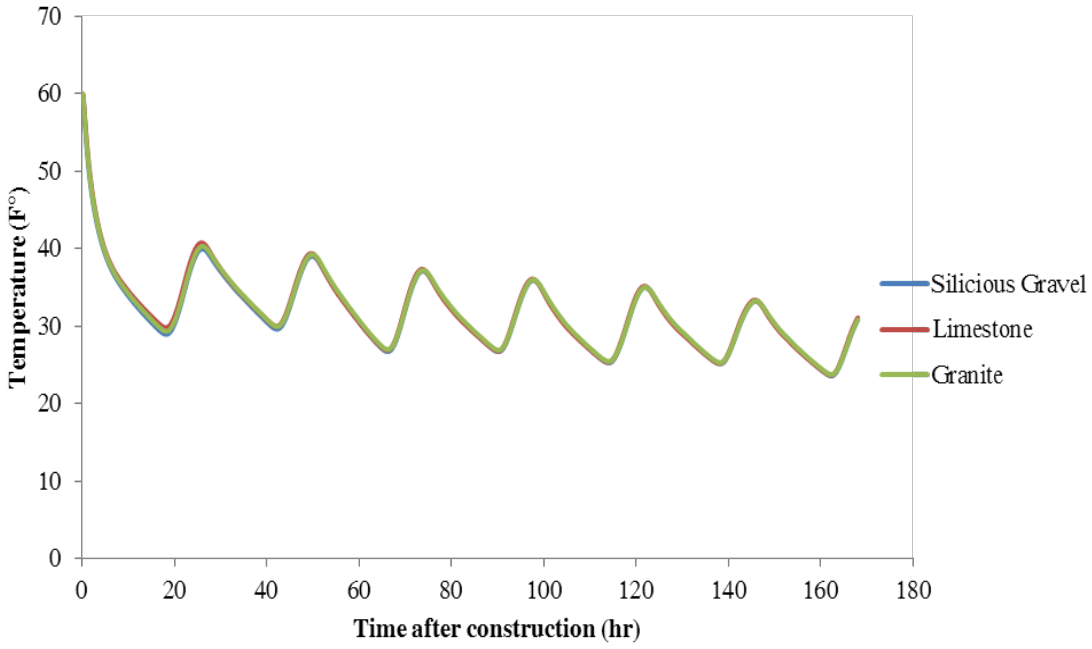

Figure 5.11 Variation of temperature at the mid-point for three different types of aggregate

A change in the curing method did change the temperature development some as shown in Figure 5.12, but only a small amount. Figure 5.12 shows the temperatures calculated for concrete pavement with different curing methods at the OK1 site, and placed at 10 A.M. on July 26th. The increased cracking at early ages is most likely a combination of the change in temperature from the change in surface heat transfer properties and a change in the drying shrinkage from better curing. The small changes seen in the temperature development from curing changes are unlikely to cause much change in the crack pattern because of the rapid stress relaxation during early ages.

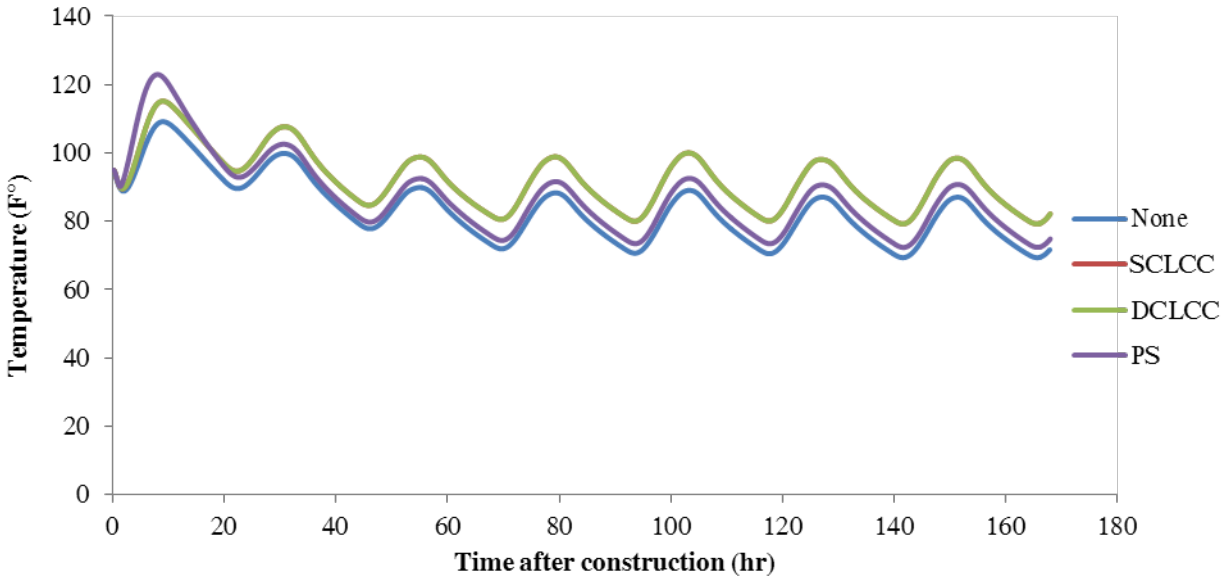

Figure 5.12 Variation of temperature at the mid-point for four different methods of curing. SCLCC = Single coat liquid curing compound, DCLCC = Double coat liquid curing compound, PS = Plastic shrinkage

5.8 Summary

The HIPERPAV III results show that the concrete placement time and date should be controlled in order to reduce the probability of closely spaced cracks, with afternoon placements in the fall showing less early-age cracking, which should translate into less Y-cracking. The time of placement showed less difference in the cracking at 1 year. The smoothness of the asphalt concrete subbase was shown to have a significant effect on the pavement cracking, especially at 1 year because of the lower degree of restraint on the provided by the subbase.

PAVEMENT STRESS MODELING

6.1 Introduction

Finite element methods (FEMs) were used to model the change in principal stress direction based on design and construction conditions. The modeling was undertaken to determine any changes in stress direction or concentrations that occur from changes in design and construction. It is expected that any changes in the stress magnitude will influence crack spacing and crack initiation time. Changes in the

maximum principal stress direction will cause a change in the crack direction, potentially causing y-cracking. A change in the distribution of the maximum principal stress across the pavement width will also cause cracks to meander and contribute to y-cracking.

The computational model of a pavement was assembled including concrete, subbase, and subgrade. Models were also assembled with areas of differing subbase friction, shoulders, and different amounts of reinforcing steel. The finite element software package used consists of several modules, which enable the complete formulation of the computational model including pavement geometry and mechanical properties. The analysis module performs the finite element calculations and creates an output data base file. The output data base file is then used to access the results and determine changes in the stress distribution and principal stress directions.

6.2 Pavement Structure Finite Element Model

A FEM was built for CRCP pavement structures in Oklahoma. The pavement geometry and layer properties were based on typical values of Oklahoma CRCP. Pavement layers were 3-dimensional, linear elastic layers. The pavement consisted of three layers: 144 in. wide, 10 in. thick concrete pavement (surface layer); a 216 in. wide, 4 in thick asphalt concrete subbase layer; and a 288 in. wide, 36 in thick soil subgrade layer. 78 in. wide, 10 in. thick shoulders were used on some of the simulations to determine the effects of shoulder type on stress distributions in the mainline pavement. Figure 6.1 shows the computational model used in the mainline pavement stress analysis before shoulder placement.

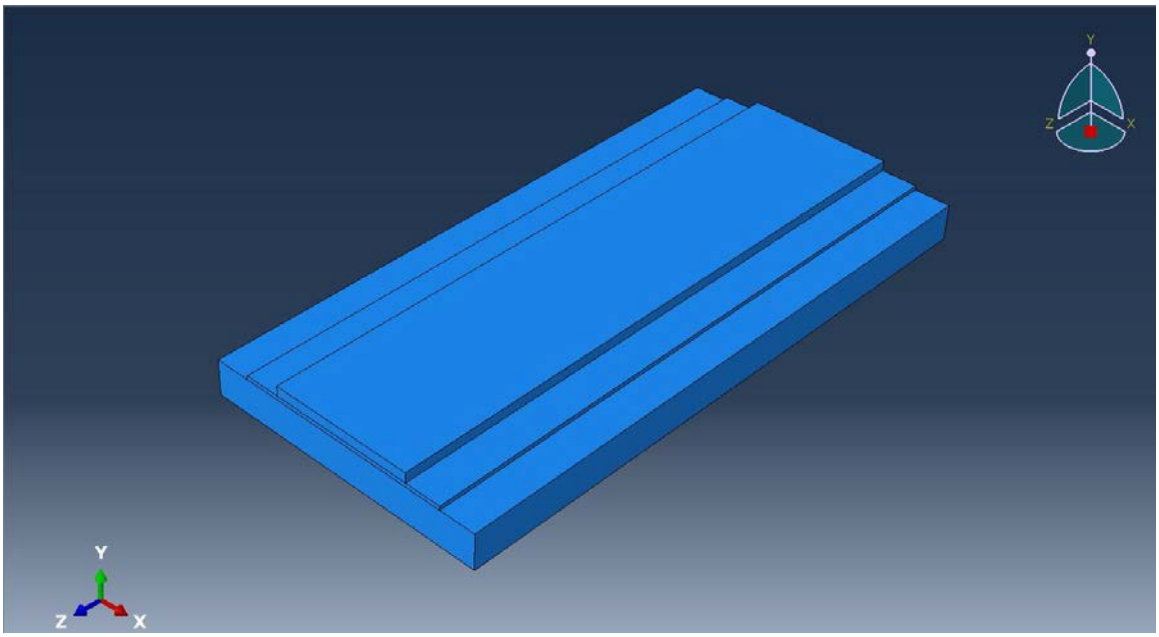

Figure 6.1 Pavement model created by Abaqus/CAE software package

Mechanical and thermal parameters defined for each material were: young's modulus (E), Poisson's Ratio (v), coefficient of thermal expansion (CTE), mass, density and thermal conductivity. Table 6.1 summarizes the layer geometry, mechanical and thermal parameters for each material used in the finite element model.

Table 6.1 Pavement layer geometry, mechanical, and thermal properties

Inputs	Pavement (Concrete)	Subbase (AC)	Subgrade (Soil)
Young's Modulus E(psi)	3122019	435000	4000
Poisson's Ratio	0.17	0.4	0.3
Coefficient of Expansion CTE(1/F`)	6.00E-06	1.38E-05	5.00E-06
Mass Density (lb/ft^3)	145	150	106
Thermal Conductivity(Btu/in.hr.F`)	0.0616	0.0361	0.0385
Length(inch)	600	600	600
Width(inch)	144	216	288
Thickness(inch)	10	4	36

Two interactions were created for these three layers in the model. The friction coefficient between the pavement layer and subbase layer was varied between 1 and 20 (unitless), with the results from the 1 and 20 values shown as the lower and upper friction bounds. These friction coefficients account for the friction provided by the surface roughness and the cohesion between the two surfaces, which is why they may appear higher than that expected for surface roughness alone. A surface-to-surface contact with a friction coefficient of 20 was defined for the interaction between the pavement and subbase layers. Another interaction was defined using the same procedure with a friction coefficient of 20 for the interaction between the subbase and subgrade. Figure 6.2 shows the location of the interactions between the pavement and subbase. Figure 6.3 shows the location of the friction interactions between the subbase and subgrade.

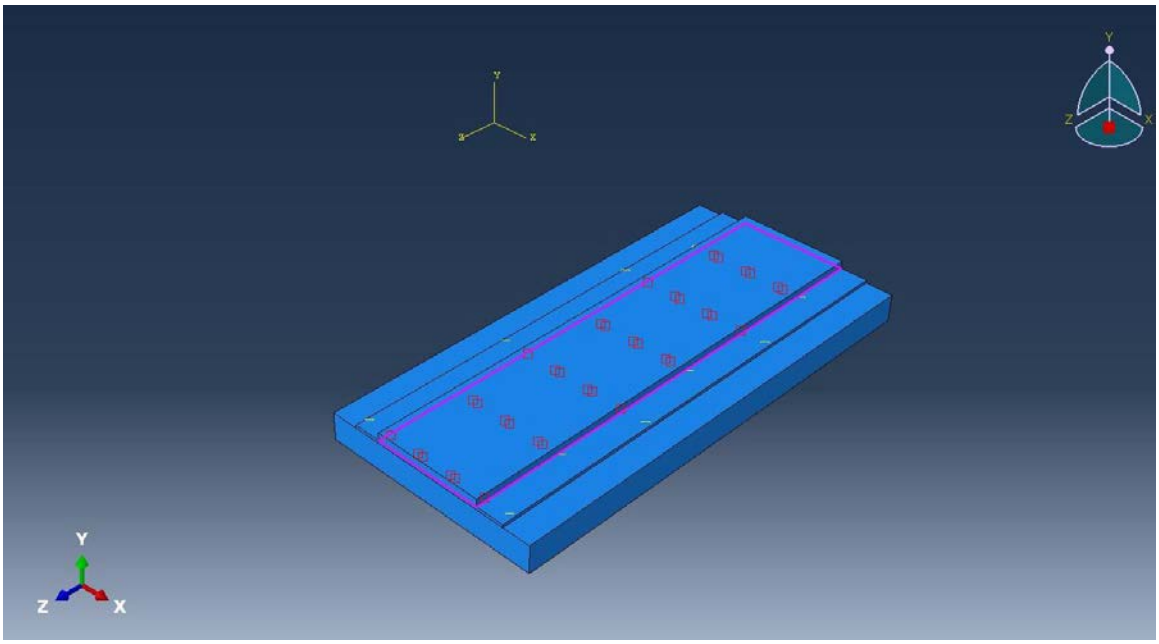

Figure 6.2 - Friction interaction location between pavement and subbase

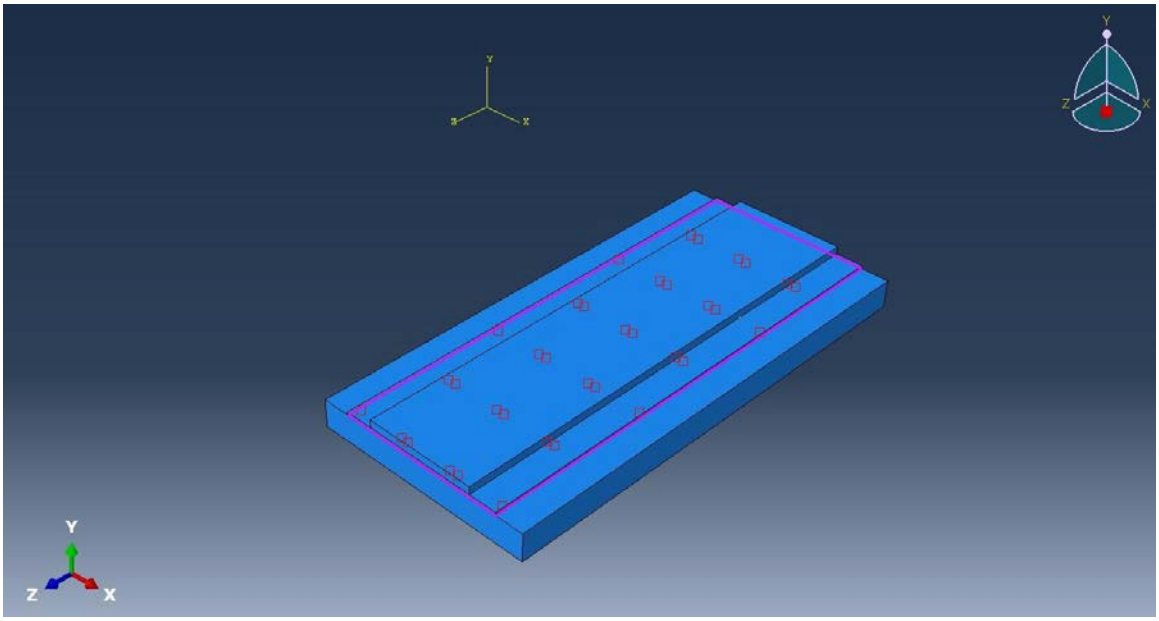

Figure 6.3 - Friction interaction location between subbase and subgrade

The bottom of the subgrade was fixed against displacement in all directions and rotation as shown in Figure 6.4. Subgrade sides were restrained against displacement in the transverse and longitudinal directions as shown in Figures 6.5 and 6.6.

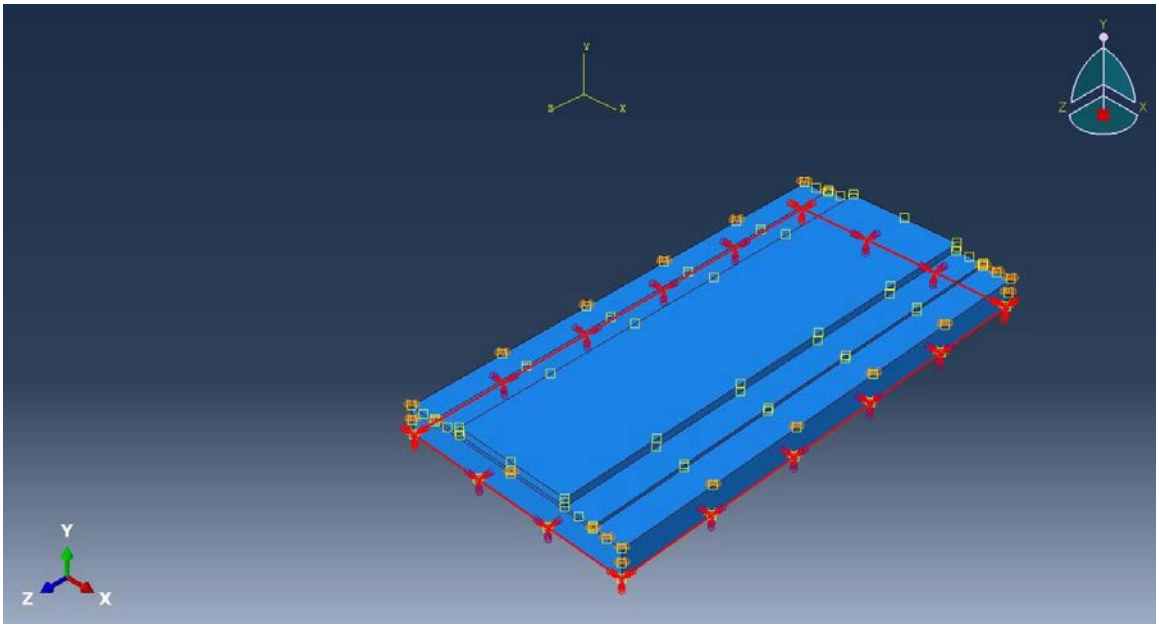

Figure 6.4 - Boundary conditions at the bottom of the subgrade

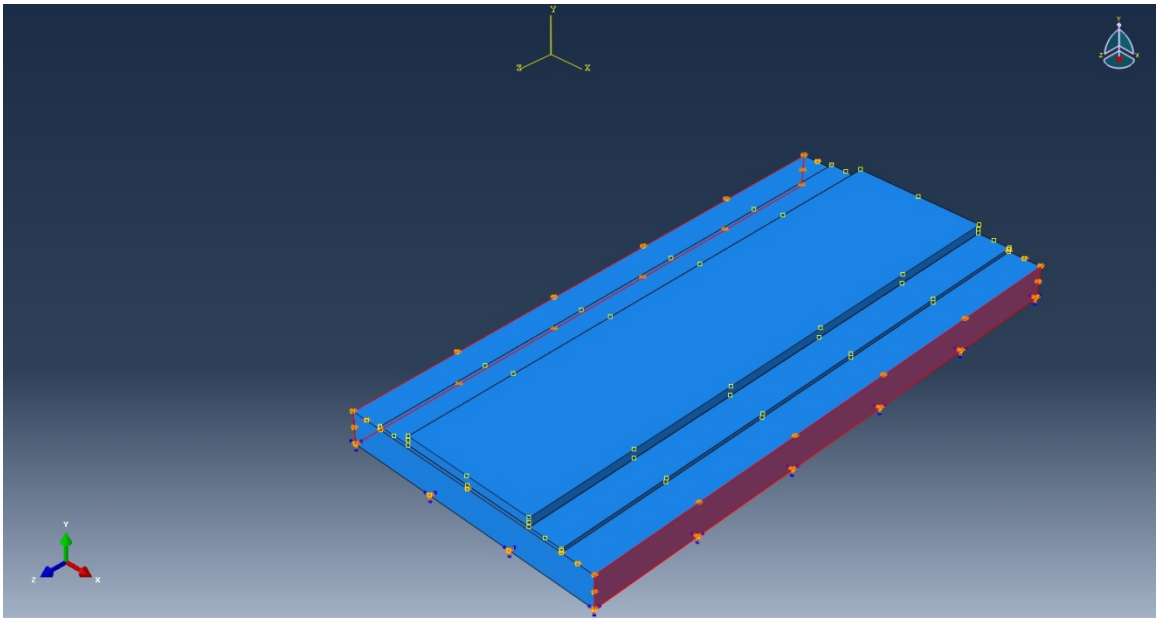

Figure 6.5 - Boundary conditions on the subgrade longitudinal direction sides

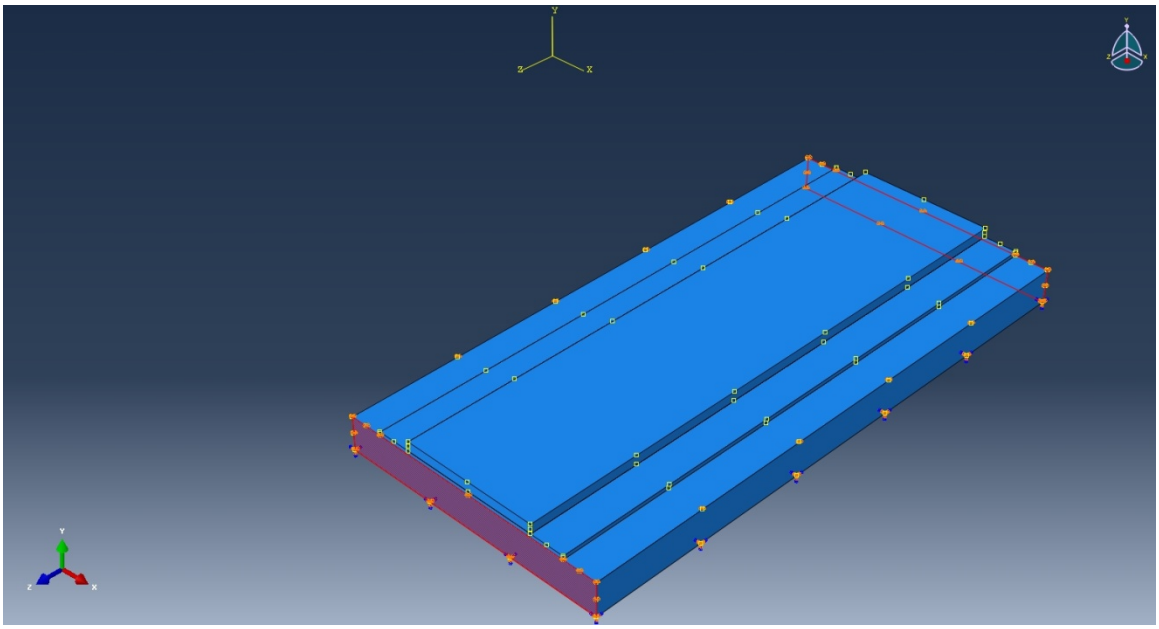

Figure 6.6 - Boundary conditions on the subgrade transverse direction sides

The gravity load was applied uniformly to the whole model. The gravity load with a vertical acceleration component of 386 in/s^2 was applied downward to the whole model as shown in Figure 6.7. It is essential to apply the gravity load to ensure that the friction between layers is engaged. A temperature decrease of 50^{o}F was applied to concrete pavement while the temperature underneath the pavement was kept constant. This temperature loading was used to simulate the effects of drying shrinkage and temperature change seen by the pavement and not by the subbase and subgrade. The primary purpose of this modeling is to determine the stress distribution patterns. This will show if there are locations that are prone to higher densities of cracks or cracks with a tendency to change direction for crack branching.

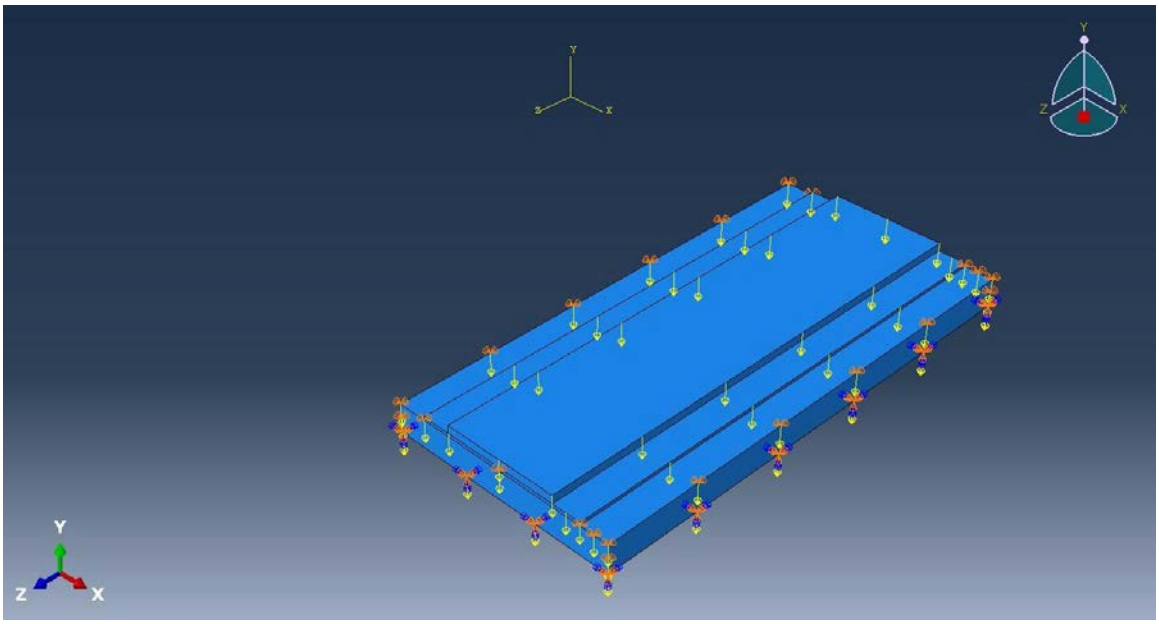

Figure 6.7 - Gravity load applied uniformly to the pavement and substructure

Coupled Temperature-Displacement elements were used in this finite element model. Automatic meshing was used to generate the model elements, referred to as the model mesh, that were used to numerically build the pavement and simulate the stress distributions. Figure 6.8 shows the finite element mesh used for the mainline pavement section. This mesh was used for all three layers in model. The number of elements used for the pavement (surface layer), subbase, and subgrade were 4,800, 3,600 and 28,800 respectively.

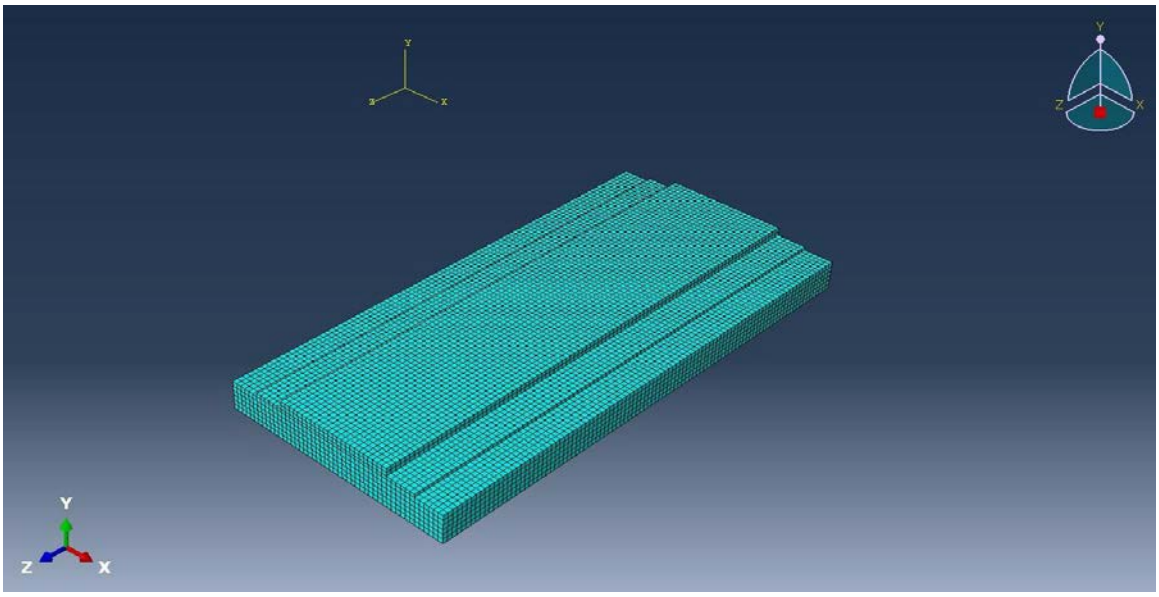

Figure 6.8 - Mainline pavement lane model mesh

Load was applied in two steps: 1) gravity load, 2) thermal load in the presence of gravity. A graphical display of normal stresses in longitudinal direction (S33) is shown in Figure 6.9. The S11, S22, and S33 stresses are the normal stresses in the x, y, and z directions. The stresses in the S11 and S33 stresses were low compared to the S33 direction. Figure 6.9 shows that tensile stresses developed approximately in the central areas (green areas) whereas compression stresses developed approximately at the top transverse edges (blue areas). Also, the stress magnitude in the middle of the pavement was the largest and decreased towards the ends (in the longitudinal direction). Since there was a high tensile stress halfway between the two longitudinal ends, the probability of cracking in the central areas was higher than transverse edges of the pavement. The friction between the pavement and the subbase provides restraint to the pavement natural volume change that would occur from a temperature change or drying shrinkage. When the pavement undergoes volume change, the pavement's natural unstressed position consequently changes. Since the pavement ends are prevented from moving all of the way to their new natural unstressed location by the friction with the subbase, stresses are generated in the pavement. The stresses build up in the pavement moving away from the end to the very high stresses that occur in the

middle of the pavement. The longer the distance between a point on a pavement and the pavement end, the larger the restraint provided and consequently the larger the stresses. Figure 6.10 shows the calculated stress in the pavement longitudinal direction along the length of the pavement. Figure 6.11 shows how the stresses build up in the pavement as the pavement moves away from the free end.

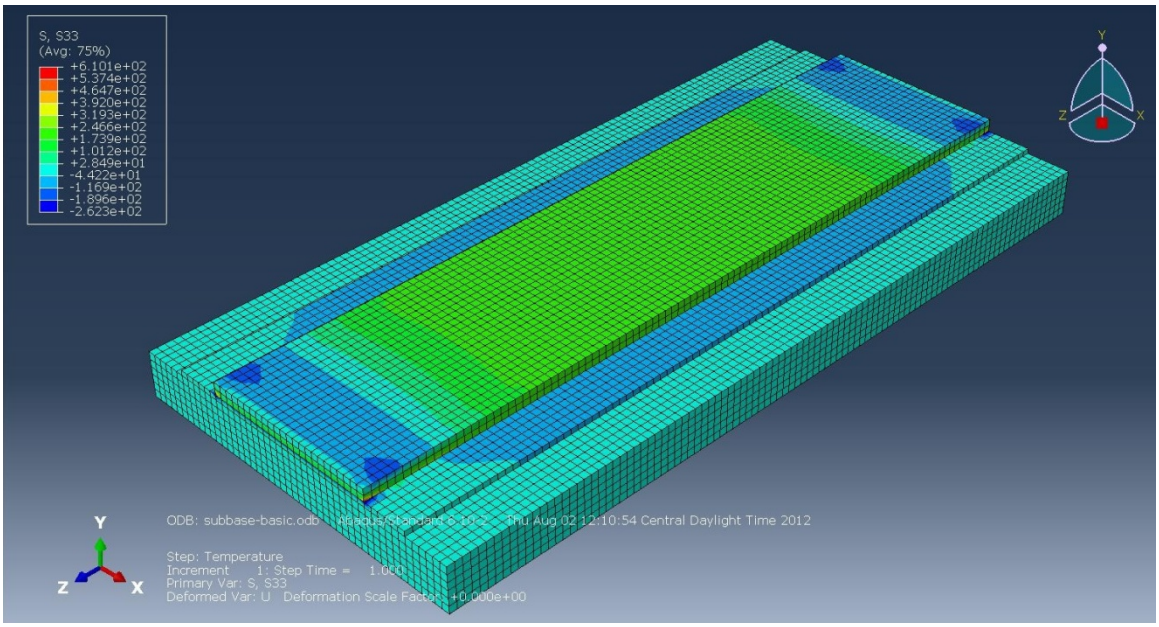

Figure 6.9 Distribution of normal stress in the longitudinal direction (S33)

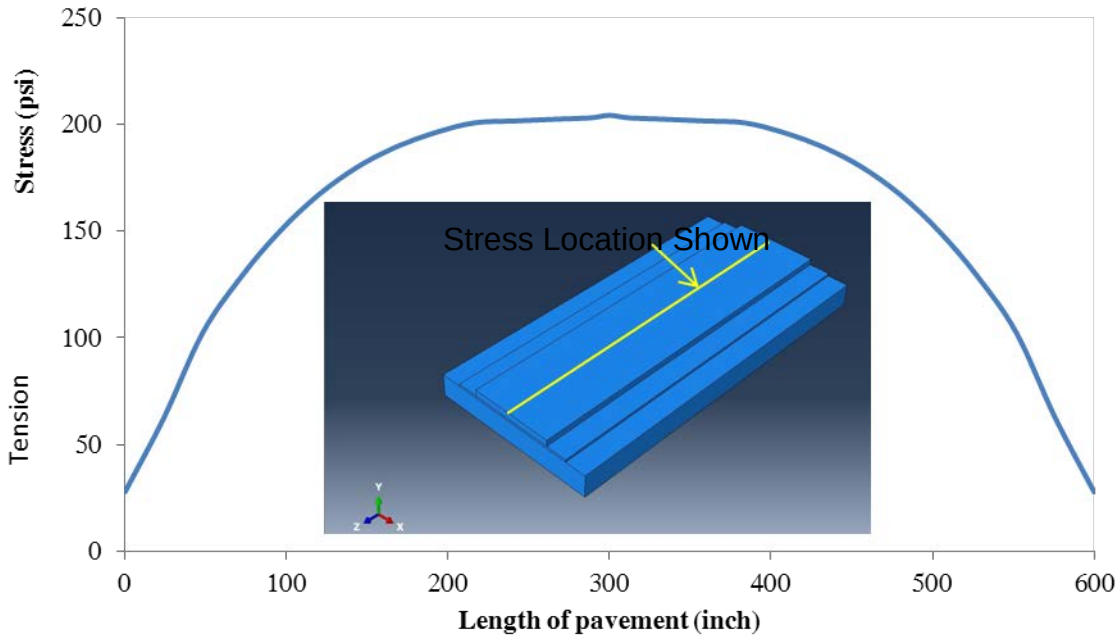

Figure 6.10 Pavement stress in the longitudinal direction (S33) along the length of the pavement

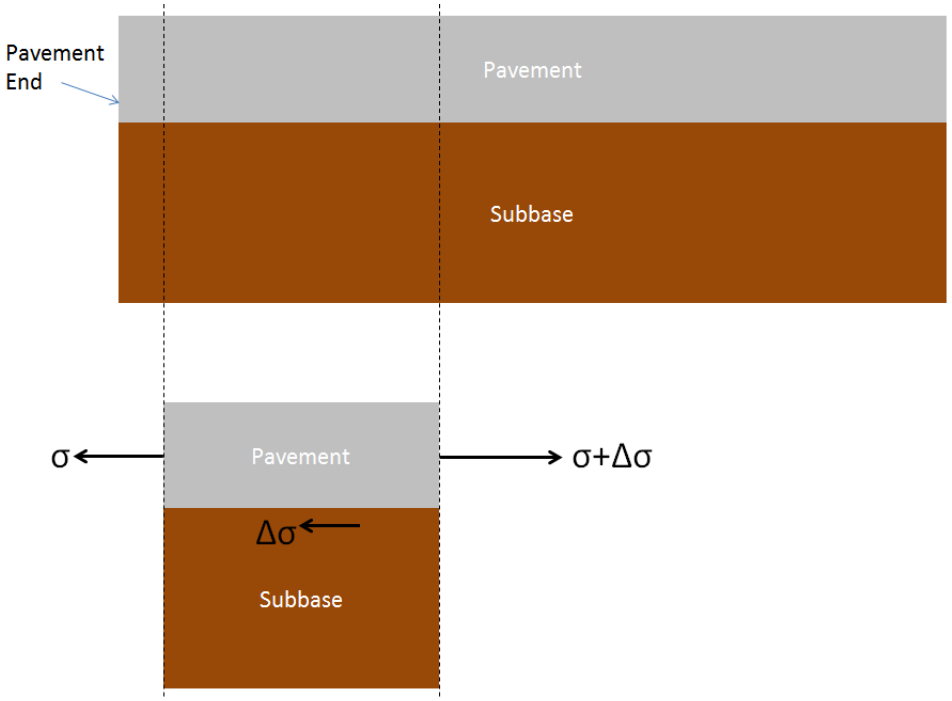

Figure 6.11 Pavement section showing how pavement stresses build up from subbase friction restraint

Distributions of stresses and displacements induced by the temperature reduction in the pavement were obtained by sampling the stresses along the transverse directions in the middle and at the edge, shown in Figure 6.12.

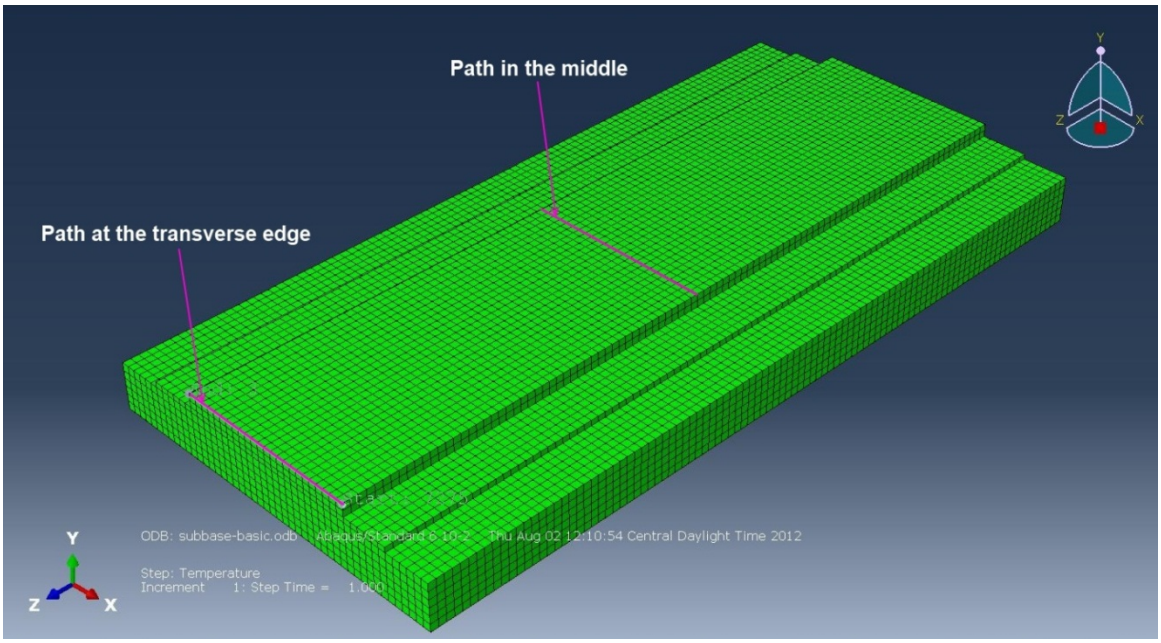

Figure 6.12 Path examined for stress at the pavement middle and transverse edge

Figure 6.13 shows the distribution of normal stresses in the transverse direction (S11) and longitudinal direction (S33) along the width of the pavement in the middle of the pavement section. As seen, the stress in the transverse direction (S11) was symmetric along the width of the pavement and varies from approximately 16 to 70 psi along the width. Stresses in the transverse direction were lower than stresses in the longitudinal direction because of the lower restraint created by the shorter pavement length in the transverse direction. This is because the distance between the middle and edge in the transverse direction is very short. In this 6’ length, the friction cannot fully build up to 100% restraint. This is analogous to having a prestressed concrete beam

that is shorter than twice the prestressed strand transfer length. For the prestressed beam, the distance is too short for all of the prestressed force to transfer to the concrete by strand-concrete bond. Figure 6.14 shows the distribution of longitudinal normal stress (S33) along the width of the pavement at the transverse edge.

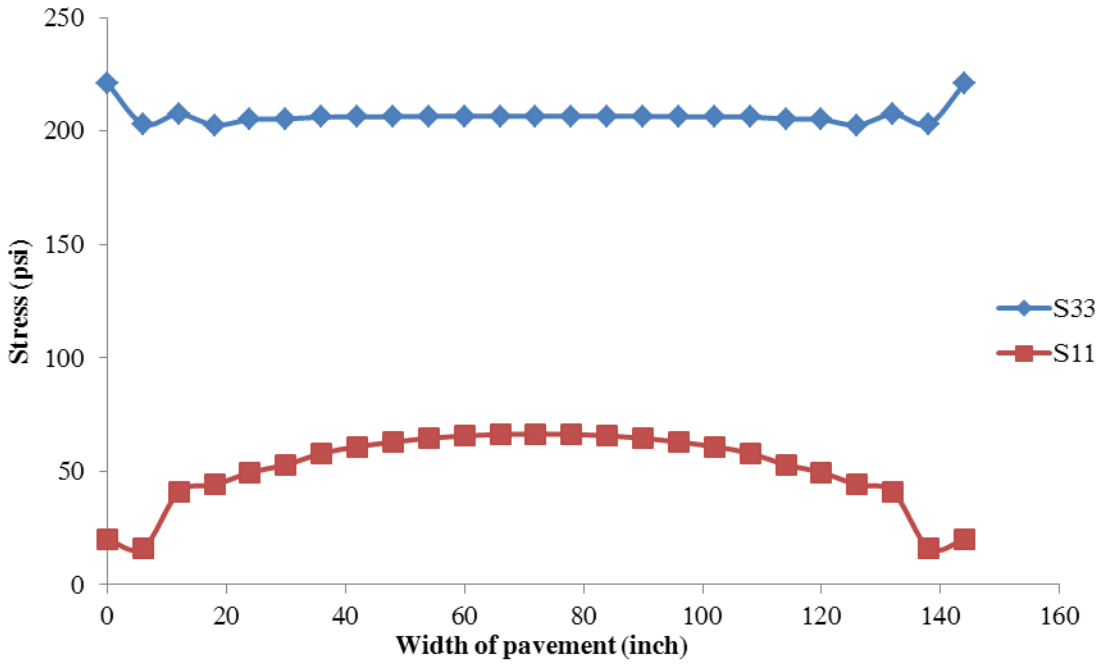

Figure 6.13 Variation of transverse stress S11 and S33 along the width of the middle of the pavement

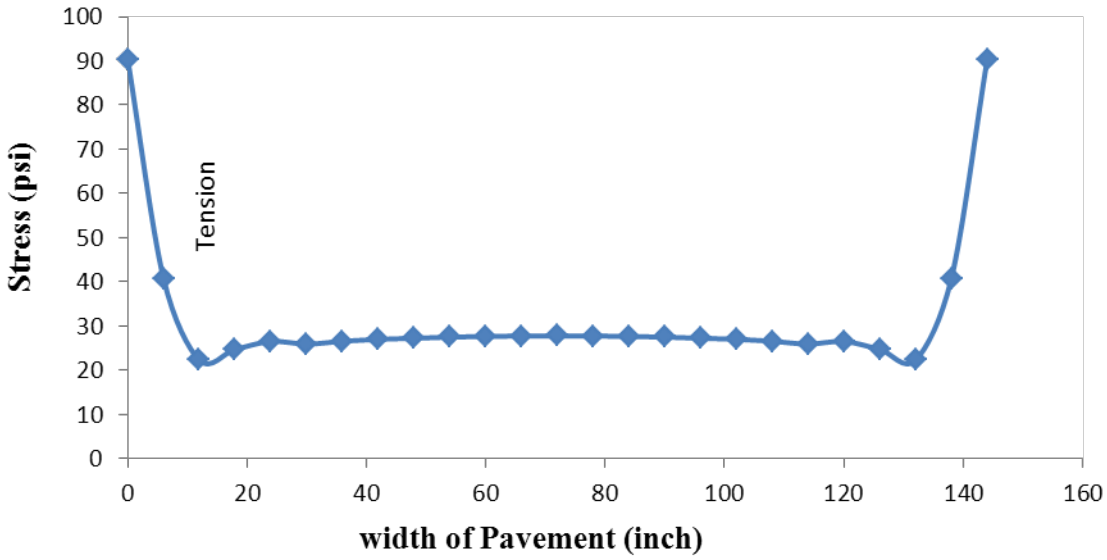

Figure 6.14 Variation of S33 along the width of the transverse edge of the pavement

There is much less of a difference in stress along the pavement width in the longitudinal direction than in the transverse direction. The stresses in the longitudinal direction are also higher, notably because of the higher amount of restraint provided by the pavement length in contact with the subbase in the longitudinal direction. The S33 stresses are symmetric along the width of the pavement, as expected because of the symmetric pavement modeled. Figure 6.15 shows that pavement displacement in the transverse direction (U1) is constant along the length of the pavement.

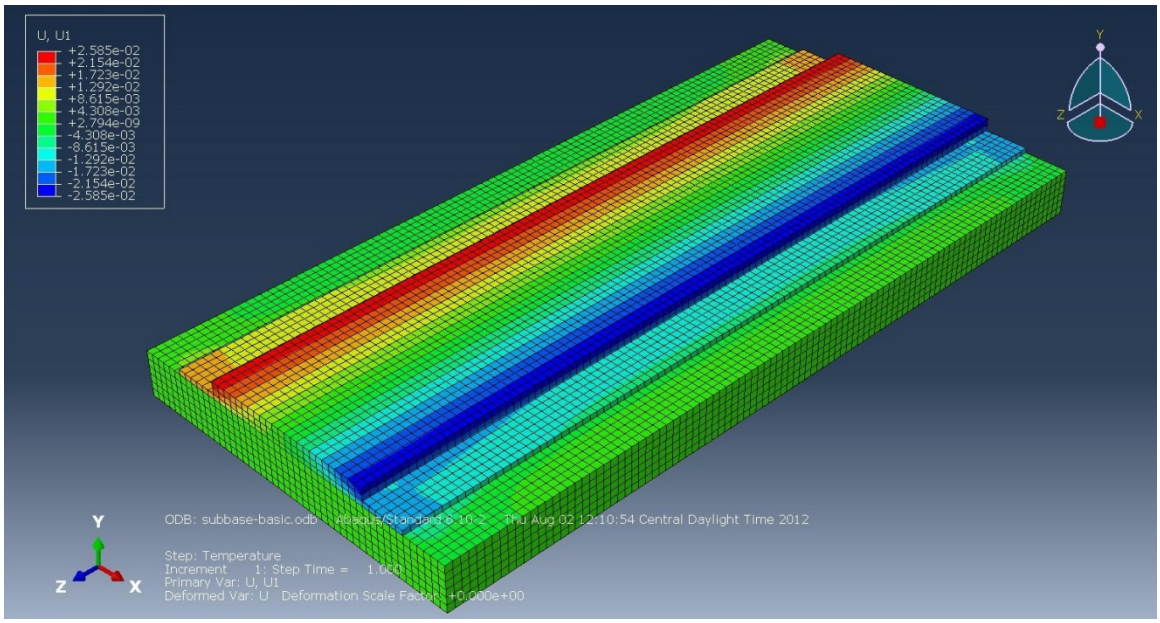

Figure 6.15 Color map of U1 in whole pavement model

6.3 Effect of Localized Changes in the Layer Interfaces

A localized change in friction between the concrete and supporting layers was modeled to determine how subbase construction uniformity could affect y-cracking. The impact of this change in subbase uniformity on the maximum principal stress direction was studied by varying the changed friction area size, location, and friction coefficient (FC).

6.4 Changed Friction Section Location

Areas of different interface frictions were placed at two different locations in the pavement: an area at the corner of the pavement and an area at the longitudinal edge in the middle of the pavement. Figure 6.16 shows the location of changed friction areas at the corner and middle of the pavements.

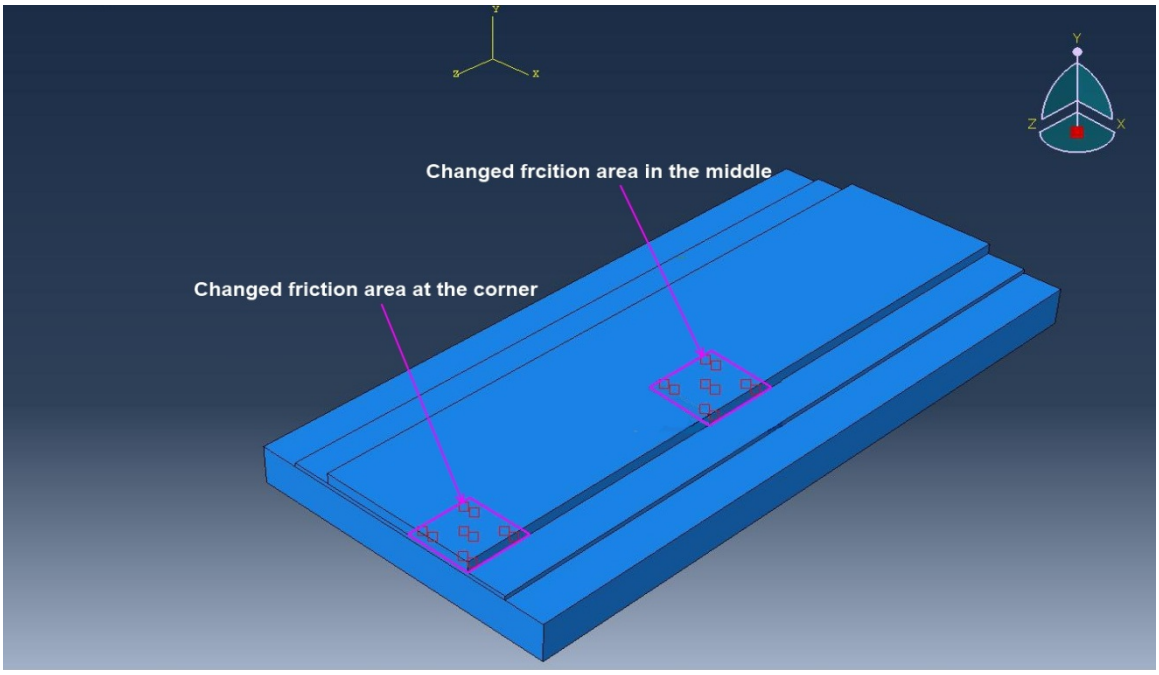

Figure 6.16 Changed friction area at the longitudinal edge in the pavement middle and corner

Changed friction area sizes used were 3’ x 3’, 5’ x 5’ and 7’ x 7’. The friction coefficient (FC) of interaction between the pavement and subbase for all changed friction areas was 1, while the FC was 20 for the interaction between the rest of the pavement and subbase. Normal stresses in the transverse direction (S11) were sampled across the width of the pavement. Figure 6.17 shows the distribution of the transverse direction stresses (S11) at the edge of the changed friction area for these areas located at the corner. Figure 6.18 shows the change in S11 at the halfway point between the two ends for changed friction areas at the longitudinal edge in the middle of the pavement section.

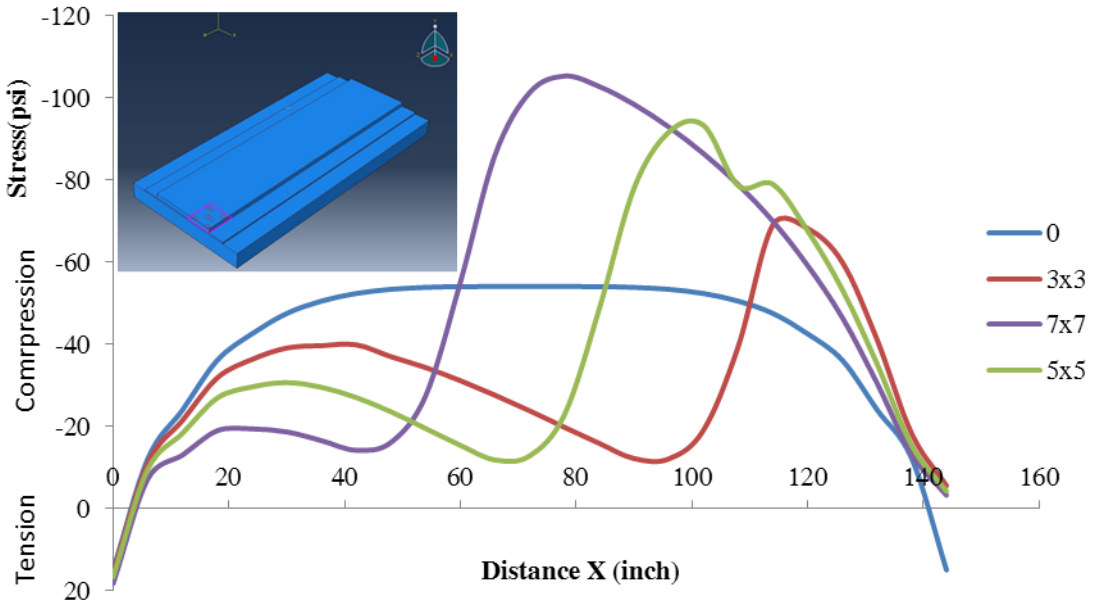

Figure 6.17 Distribution of S11 for changed friction areas at the corner (FC-Area=1 and FC-Rest of the Pavement=20).

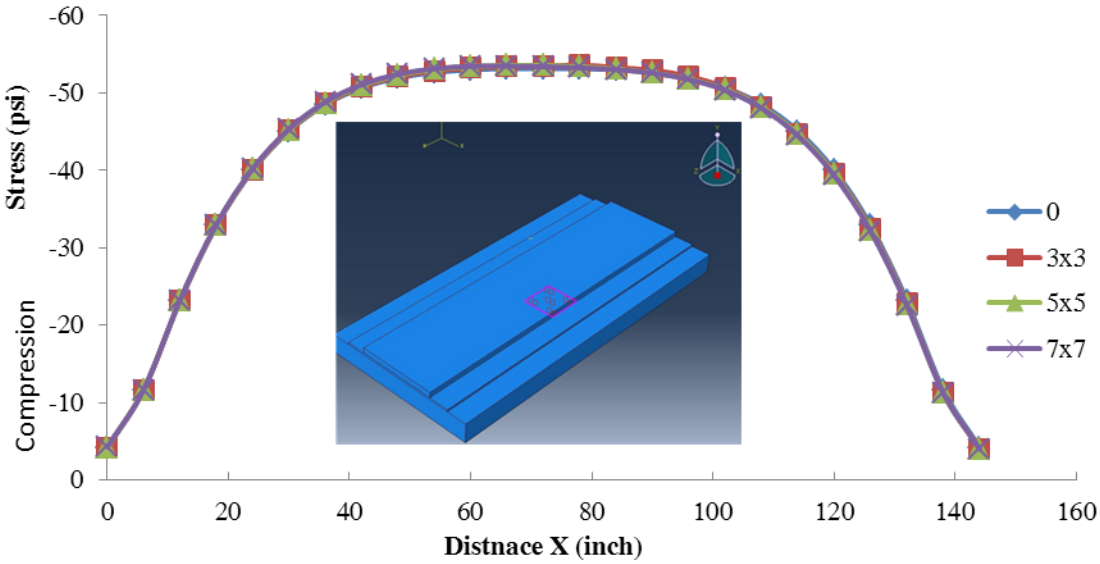

Figure 6.18 Distribution of S11 for changed friction areas placed halfway between two ends (FC-Area=1 and FC-Rest of the Pavement=20)

A change in the friction at the corner had a large effect on the stress magnitude and direction at the edge of the area. An area with different friction placed halfway

between the pavement ends did not significantly change the pavement stress state. As seen in Figure 6.17, the changed friction area size has a large effect on the stress magnitude when the area is near the transverse edge of the pavement. When the changed friction area location is near the middle of the section in the longitudinal direction however, the transverse stresses did not change significantly. This occurs because at the end of the pavement, a change in the friction coefficient would have a large effect on the amount of volume change converted to stress by the restraint. In the pavement middle section the pavement has already reached a high degree of restraint close to 100% restraint from the friction provided by the pavement on both ends, limiting the effect of a change in friction in middle.

6.5 Effect of Changed Friction Section Size and Friction Coefficient

Four models were run to understand the effect of changed friction area size and friction coefficient (FC) on how the direction of maximum principal stresses varies across the width of the pavement. To determine the effects of changed friction area size on stress magnitude and direction, the changed friction area size was changed for the area at the corner. The friction coefficient for the area was then changed for both the 5’ x5’ and 7’x7’ sections as follows:

1- Model with a 5’x5’ changed friction area, area FC=1, FC=20 for the rest of the pavement.
2- Model with a 5’x5’ changed friction area, area FC=20, FC=1 for the rest of the pavement.
3- Model with a 7’x7’ changed friction area, area FC=1, FC=20 for the rest of the pavement.
4- Model with a 7’x7’ changed friction area, area FC=20, FC=1 for the rest of the pavement.

The principal stress directions across the width of the pavement at the transverse edge were calculated from the finite element output data. After extracting all six components of stress state from the finite element output data, a stress tensor was assembled for calculation of principal stress directions.

Angles between maximum principal stress direction and the transverse, vertical and longitudinal axis are referred to as α, β, and γ angles, respectively. Figure 6.19

shows the angle between the maximum principal stress and longitudinal axis (γ angle) across the width of the pavement at the transverse edge for the two models with two different sizes of different friction areas.

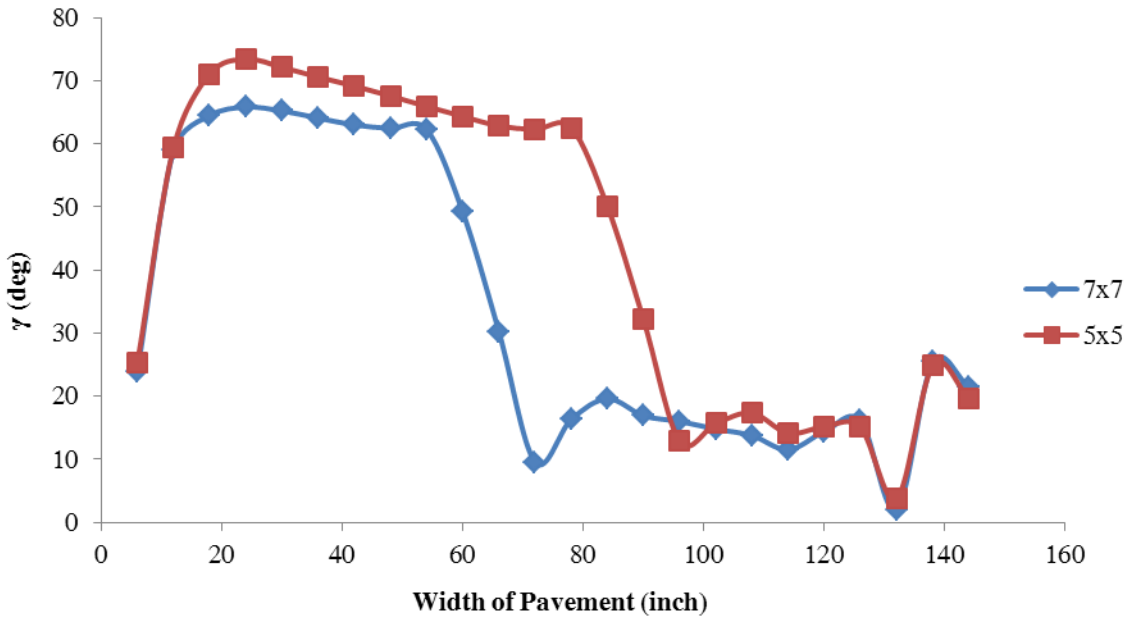

Figure 6.19 Distribution of γ along transverse edge (Area FC=20 and Rest of the Pavement FC=1)

The changed friction areas showed an abrupt change in the principal stress direction at 60 in. for the 7'x7' and at 84 in. for the 5'x 5' areas, corresponding to the edge of each patch. Both areas showed principal stress directions at least 25° from the transverse direction, indicating a high potential for branching cracks and Y-cracking.

Figure 6.20 and 6.21 compare two different models with different friction coefficients for the 7' x 7' areas and 5'x 5' areas, respectively. Figures 6.22 and 6.23 show diagrams for the distribution of γ along the width of the pavement at the transverse edge for the simulations with the mainline pavement FC = 1 and the changed friction area FC=20 for the 5'x5' and 7'x7' changed friction areas, respectively. For these models, FC was changed from 1 to 20, with the friction coefficient for the remaining

pavement changed from 20 to 1. This data shows that a change in friction over a section of the pavement, whether an increase or decrease, will give non-uniform restraint and cause the principal stress direction to meander. A decrease or increase in the pavement friction will cause the meandering to go in opposite directions. Friction coefficients of 1 and 20 were chosen as upper and lower bounds. The amount of meandering will depend on the relative difference in friction coefficient between the pavement and an area of different subbase properties. It appears that a key to preventing y-cracking is subbase surface uniformity.

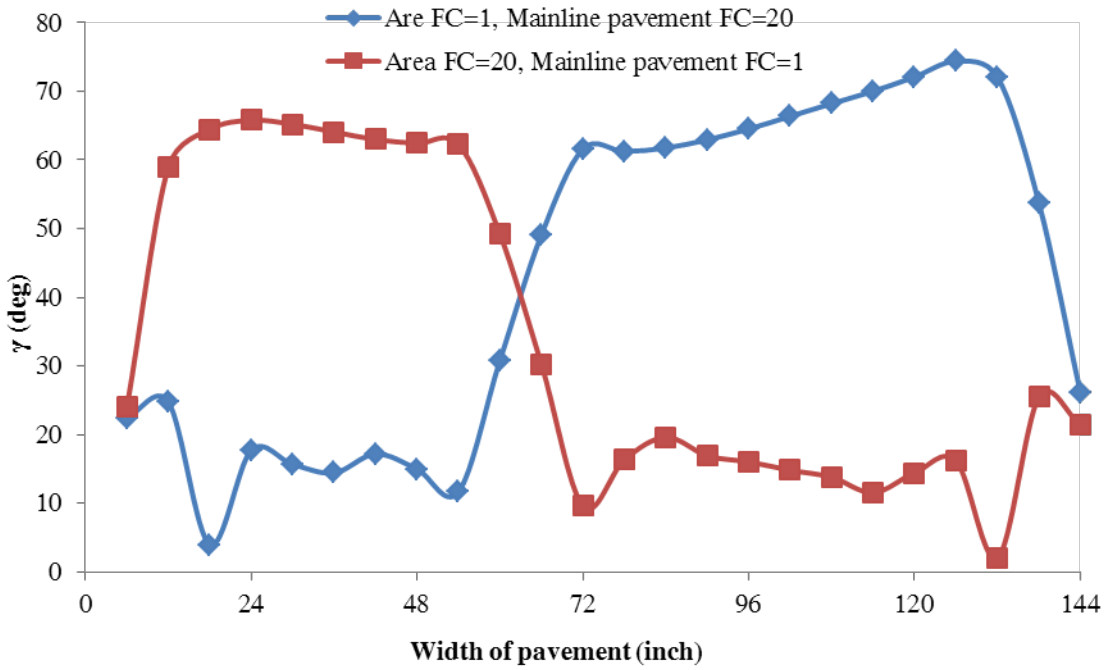

Figure 6.20 Distribution of γ along transverse edge (Area FC=20 and Rest of the Pavement FC=1)

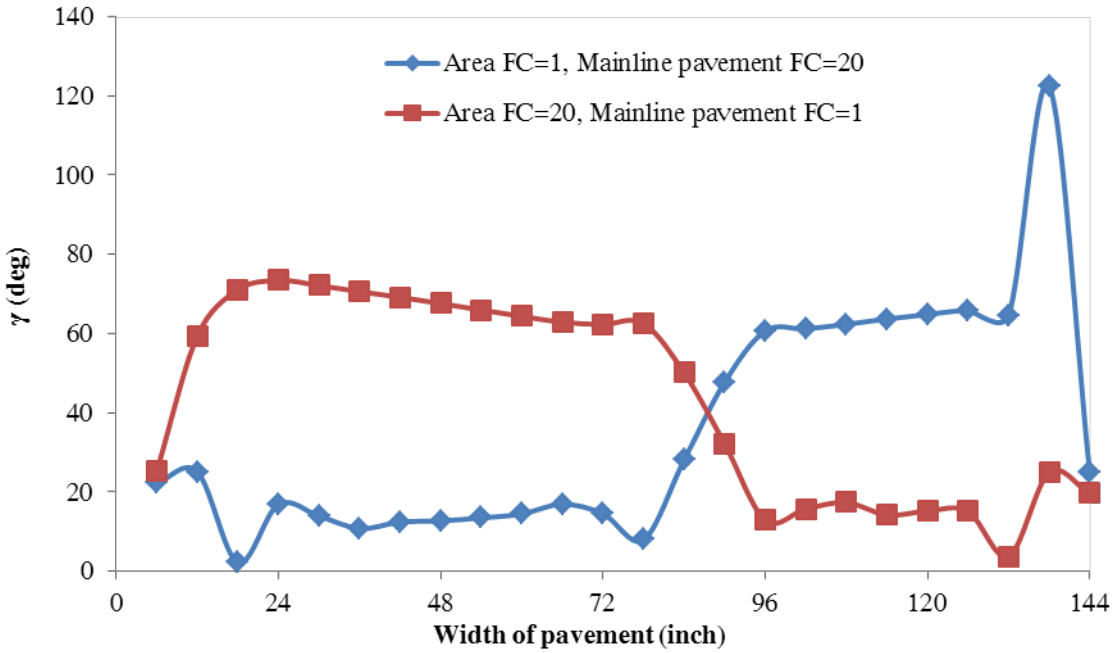

Figure 6.21 Distribution of γ along width of the pavement at transverse edge for 5'x5' changed friction areas

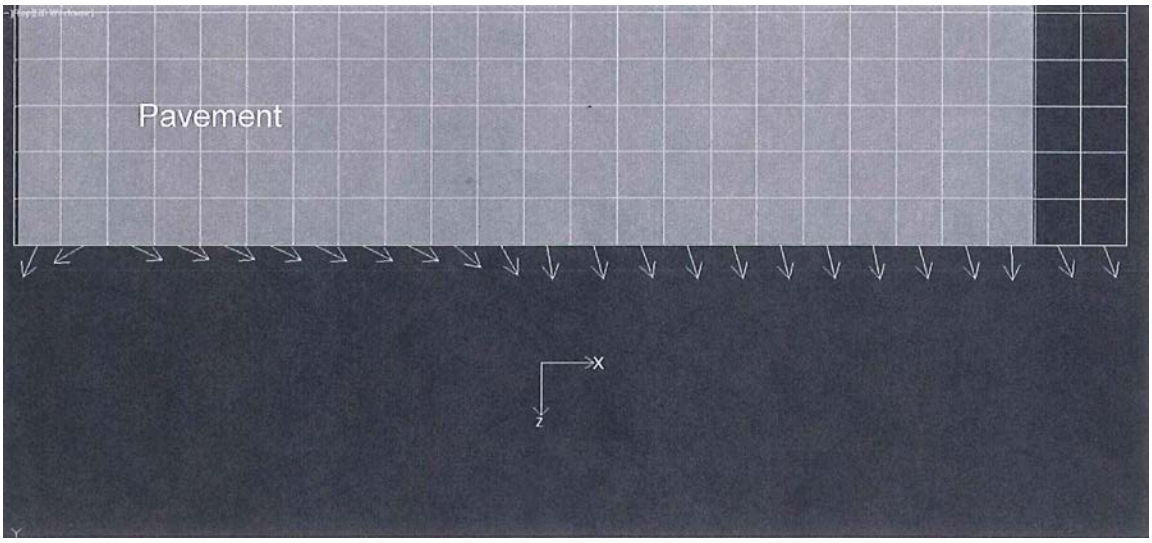

Figure 6.22 Pavement plan view diagram showing the direction of the pavement maximum principal stress direction for the 7' x 7' changed friction areas for the mainline pavement having a FC=1, and the changed friction area having a FC=20

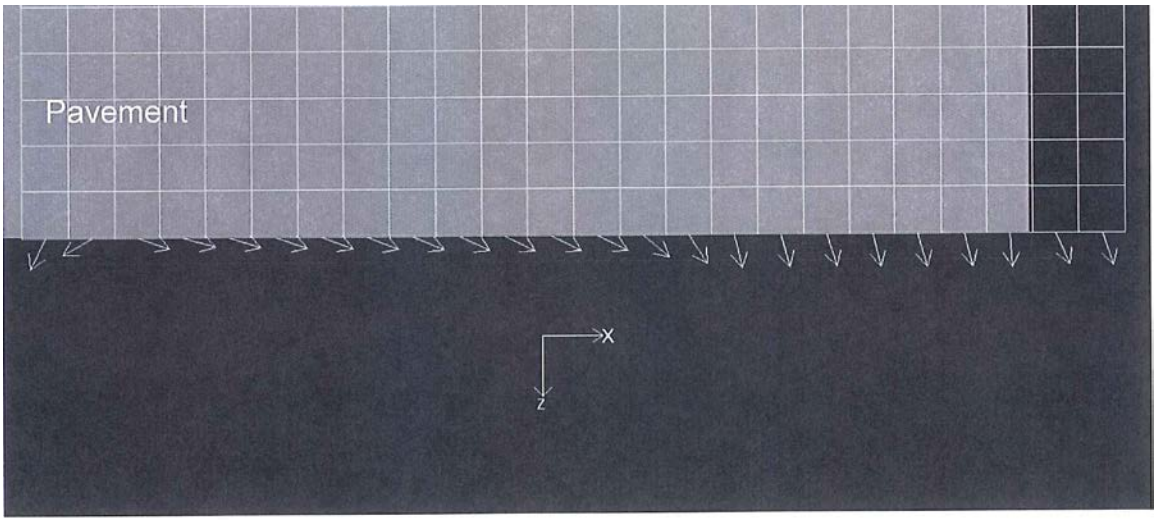

Figure 6.23 Diagram showing the direction of the pavement maximum principal stress direction for the 5’ x 5’ changed friction areas for the mainline pavement having a FC=1, and the changed friction area having a FC=20

6.6 Pavement Shoulders

6.6.1 Shoulder without Joints

A 10 in. thick shoulder with 78 in. width was added to the side of the mainline pavement to investigate the effects on y-cracking of shoulders placed after the mainline pavement. The materials used on the mainline pavement were also used on the pavement shoulder section. Figure 6.24 shows the model generated for this case.

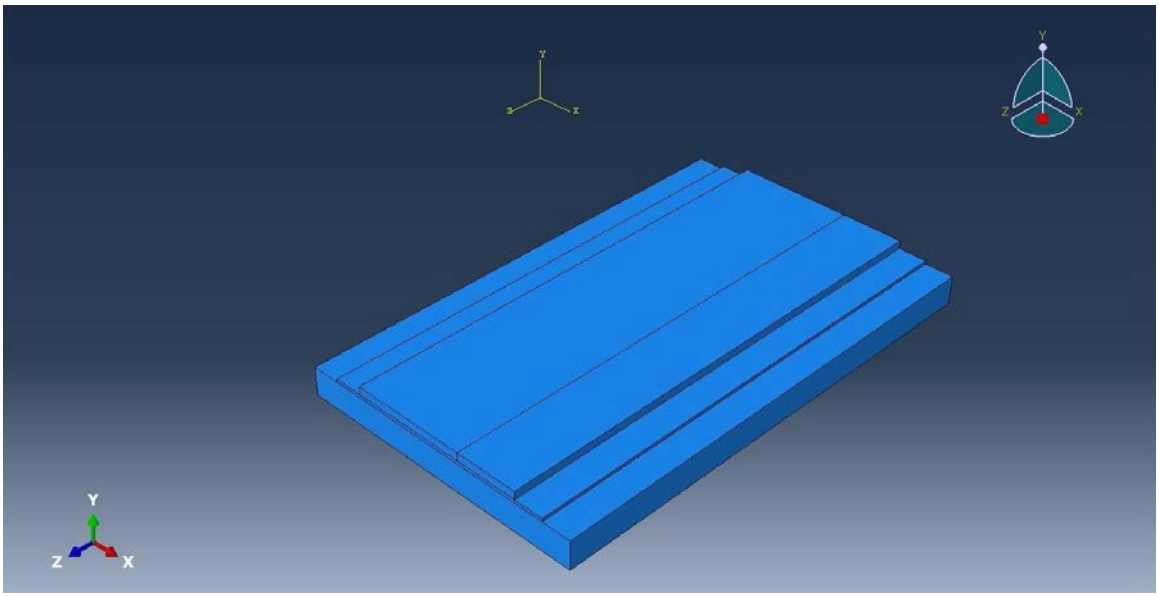

Figure 6.24 Concrete pavement model with CRCP shoulder

Two interactions were created for these three layers. A surface to surface contact with friction coefficient of 20 was defined for interaction between the pavement layer and subbase layer. Another interaction was defined with a friction coefficient of 20 between the subbase layer and the subgrade layer.

The bottom of the pavement structure was completely fixed, thus disabling all displacement and rotation components at this location. Also, the vertical sides of the subgrade were prevented from translating in both transverse and longitudinal directions.

As in the mainline pavement model, the gravity load was applied uniformly to the pavement layers. This gravity acceleration of 386 (in/s^2) was applied in the downward vertical direction. It is essential to apply the gravity load to ensure that the friction between layers is engaged. A temperature decrease of 50°F was applied to the entire concrete pavement including the mainline and shoulder sections while the temperature in the subbase and subgrade underneath the pavement was kept constant.

A color map of the normal longitudinal stresses (S33) is shown in Figure 25. Since the pavement modeled was symmetric in the longitudinal direction, the stresses were symmetric. Figure 6.25 shows that tensile stresses developed approximately in the central areas (green areas) whereas compression stresses developed approximately at

the transverse top surface pavement edges (blue areas). The quantity of stress in the middle of the pavement was the highest and started to decrease as it went farther from the middle as shown in Figure 6.26. Since there was a high tensile stress in the middle, the probability of cracking in the central regions of the pavement was higher than at the transverse edges of the pavement.

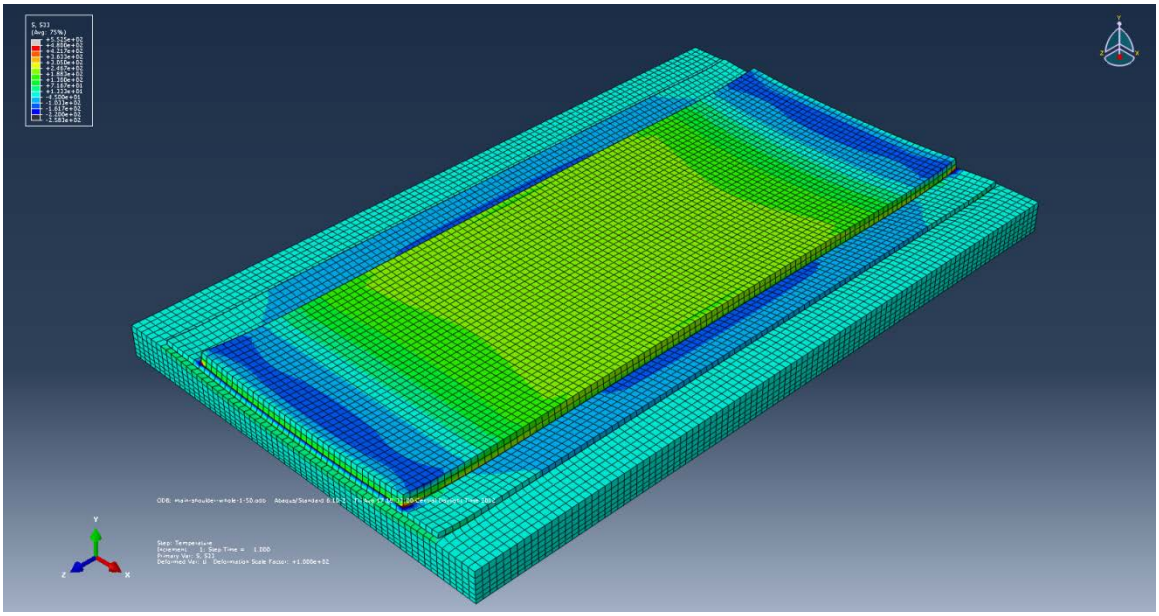

Figure 6.25 Stress map for longitudinal stresses

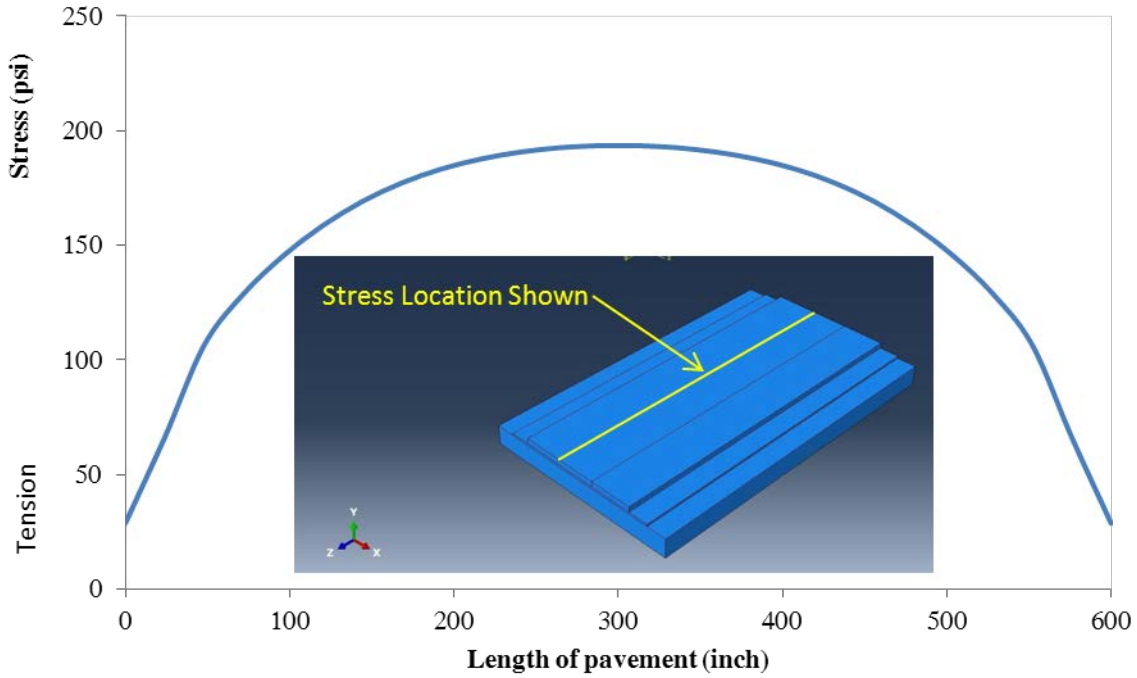

Figure 6.26 Pavement stress in the longitudinal direction (S33) along the length of the pavement with shoulder for a 50°F temperature reduction over the mainline pavement and shoulder

6.6.2 Shoulder with Joints

Another model was assembled for the pavement with jointed shoulders. All parameters were equal to those used in the previous models except for 3 transverse joints created in the shoulder as shown in Figure 6.27.

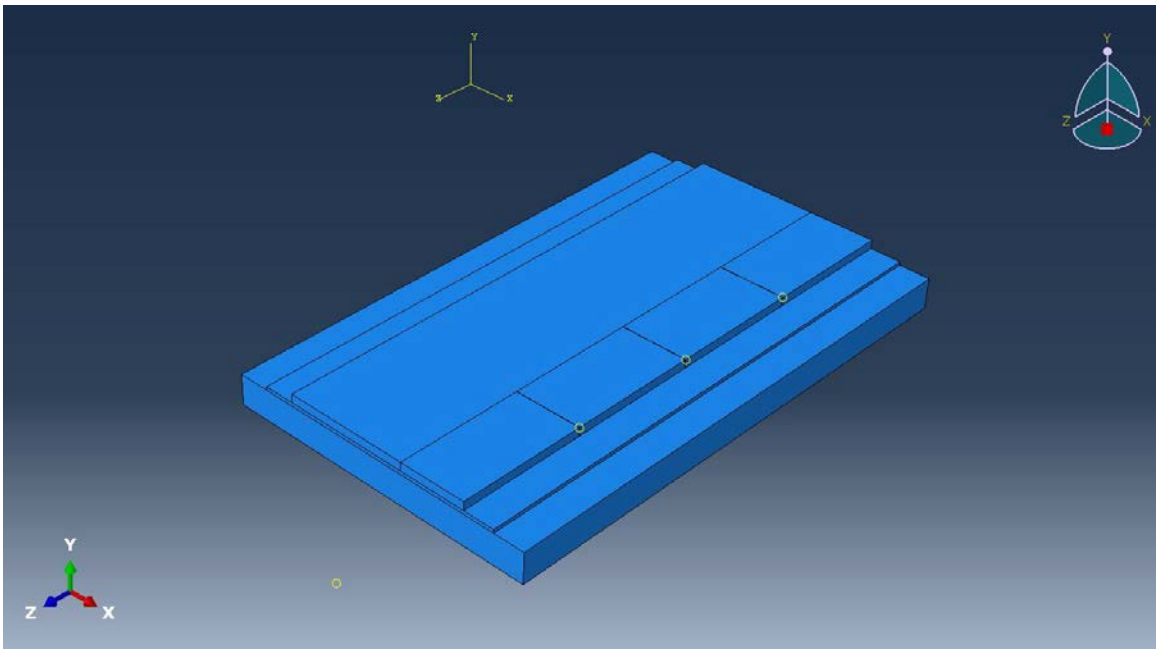

Figure 6.27 Computational model that includes a jointed pavement shoulder

Coupled Temperature-Displacement elements were used in this finite element model. Cubic elements were used in the subbase and subgrade. Elements in the pavement portion of the model however were triangular because of the geometry imposed by the joint – mainline pavement intersection. Figure 6.28 shows the mesh generated for this model.

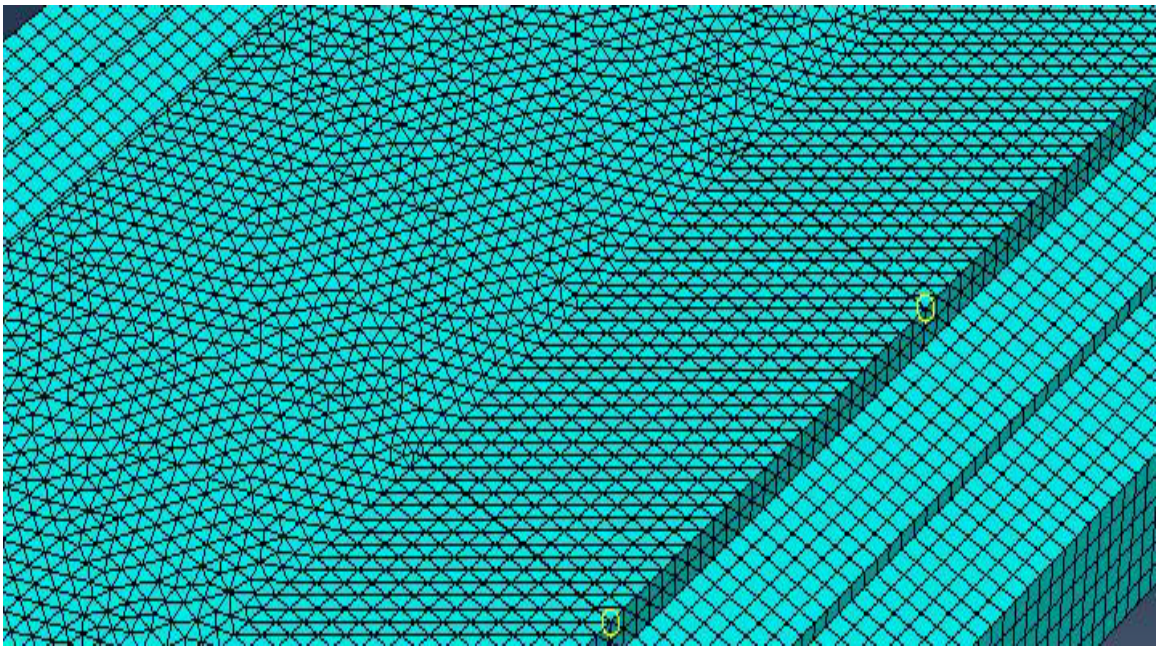

Figure 6.28 Close-up model of jointed shoulder after meshing

A temperature decrease of 50°F was applied to the concrete pavement including mainline and shoulder sections while the temperature for the subbase and subgrade was held constant. The temperature for the pavement layer decreased from 100° F to 50° F, whereas the temperature for subbase and subgrade was constant and equal to 50° F.

Figure 6.29 shows a color map of the normal longitudinal stress (S33). From Figure 29, it appears that when the shoulder is jointed, S33 is higher in the mainline than in the shoulder. Also, for the model with joints in the shoulder, stresses in the main line pavement were higher than stresses in the main line pavement with CRCP shoulders for the same temperature reduction in both models. As shown in Figure 29, there is a high concentration of stress at the sharp corners close to the joints. Also, it can be seen that stresses were not symmetric and change along the width of the pavement. This meandering in stress patterns can show a high potential for Y-cracking in the pavement with a jointed shoulder. The pavement cracking probability is a function of the maximum principal stress-to-tensile strength ratio. Cracks usually occur perpendicular to the direction of the maximum principal stress. When the direction of the

maximum principal stress changes from, the perpendicular direction and consequently the crack direction will also change. The high stresses at the joints occur because the shoulder strains concentrate at the joint. This could lead to a situation where if the pavement cracks on the side opposite the shoulder, it would have a tendency to meander to the joint to relieve the stresses. This supports the empirical data from the ODOT pavement surveys that a jointed shoulder with CRCP could lead to an increase in Y-cracking.

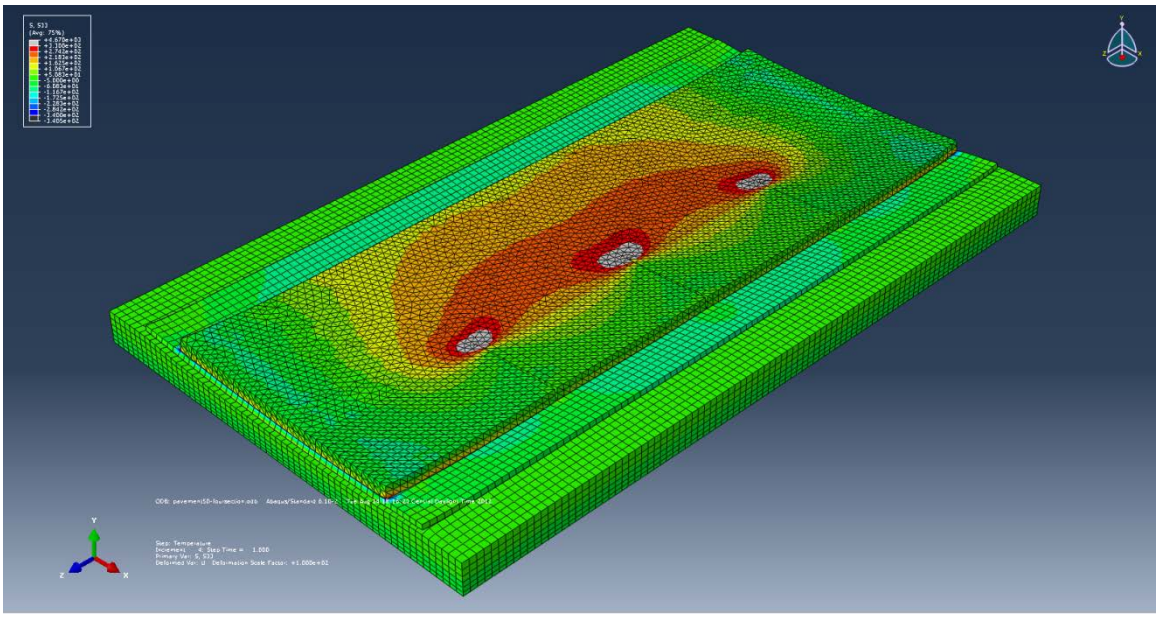

Figure 6.29 Color map for longitudinal stresses S33 (psi)

6.6.3 Different Shrinkage between Mainline and Shoulder Pavements

Different temperature changes were imposed on the mainline and shoulder pavements in order to simulate the effects of the differential drying shrinkage between the hardened mainline concrete and the newly cast shoulder. A temperature reduction of 50°F was imposed on the shoulder in all models while the temperature reduction for the mainline was varied between 5, 10 and 40°F in the models with continuous shoulder. The subgrade and subbase temperatures were kept constant. For three models with CRCP

shoulders, principal stress directions were calculated at the transverse edge and in the middle transverse cross section.

Principal stress directions were computed for the models with the 5, 10, and 40° F temperature reduction in the mainline pavement. The angle between the maximum principal stress and longitudinal axis in each element was calculated along the width of the pavement. Figures 6.30 and 6.31 show the principal stress direction angles at the transverse edge and in the middle of pavement, respectively. Figure 6.32 shows a diagram of the principal stress directions in the pavement middle for the simulations with the 10°F temperature reduction in the mainline pavement.

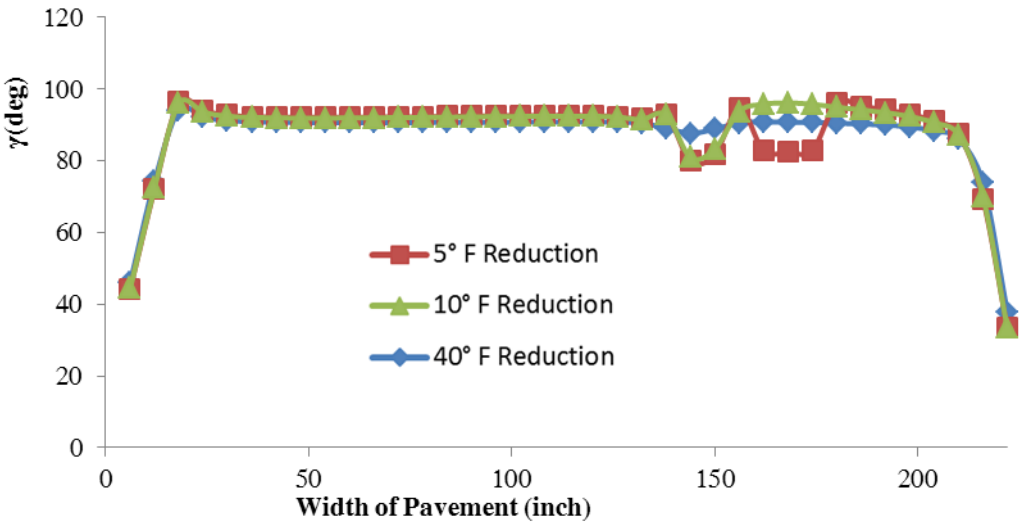

Figure 6.30 Direction of maximum principal stress at the transverse edge for simulations with temperature reductions of 5°, 10° and 40° F in the mainline pavement temperature.

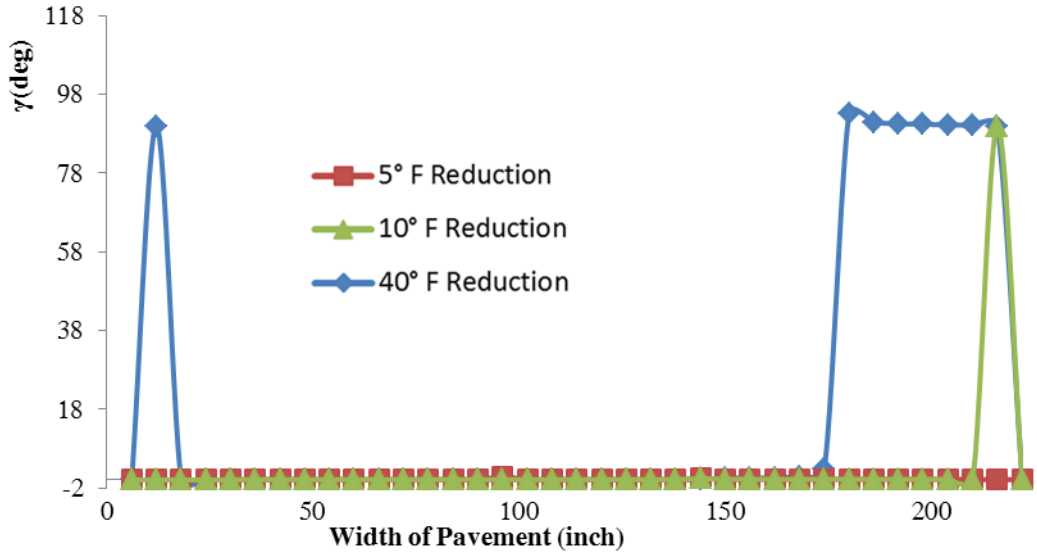

Figure 6.31 Direction of maximum principal stress in the pavement middle for simulations with temperature reductions of 5°, 10° and 40° F in the mainline pavement temperature

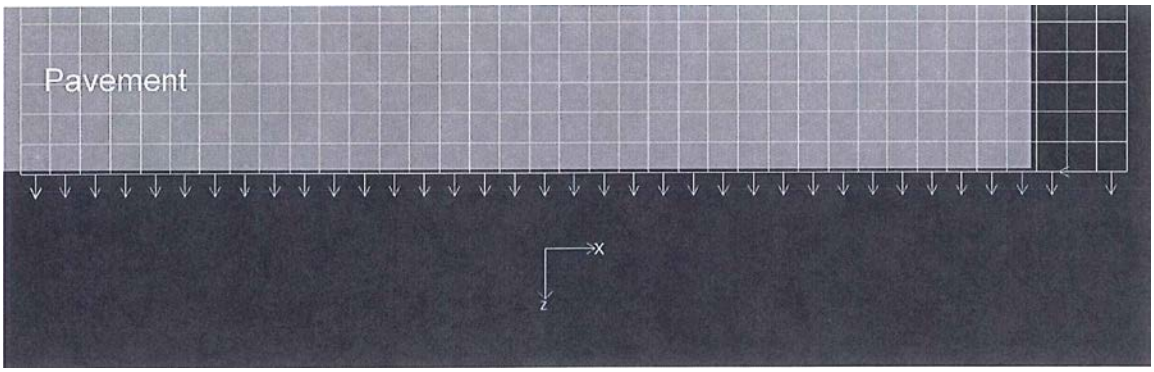

Figure 6.32 Direction of principal stress in the pavement middle for the simulation with a 10° F temperature reduction in the mainline pavement

From Figure 6.30, it can be seen that the orientation of the maximum principal stress was not significantly changed for the different amounts of temperature decrease modeled. Figure 6.31 shows the direction of principal stresses in the middle of the pavement for simulations with temperature reductions of 5°, 10° and 40° F in the mainline pavement. The principal stress direction for all three models was similar except

for the shoulder, where the simulation with the 40° F temperature reduction showing a change in γ from 90° to 0° degrees in the right hand of width of the pavement. The pavement locations with 0° angles mean that the cracking would occur transverse to the pavement.

Figures 6.33-6.35 show the color map of the normal longitudinal stresses (S33) for models with temperature reductions of 5°F, 10°F and 40°F, respectively in the mainline when continuously reinforced concrete shoulder was used.

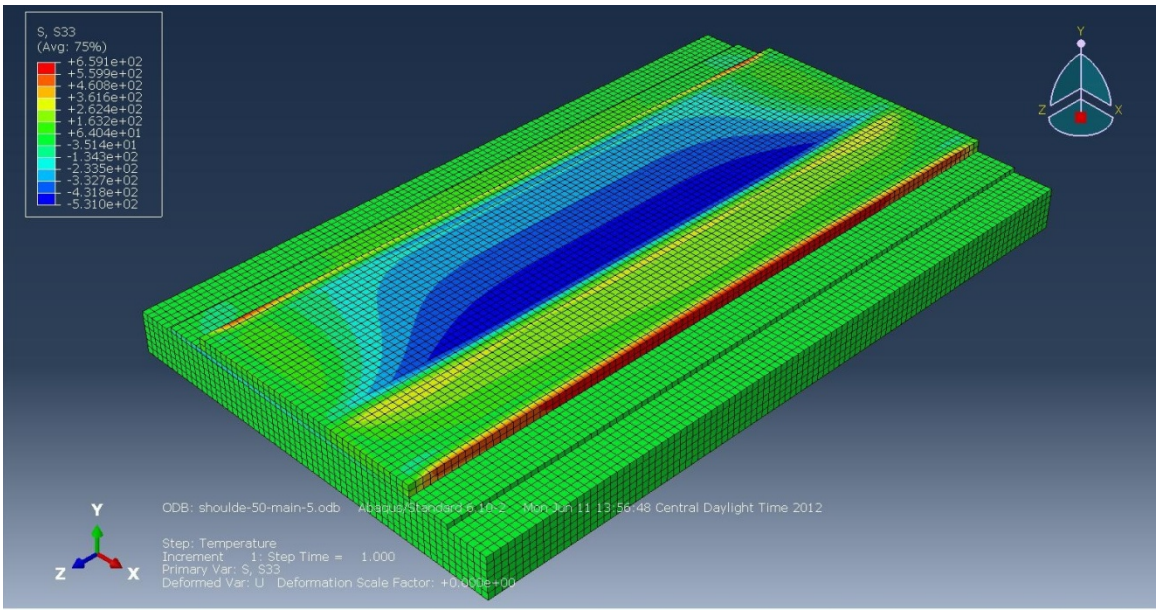

Figure 6.33 Color map of longitudinal stress (S33) for 5° F temperature reduction in the mainline for the pavement with continuous shoulders

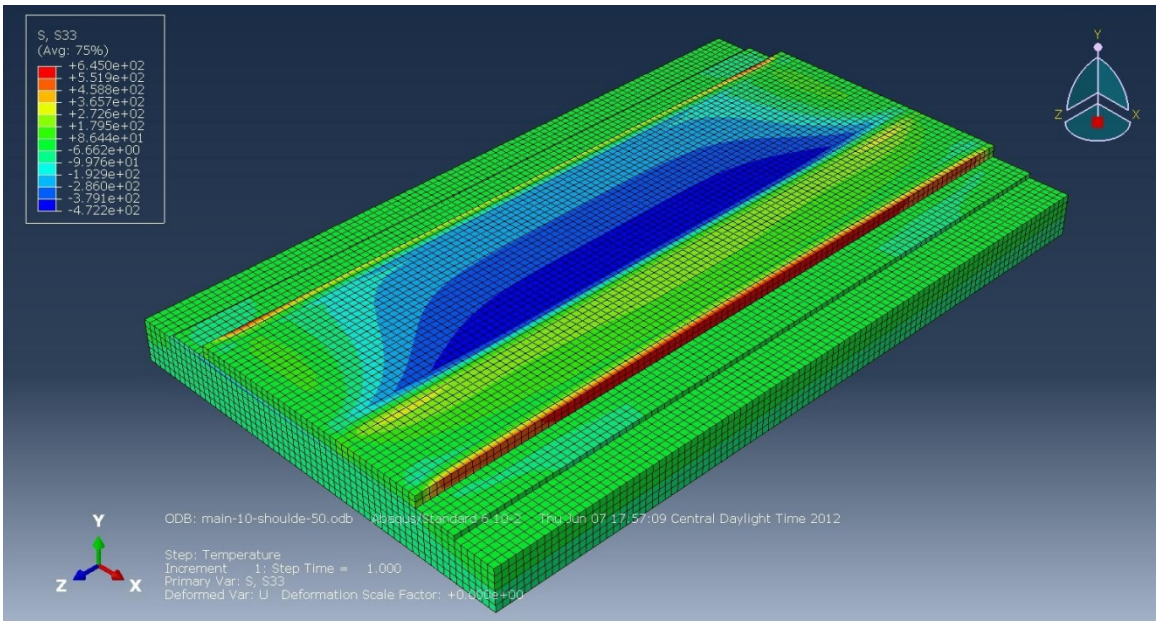

Figure 6.34 Color map of longitudinal normal stress (S33) in (psi) for 10° F temperature reduction in the mainline for pavement with continuous shoulder

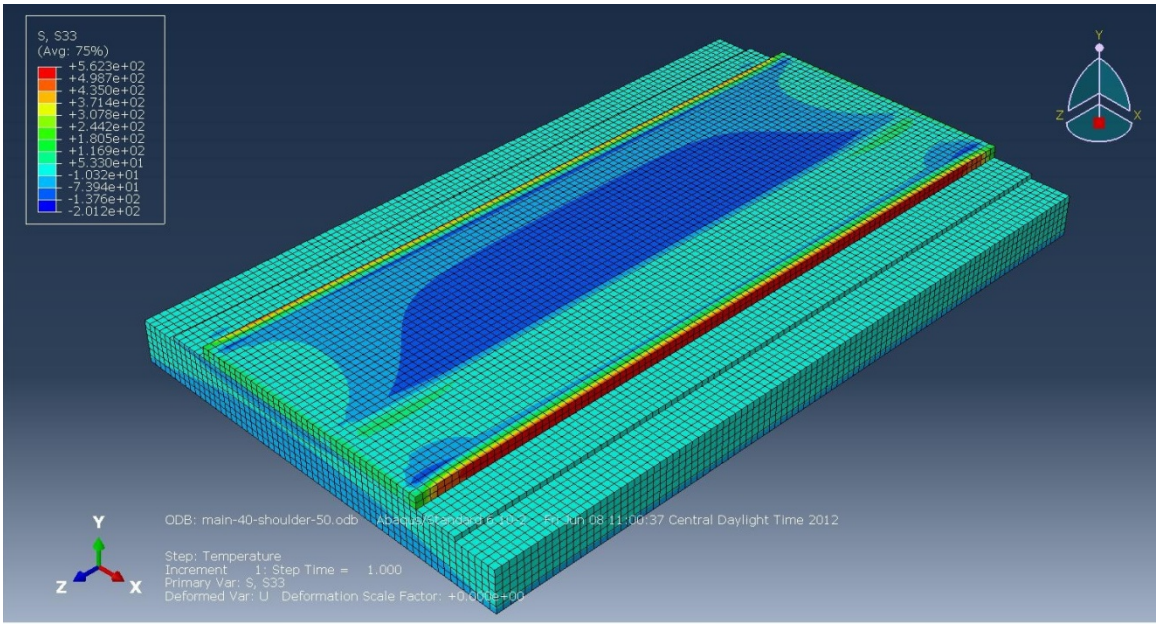

Figure 6.35 Color map of longitudinal normal stress (S33) in (psi) for 40° F temperature reduction in the mainline for pavement with continuous shoulder

It can be seen from Figures 6.33-6.35 that larger differences in shrinkage between the mainline and shoulder pavement generates larger stresses in the mainline

pavement. The shrinkage difference causes tension stresses in the shoulder and compression in the mainline pavement near the shoulder. The mainline pavement experienced pavement tension on the side located opposite to the shoulder. This differential shrinkage has the ultimate effect of causing bending stresses for the mainline pavement in the horizontal plane about an axis in the longitudinal direction. This does not mean that the mainline pavement overall was in compression, just that the differential shrinkage between the shoulder and mainline pavement caused compression stresses in the mainline pavement that would be superimposed on the mainline pavement stresses that occurred before the shoulder was placed.

Another model was assembled for the pavement with jointed shoulders, but with a temperature reduction of 10°F imposed on the mainline pavement and a temperature reduction of 50°F imposed on the jointed shoulder. Figure 6.36 shows a color map of longitudinal normal stresses for this model.

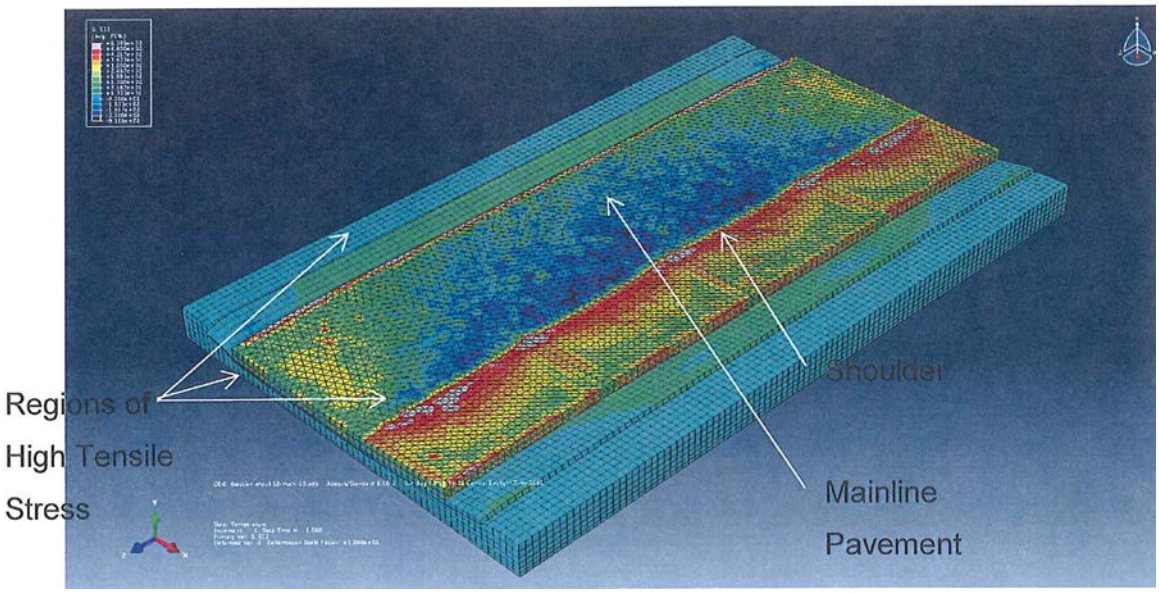

Figure 6.36 Color map of normal longitudinal stresses (S33) in (psi) for pavement with jointed shoulder

From Figure 6.36, the stress distribution is seen to be different in the pavement with the jointed shoulder. There were high tensile stresses in the jointed shoulder, especially at the interface between the shoulder and mainline pavement (shown in red color). Additionally, there were regions of high tensile stress in the mainline pavement at

the location of the joint, the side opposite the shoulder, and the region located at the mainline pavement near the pavement end. Shoulder movements could concentrate at the joint, leading to high strains in the mainline pavement near the joint. This leads to high cracking potential in the mainline pavement near the shoulder joint. Cracking could also occur at the high stress levels on the mainline pavement opposite the shoulder.

If a crack in the mainline pavement existed before placement of the shoulder and was located between the joints, the pavement would resemble that of a z-shaped shear specimen commonly used to measure concrete shear strength as shown in Figure 6.37 These high shear stresses would cause the concrete principal stress to change direction. The crack direction would likewise change with the principal stress direction. Although there exists a longitudinal joint between the shoulder and the mainline pavement, tie bars reduce differential movement between the mainline pavement and shoulder, allowing shear stresses to develop.

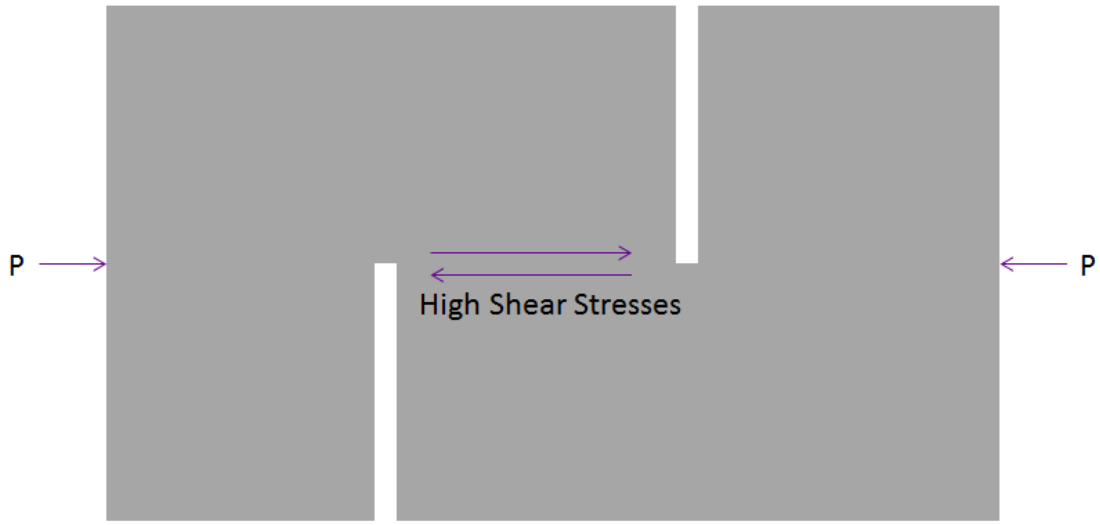

Figure 6.37 Schematic of Z-shaped concrete shear specimen

6.7 Reinforcement

Two finite element models with different percentages of longitudinal steel reinforcement were investigated. All other parameters were equal to those in the

previous model with continuously reinforced concrete shoulders. Thirty #6 (0.75 in. diameter) longitudinal bars were embedded in the pavement for the model with 0.6 % longitudinal steel. Thirty five #6 bars (0.75 in. diameter) were used for the model. This provided 0.7 % longitudinal steel. #5 bars (0.625 in diameter) with 44 in. spacing for the transverse steel. Tie bars that were 30” in length were spaced at 30” and were used to tie the mainline to the shoulder. Figure 6.38 shows the arrangement of steel bars inside the pavement for models with 0.6 % longitudinal steel.

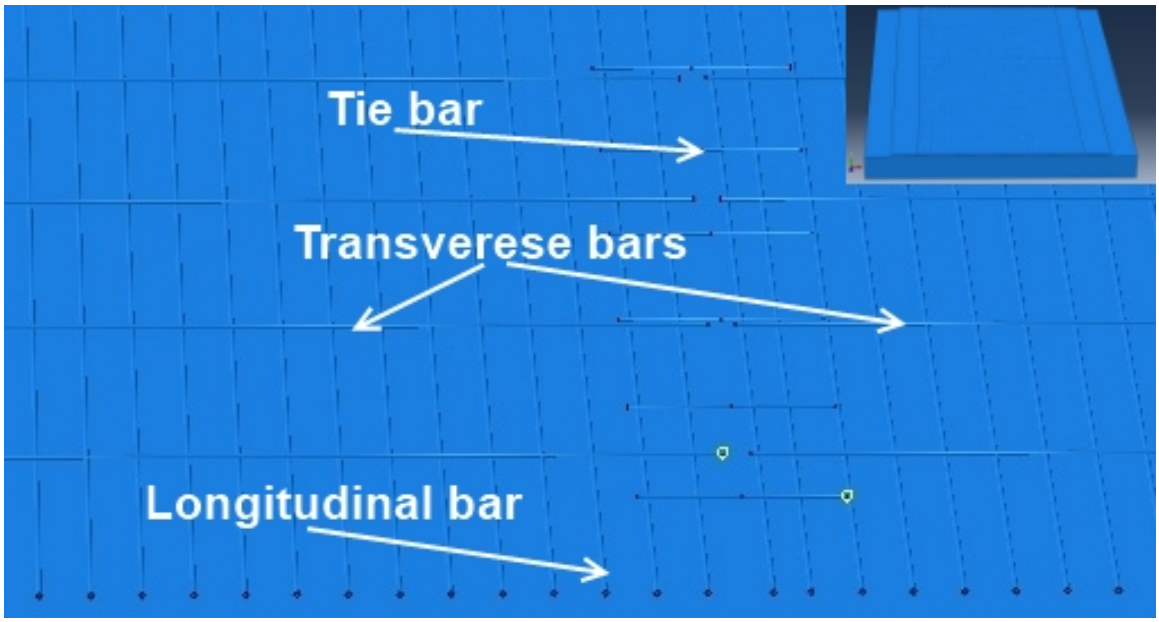

Figure 6.38 Arrangement of reinforcing bars in the pavement with 0.6 % longitudinal steel

A temperature reduction of 50°F was imposed on the shoulders while the mainline temperature reduction used was 10°F. The subgrade and subbase temperatures were kept constant in these simulations. Figure 6.39 shows the longitudinal normal stress map for model with 0.6 % longitudinal steel. The inclusion of 0.7% instead of 0.6% reinforcing steel did not change the maximum stress magnitude by a large amount. The greater reinforcing steel content did provide a slightly more varying stress pattern which is seen by comparing the stresses and is shown in Figures 6.40 and 6.41. The presence of discrete reinforcing bars increases localized stress

concentrations at the bar locations. More reinforcing bars provide more locations of localized stress concentrations.

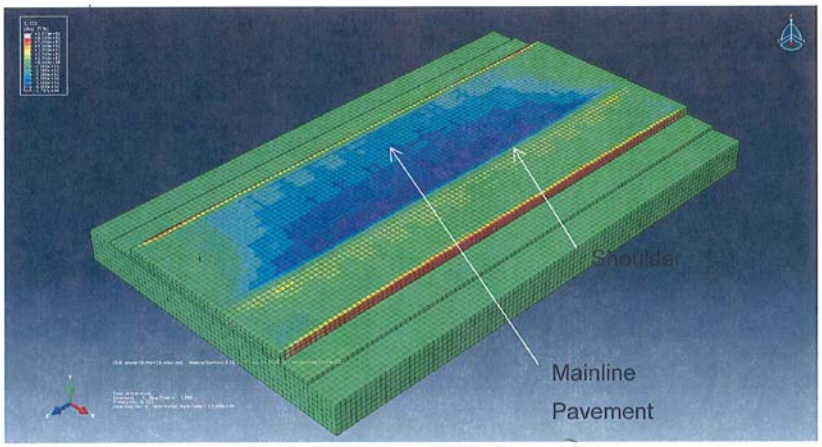

Figure 6.39 Color map of longitudinal normal stress S33 (psi) for pavement with 0.6 % longitudinal steel

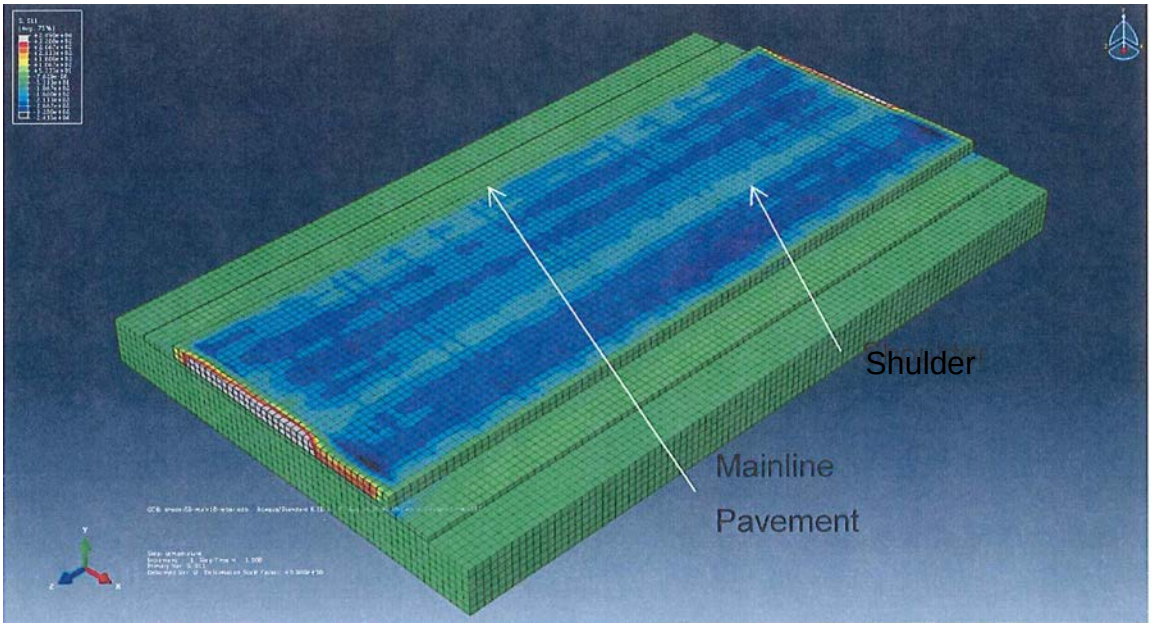

Figure 6.40 Transverse stress (S11) map for pavement with 0.6 % longitudinal steel

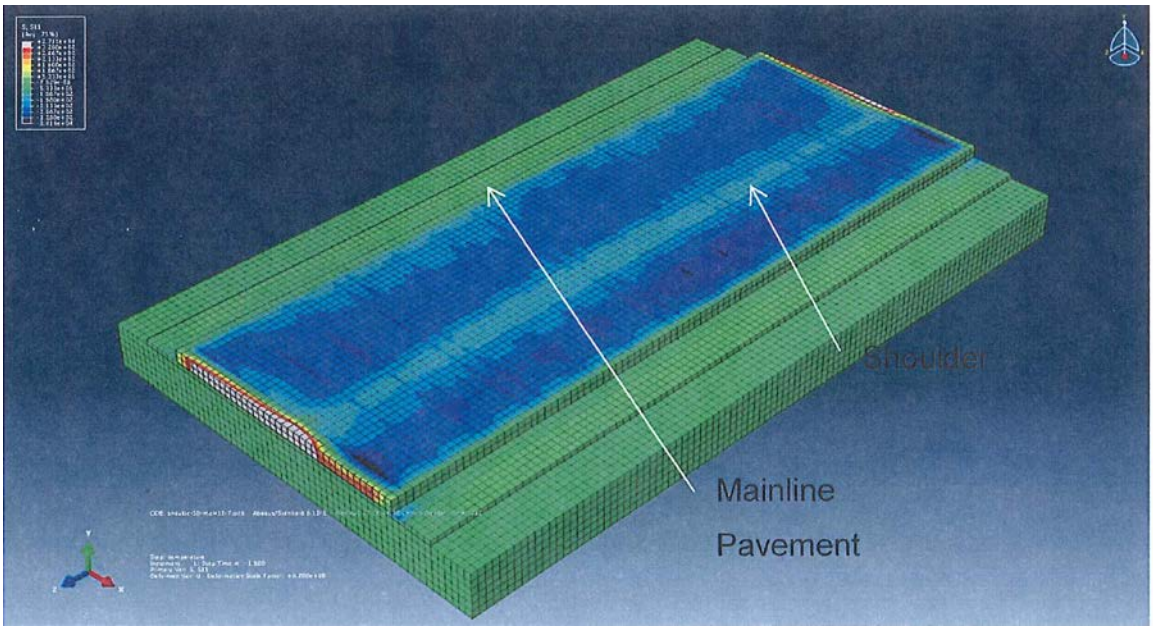

Figure 6.41 Transverse stress (S11) map for pavement with 0.7 % longitudinal steel

Reinforcing bars did change the stress magnitudes from those seen in the unreinforced model as shown in Figure 6.42. This is because the reinforcing steel has a much higher elastic modulus and can carry a larger portion of the total force than an equivalent amount of concrete in its place in the unreinforced model.

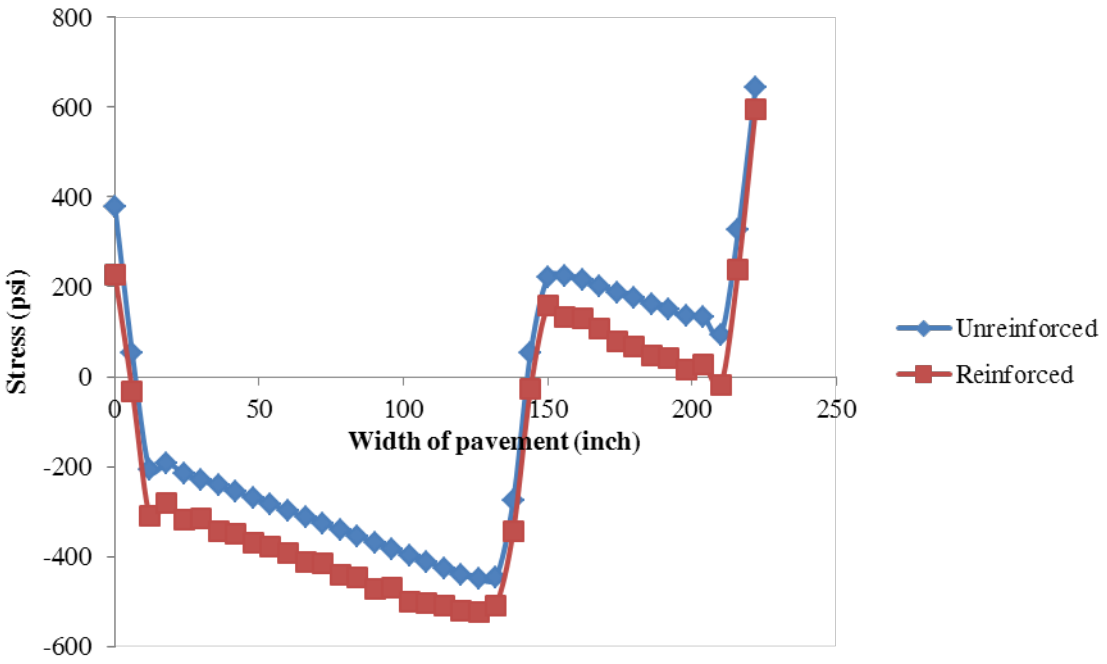

Figure 6.42 Concrete stress for pavement with and without steel reinforcement for the case of the shoulder temperature reduction of 50°F and the mainline pavement temperature reduction of 10°F

6.8 Conclusion

Changes in the maximum principal stress direction will cause the crack to change direction, potentially causing y-cracking. A change in the maximum principal stress along the width of the pavement also causes cracks to meander and contribute to y-cracking. In this research, several finite element simulations were run to understand the effect of friction coefficients between pavement layers, localized changes in pavement friction, differential shrinkage between mainline and the shoulder, joints in shoulders and steel in the pavement on principal stress direction.

Models with different friction coefficients between pavement layers were developed. Different size sections with different friction coefficients between the pavement and subbase than the rest of the pavement were added to the pavement simulations. The impact of these area friction properties on the maximum principal stress direction was studied by changing the location of the changed friction area in the

pavement, area size, and friction coefficient of interaction between and the underneath layer. To understand the effect of section location, areas were placed halfway between the pavement ends in three models and in the other three models they were located at the corner. A change in the friction at the corner had a large influence on the amount of stress and direction at the edge of the area. A changed friction area placed midway between the pavement ends did not significantly affect the pavement stress distribution. The changed friction area size has a large effect on the stress magnitude when the area is near the transverse edge of the pavement or an existing crack. When the changed friction area location is near the middle of the section between cracks in the longitudinal direction, the stresses did not change significantly. Results showed whether an increase or decrease in friction coefficient interaction will give non-uniform restraint and cause the principal stress to change direction. This data suggests that subbase non-uniformity could cause the meandering of cracks and lead to Y-cracks.

Different temperature changes were imposed on the mainline and shoulders in order to simulate the effects of the differential drying shrinkage and temperature change between the hardened mainline concrete and the newly cast shoulder. The stress magnitudes were higher for larger differences in shrinkage between the mainline and shoulder pavement. This wavy stress patterns seen through the pavement with jointed shoulders could help explain the high potential for Y-cracking. High local stresses occur where the joints in the shoulder meet the mainline pavement. This high local stress can initiate a crack.

To understand the effect of reinforcement amounts on stress distribution, two finite element models with different percentages of longitudinal steel were developed. It appears that the pavement with 0.7% steel shows more variation in the stress than the model with 0.6% longitudinal steel, potentially leading to more crack direction divergence.

CONCLUDING REMARKS AND RECOMMENDATIONS

This report has combined literature reviews, updates of historical databases, field surveys, construction records, and simulations to investigate the prevalence and long-term impact of Y-cracks on CRCP. Through this work many things have been observed.

The primary findings from the field observations were:

- Pavements with CRC shoulders and open graded bituminous bases contained 35% less Y-cracks per mile than pavements with non-CRC shoulders.
- Pavements with higher transverse steel contents contained more Y-cracks per mile
- Pavements that did not contain transverse steel showed poor performance
- Pavements in this study did not experience a change in Y-cracks per mile when the longitudinal steel content was increased to 0.71% and 0.73%, when compared to steel contents of 0.50% and 0.61%
- When pavements contained more than 60 Y-cracks per mile then the patches tend to increase as well.

This last point is significant as it suggests that if the amount of Y-cracks in a pavement can be minimized then the overall quality of the roadway can be preserved.

A number of useful observations were found in the simulations. These include:

- Concrete placement time and date can impact the probability of closely spaced early age cracks with less difference at 1 year
- Differential friction between pavement layers may be a cause for meandering of cracks with FEM models and an increase in cracks with Hyperpave III modeling. These areas of differential friction had an especially large impact at the edge of a pavement
- The larger the area of differential friction the larger the impact was on the stress distribution
- Differential shrinkage between the mainline pavement and the shoulders was seen to cause an increase in stress and possible cracking
- The modeling confirmed that JCP shoulders would cause increases in Y-cracks and therefore punchouts in CRCP

Based on these findings of this work CRCPs that were 10 to 12 inches in thickness, with longitudinal steel content between 0.61% and 0.73%, transverse steel at 0.06% with CRC shoulders and an open graded bituminous base showed the best performance. Any differential bonding or friction should be minimized between layers if possible.

REFERENCES

Al-Qadi, I. L., and M. A. Elseifi. "Mechanism and Modeling of Transverse CRacking Development in Continuously Reinforced Concrete Pavement." International Journal of Pavement Engineering, Vol. 7 , No.4, 2006: 341-349.

American Association of State Highway and Transportation Officials. "AASHTO Guide for Design of Pavement Structures." Washington, D.C., 1993.

Barragán, B., Gettu, R., Agulló, L., and Zerbino, R. (2006), “Shear Failure of Steel Fiber-Reinforced Concrete Based on Push-Off Tests,” ACI Materials Journal, Vol. 103, No. 4, pp. 251-257.

Beyer, Matthew, and Jeffery Roesler. Mechanistic-Empirical Design Concepts for Continuously Reinforced Concrete Pavements in Illinois. Springfield, IL, IL: Illinois Department of Transportation, 2009.

Choi, Jeong-Hoon, and Roger H. L., Ph.D. Chen. Design of Continuously Reinforced Concrete Pavements Using Glass Fiber Reinforced Polymer Rebars. McLean, VA: Federal Highway Administration, 2005.

Darter, Michael I., Scott A. LaCoursiere, and Scott A. Smiley. "Structural Distress Mechanisms in Continuously Reinforced Concrete Pavement." Transportation Research Board, 1979: 1-7.

Du, Lianxiang, and Elizabeth Lukefahr. "Summary of Thirty Years of TxDOT-Funded Research on Coarse Aggregate Issues in Concrete Paving." 2007 Mid-Continent Transportation Research Symposium. Ames: Iowa State University, 2007. 1-16.

ERES Consultants, Inc. Summary of CRCP Design and Construction Practices in the U.S. Schaumburg, Illinois: Concrete Reinforcing Steel Institute, 2001.

Huang, Yand H. Pavement Analysis and Design. Upper Saddle River, NJ: Pearson Prentice Hall, 2004.

Huang, Yang H. Pavement Analysis and Design. 2nd Edition. Upper Saddle River, New Jersey: Pearson Education, Inc., 2004.

Johnston, Daniel P. "Effects of Design and Material Modifications on Early Cracking of Continuously Reinforced Concrete Pavements in South Dakota." Construction, 2008, 2008: 103-109.

Johnston, Daniel P., and Roger W. Surdahl. "Effects of Design and Material Modifications on Early Cracking of Continuously Reinforced Concrete Pavements in South Dakota." Transportation Research Record 2081 (2008): 103-109.

Kohler, Erwin. Experimental Mechanics of Crack Width in Full-Scale Sections of Continuously Reinforced Concrete Pavements. Urbana, IL.: PhD dissertation, University of Illinois at Urbana-Champaign, 2005.

Kohler, Erwin, and Jeffery Roesler. Accelerated Pavement Testing of Extended Life Continuously Reinforced Concrete Pavement Section. Springfield, IL: Illinois Department of Transportation, 2006.

Kohler, Erwin, and Jeffery Roesler. "Active Crack Control for Continuously Reinforced Concrete Pavements." Transportation Research Record 1900 (2004): 19-29.

Kohler, Erwin, and Jeffery Roesler. "Active Crack Control for Continuously Reinforced Concrete Pavements." Construction, 2004, 2004: 19-29.

McGovern, Ginger, David A. Ooten, and Lawrence J. Senkowski. Performance of Continuously Reinforced Concrete Pavements in Oklahoma - 1996. Oklahoma City, OK: Oklahoma Department of Transportation, 1996.

Oregon Department of Transportation. "Distress Survey Manual." 2009. http://www.oregon.gov/ODOT/HWY/CONSTRUCTION/docs/pavement/Distress_Survey_Manual.pdf (accessed April 17, 2010).

Riding, Kyle A. "Early Age Concrete Thermal Stress Measurement and Modeling." Doctoral Dissertation. The University of Texas at Austin, 2007. 588 pp.

Riding, Kyle A., Jonathan L. Poole, Anton K. Schindler, Maria C.G. Juenger, and Kevin J. Folliard. "Effects of Construction Time and Coarse Aggregate on Bridge Deck Cracking." ACI Materials Journal 106, no. 5 (2009): 448-454.

Ruiz, J. M., P. J. Kim, A. K. Schindler, and R. O. Rasmussen. "Validation of HIPERPAV for Prediction of Early-Age Jointed Concrete Pavement Behavior." Transportation Research Record. 2001. 17-25.

Ruiz, J. Mauricio, Robert O. Rasmussen, George K. Chang, Jason C. Dick, and Patricia k. Nelson. Computer-Based Guidelines For Concrete Pavements Volume II—Design and Construction Guidelines and HIPERPAV II User's Manual. Final Report, FHWA, 2005.

Ruiz, J. Mauricio, Robert O. Rasmussen, George K. Chang, Jason C. Dick, Patricia K. Nelson, and Ted R. Ferragut. Computer-Based Guidelines for Concrete Pavements Volume I: Project Summary. McLean, VA: Federal Highway Administration, 2005.

Schindler, Anton K., and Frank B. McCullough. The Importance of Concrete Temperature Control During Concrete Pavement Construction in Hot Weather Conditions. Washington, D. C.: Transportation Research Board, 2002.

Suh, Young-Chan, and B. F. McCullough. "Factors Affecting Crack Width of Continuously Reinforced Concrete Pavement." Design and Rehabilitation of Pavements (National Academy of Sciences), 1994: 134-140.

Suh, Young-Chan, and B. Frank McCullough. "Factors affecting crack width of continuously reinforced concrete pavement." Transportation Research Record, 1994: 134-140.

Tayabji, Shiraz D., Dan G. Zollinger, Jaganmohan R. Vederey, and Jeffrey S. Gagnon. "Performance of Continuously Reinforced Concrete Pavements Volume III - Analysis and Evaluation of Field Test Data." 1998.

Tayabji, Shiraz D., Dan G. Zollinger, Jaganmohan R. Vederey, and Jeffrey S. Gagnon. Performance of CRC Pavements - Volumes 2 & 3. McLean, VA, Maryland: Federal Highway Administration, 1998.

Tayabji, Shiraz D., Peter J. Stephanos, Jeffrey S. Gagnon, and Dan G. Zollinger. "Performance of Continuously Reinforced Concrete Pavements Volume II - Field Investigations of CRC Pavements." 1998.

Texas Department of Transportation. "TxDOT Specifications." TxDOT Expressway . June 1, 2004. ftp://ftp.dot.state.tx.us/pub/txdot-info/des/specs/specbook.pdf (accessed June 30, 2011).

The Transtec Group, Inc. CRCP in Texas Five Decades of Experience. Schaumburg, IL: Concrete Reinforcing Steel Institute, 2004.

Triola, Mario F. Elementary Statistics. Boston, MA: Pearson Education, Inc., 2006.

Zollinger, Dan G., and E.J. Barenberg. "Continuously Reinforced Pavements: Punchouts and Other Distresses and Implication for Design," Report No. FHWA/IL/UI 227. Urbana, Illinois: University of Illinois, 1990.

APPENDIX A - DETAILED FIELD INSPECTIONS

A.1 Logan County

A.1.1 Overview

The continuously reinforced concrete pavement (CRCP) studied in Logan County is located on Interstate 35 just south of the town of Guthrie. As shown in Figure A.1, the pavement begins at the Oklahoma-Logan County line and extends north nearly six miles. Each square in Figure A.1 represents one square mile. Information provided by ODOT shows that the 2011 Annual Average Daily Traffic (AADT) for the project was estimated at 35,200 vehicles per day (VPD); meanwhile, the plan-sets provided by ODOT for the project show that the design average daily traffic (ADT) was 42,000 VPD.

The CRC pavement was completed in 1988 by Koss. It is 10 inches thick with 0.51% longitudinal and 0.11% transverse steel, according to the specifications for the project provided by ODOT. The pavement sits atop three inches of Type-A asphalt concrete and eight inches of select subbase, with jointed plain concrete shoulders. Type-A asphalt concrete has a ¾ inch nominal maximum aggregate size (NMS).

A visual inspection was conducted on July 5 and 26, 2011. The visual inspection consisted of counting Y-cracks and patches, while photographing subjects of interest.

The chainage of each patch and photograph taken was documented for future reference. A thousand foot section was also inspected for results comparable to Federal Highway Administration (FHWA) Report Number: FHWA-RD-94-174. This study consisted of 10.56 lane miles, consisting of 5.36 miles in the north bound direction and 5.20 miles in the south bound direction.

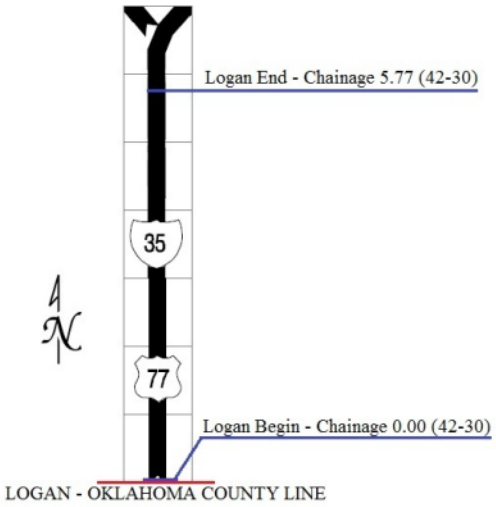

Figure A.1 Layout of the Logan County CRCP visited during inspection. The pavement is marked by county name, begin and end points, along with chainage (the length in miles from the beginning of the control section to a specified point) and the control section number.

A.1.2 Inspection Details

The southbound lane of his project had several more distresses and failures than the north bound lane. The southbound lane had several large areas of map cracking as seen in Figure A.2. The lane also exhibited multiple Y-cracks, or transverse cracks with several branching cracks, shown in Figure A.3 below.

Figure A.2 Photo shows transverse cracks with inter-connecting longitudinal cracks.

Figure A.3 Photo shows Y-cracks with multiple branches

The overall crack spacing in the southbound lane was fairly irregular. Cracks seemed to range in spacing from two to ten feet. There were several instances of close transverse cracks (less than one foot) starting to break up, by way of longitudinal cracks, shown in Figure A.4. During the south bound lane inspection it was noted that

areas with deeper tines made it more difficult to count Y-cracks, but seemed to make the cracks meander less.

Figure A.4 Photo showing closely spaced transverse cracks developing into punchouts

The northbound lane also exhibited irregular crack spacing, with cracks ranging from three to eight feet in spacing. There were a few developing punchouts that had not been patched (Figure A.5); however, these appeared to be close transverse cracks and not Y-cracks. Many of the Y-cracks had spalling along their length. It was noted during the inspection that Y-cracks seemed to be spaced both far apart and in clusters. In areas of increased crack spacing, such as eight to ten foot, Y-cracks were scarce.

Figure A.5 Developing punch-out between two close transverse cracks

A.2 Oklahoma County

A.2.1 Overview

The CRC pavement studied in Oklahoma County is located on Interstate 35. The project begins two miles north of the Oklahoma-Cleveland County line and extends north for just over a mile. Figure A.6 shows the location of the project with each square representing one square mile of area. The 2011 AADT data provided by ODOT estimated 120,000 VPD for the pavement, while the plan-sets showed the design ADT to be 94,000 VPD. The inspection consisted of 0.73 miles in the northbound lane and 1.01 miles in the south bound lane, for a combined total length of 1.74 miles.

The pavement project was completed in 2001 by Neilson Inc. It is ten inches thick with 0.61% and 0.07% longitudinal and transverse steel respectively according to ODOT plan sets. The pavement is sitting atop four inches of open graded bituminous base and twelve inches of aggregate base with CRCP shoulders.

A visual inspection was conducted on July 5, 2011. The visual inspection consisted of counting Y-cracks and patches, while photographing subjects of interest. The chainage of each patch and photograph was also noted for future reference.

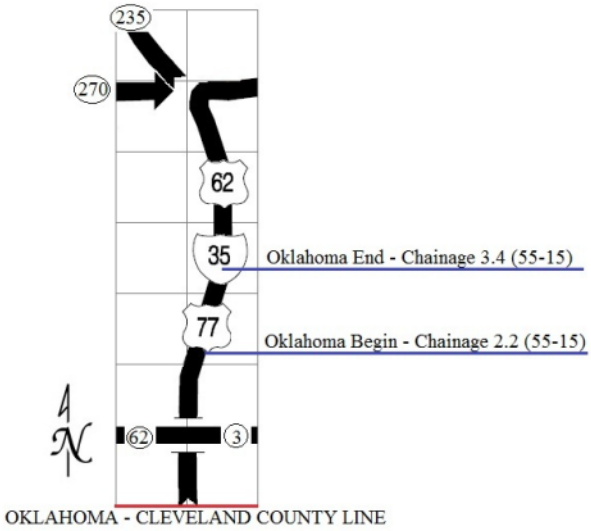

Figure A.6 Layout of the Oklahoma County CRCP visited during inspection. The pavement is marked by county name, begin and end points, along with the chainage and control section number.

A.2.2 Inspection Details

The northbound lane of this project had isolated areas of heavy Y-cracking and closely spaced transverse cracks connected by longitudinal cracks (see Figure A.7). It was noted that the crack width seemed to be very small, with a crack spacing of eight to ten feet between clusters of cracks.

Figure A.7 Closely spaced transverse connected by longitudinal cracks

Before the project was inspected, ODOT commented that they had a particular concern within mileposts 124.1 and 124.2. Figures A.8 and A.9 show the distresses in this particular region. The transverse steel in this region appears to be high in the pavement, leaving only ¾-1 inch of concrete cover over the bar. It was also noted that the transverse steel in this region does not appear to be perpendicular to the direction of traffic. Chris Westlund, an ODOT employee, said that the steel on this project was placed with a machine during the paving process and he recalled that the machine was having problems. Nevertheless, the distresses in this section of pavement seemed to be caused by inadequate steel cover and not related to Y-cracking, or any other cracking patterns. None of the distresses caused by the transverse steel have been patched in the northbound lane. The northbound lane also exhibited several stretches where the road surface was extremely worn. The tines in the wheel paths were barely visible. Several stretches of pavement had to be skipped while performing the visual inspection due to exits, entrances, and barrier walls not providing a shoulder to conduct the inspection.

Figure A.8 Distresses in ODOT's region of concern

Figure A.9 More distresses in ODOT's region of concern

The southbound lane appeared to be in slightly better condition than the northbound lane. The southbound lane still had distress caused by steel placement but significantly fewer than the other direction. Only one of the steel placement distresses had been patched, see Figure A.10. Figure A.11 shows images where it appears as though a Y-crack occurred over the shallow transverse steel. The steel in this area appeared to be less than an inch below the surface and is more likely to be the cause of

the distress, not the Y-crack. Ignoring the steel placement issues, the pavement appeared to be in good shape with a low number of Y-cracks observed and no Y-crack related distresses.

Figure A.10 AC patch over a distress with exposed transverse steel

Figure A.11 Possible Y-crack over shallow transverse steel

A.3 Cleveland County

A.3.1 Overview

The CRC pavement studied in Cleveland County consisted of two adjacent projects located on Interstate 35 near the town of Moore. The pavements begin at the Oklahoma-Cleveland county line and extend south for two miles, see Figure A.12. Each square in Figure A.12 represents one square mile. The CRCP projects visited in Cleveland County displayed slight differences in AADT data, according to 2011 data provided by ODOT. Cleveland 1 AADT was estimated at 126,600 VPD, while Cleveland 2 was 113,500 VPD; meanwhile, the design ADT values were 94,000 and 110,000 VPD respectively.

The two projects of interest (Cleveland 1 and Cleveland 2) have many similar characteristics with only a few minor differences. Cleveland 1 was completed in 2002 by Haskell Lemon. The pavement is ten inches thick with 0.61% and 0.07% longitudinal and transverse steel respectively, according to the specifications for the project. The pavement sits atop four inches of open graded bituminous base and twelve inches of aggregate base, with CRCP shoulders.

Cleveland 2 was completed in 2005 also by Haskell Lemon. The pavement is ten inches thick with 0.71% and 0.07% longitudinal and transverse steel respectively, according to the specifications for the project. The pavement also sits atop four inches of open graded bituminous base and twelve inches of aggregate base, with CRCP shoulders. Therefore these two projects are similar in contractor, thickness, base, and subbase. However, they differ in year constructed and percent longitudinal steel content.

A visual inspection was executed on July 5, 2011. The inspection consisted of counting Y-cracks and patches, while photographing subjects of interest along the pavement. The chainage of each patch and photograph was also noted for future reference. Together the two projects totaled 1.80 miles north bound and 1.52 miles in the south bound direction.

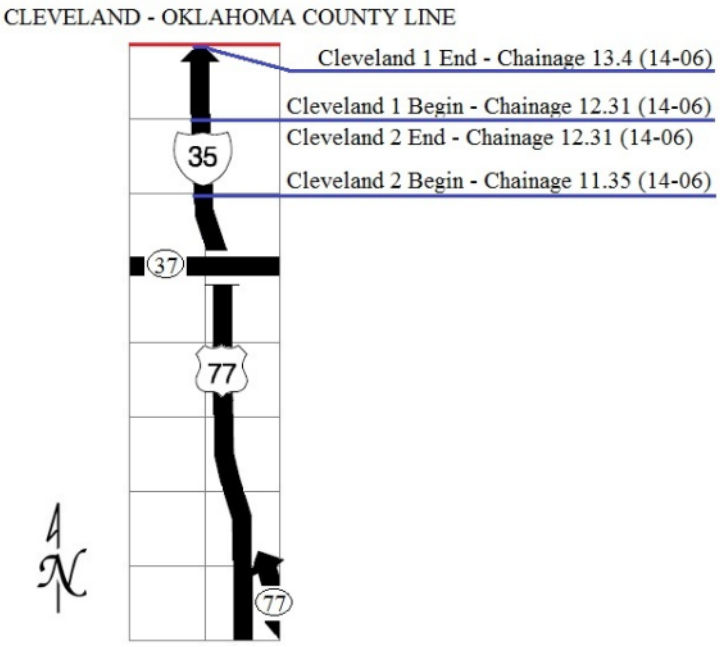

Figure A.12 Layout of the Cleveland county CRCP sites visited during inspection. The pavements are marked by designated county number, begin and end points, along with chainage and control section number.

A.3.2 Cleveland 1 Inspection Details

Inspection began at the Oklahoma-Cleveland County line with the pavement being inspected for two hundred feet, up to a bridge and then the bridge was skipped. On the south side of the bridge, in the southbound lane it was noted that the crack spacing was approximately three to four feet. A ½ mile south of the county line a construction joint was found, after the construction joint the crack spacing increased from three to four feet, to eight to ten. The southbound lane of the project was in great shape. There were no patches or punchouts observed and Y-cracking was minimal.

The northbound lane of the project was also in great shape. There were no punchouts or patches observed in the northbound lane. It was noted, though, that the northbound lane did have a lot more Y-cracks than the southbound lane, nearly triple. However, no failures were found.

A.3.2 Cleveland 2 Inspection Details

The inspection began in the southbound lane just north of exit 118 at a bridge joint. The length of pavement that was inspected was less than the full length of the project because of entrance ramps, heavy traffic, and lack of a shoulder to drive. Overall, the southbound lane was in great shape and contained no patches or punchouts.

The northbound lane of the project was more accessible which allowed the full length of the pavement to be viewed. The inspection began at the joint on the southern end of the project (Figure A.13). It was noted that the pavement had no cracks for the first forty-two feet, and then displayed a long crack spacing of approximately fifteen feet. Then cracks slowly became closer, reaching a spacing of three to four feet. Overall, the northbound lane, like the southbound lane, was in good shape with no patches or punchouts recorded.

Figure A.13 Joint at the Southern end of North bound lane

A.4 Carter County

A.4.1 Overview

The CRC pavement studied in Carter County is located along Interstate 35 near the town of Ardmore. The project begins at the Carter-Love County line and extends north for just over four miles. Figure A.14 below shows the location of the project with each square representing one square mile of area. The 2011 AADT data provided by ODOT estimated 32,700 VPD for the pavement, while the plan-sets showed the design ADT to be 52,700 VPD.

The pavement project was completed in 2007 by Koss. The CRCP is twelve inches thick with 0.73% and 0.06% longitudinal and transverse steel respectively, according to the plan sets provided by ODOT. That makes this section not only one of the thickest but also the most heavily reinforced. The pavement is sitting atop four inches of open graded bituminous base, eight inches of aggregate base, followed by eight inches of lime treated subbase. The pavement has jointed plain concrete shoulders.

A visual inspection was conducted on July 6, 2011. The inspection consisted of counting Y-cracks and patches, while photographing subjects of interest along the project. The chainage of each patch and photograph was also noted for future reference.

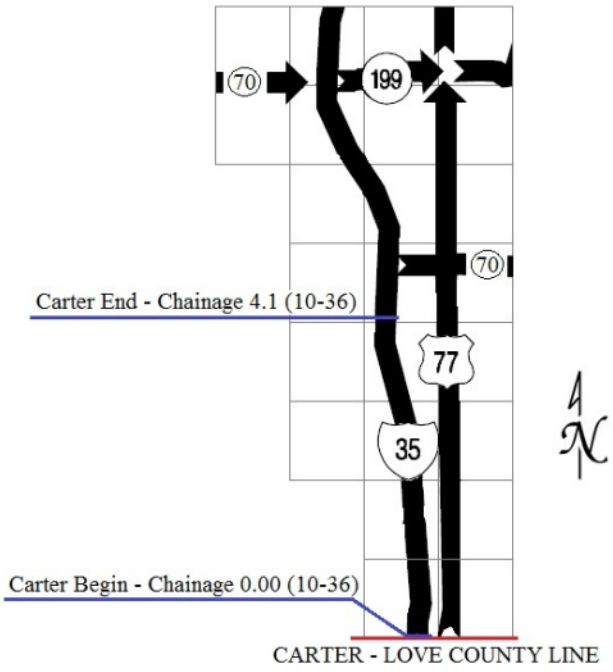

Figure A.14 Layout of the Carter county CRCP visited during inspection. The pavement is marked by county name, begin and end points, along with chainage and control section number.

A.4.2 Inspection Details

The northbound lane inspection began approximately two-hundred feet north of the county line due to a bridge. The first thing that was noted was that the pavement has its white line moved over two feet from the joint between the outside lane and the shoulder. The pavement contained a higher than usual Y-crack count for the first mile and a half but the count decreased afterward. However, the cracks for the first mile and a half displayed a regular crack spacing of approximately eight feet. Figure A.15 shows a typical Y-crack with spalling for the region on the left and spalled circular area on the right. The Y-crack shown in Figure A.15 seemed to be the most common, it was noted during inspection that there were multiple Y-cracks at the pavement edge with several of them being outside the white line (approximately 40%). This was especially noticed between mileposts 125 and 126. Figure A.16 shows two construction joints that display signs of raveling. Despite the occurrence of Y-cracks (see Figure A.17 left), more potential for distresses to develop were found by closely spaced transverse cracks (see

Figure A.17 right). These cracks displayed spalling and in several instances were connected by longitudinal cracks.

Figure A.15 (Left) Typical Y-crack for the region, (right) circular spalled area

Figure A.16 Two construction joints displaying signs of spalling

Figure A.17 (Left) Y-crack located in the region; (right) two close transverse cracks showing distress

There was a construction joint 4.15 miles north of the Carter-Love County line. According to the 2008-2009 PMS Database and the CRCP Database, the project ended at this location along with the CRCP in the area. Meanwhile, the 2009 Interstate Structural Pavement History lists the roadway as project number IMY-35-1(145)029 and simply states future construction.

Due to curiosity, approximately ½ mile of this project was inspected in both the north and south bound directions. Figure A.18 shows images of the pavement. The roadway displays a grey/silver color, possibly due to curing compound, while the surface appears to be in good shape with virtually no wear.

Figure A.18 Two images showing the glossy pavement surface with little wear

The southbound inspection began at a bridge approach joint 0.16 miles north of mile post 29. The first 0.64 miles inspected were part of the project IMY-35-1(145)029. This area of pavement displayed a low number of Y-cracks. The south bond lane appeared to be more worn than the northbound lane, and its appearance was not as glossy. The southbound lane of the original project of interest displayed various forms of Y-cracking as seen in Figure A.19. However no patches or punchouts were documented.

Figure A.19 Two different forms of Y-cracking

The CRCP pavement in Carter County seemed to be in good overall condition. There were no Y-crack related distresses observed. The 2008-2009 PMS database provided by ODOT showed that the northbound lane contained four patches, while the south bound lane contained five patches. During the inspection the chainages of the patches, according to the PMS Database, were specifically checked and no patches could be found within two tenths of a mile in either direction of the specified location.

A.5 Okfuskee County

A.5.1 Overview

The CRC pavement studied in Okfuskee County is located on Interstate 40 near the town of Okemah. The project is located five miles east of Okemah near interstate mile post 227. Figure A.20 shows the location of the pavement with each square in the figure representing one square mile of area. The investigation consisted of 4.71 miles east bound and 4.69 miles in the westbound direction. The 2011 AADT data provided by ODOT estimated 16,200 VPD for the pavement, while the plan-sets showed the design ADT to be 21,400 VPD.

The project was completed in 1985 by Koss. The CRCP is nine inches thick with 0.50% and 0.08% longitudinal and transverse steel respectively, according to the plan sets provided by ODOT. That makes this pavement not only the thinnest, but also the

lowest steel content of all of the pavements studied. The pavement is supported by four inches of course aggregate bituminous base and twelve inches of method b subbase with jointed plain concrete shoulders.

A visual inspection was conducted on July 7, 2011. A thousand foot section was also inspected for results comparable to Federal Highway Administration (FHWA) Report Number: FHWA-RD-94-174. An additional five-hundred foot crack spacing survey was also performed on the first five-hundred feet of the thousand foot section studied in the FHWA report.

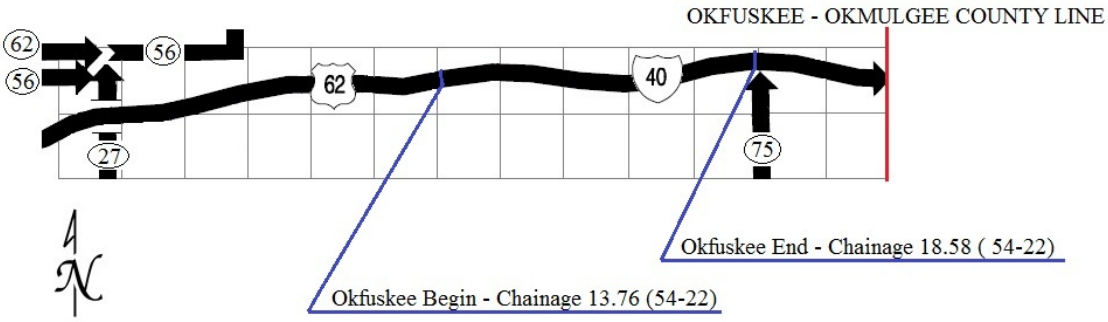

Figure A.20 Layout of the Okfuskee county CRCP visited during inspection. The pavement is marked by county name, begin and end points, along with chainage and control section number.

A.5.2 Inspection Details

The inspection began in the eastbound direction; Figure A.21 shows the terminal joint at the project beginning. The terminal joint has some signs of deterioration. The eastbound direction contained several types of Y-cracks (Figure A.22), but seemed to have many places where the transverse cracks were close together. Figure 2.23 shows a place where five transverse cracks all occurred within an eight-foot section of pavement. Figure A.22 right does contain a Y-crack on the far left, but in most cases the closely spaced transverse cracks did not consist of Y-cracks, and in most cases the

close transverse cracks did not show signs of punch-out or failure. However, a few did, as shown in Figure A.22.

Figure A.21 Deteriorated terminal joint at project beginning

Figure A.22 Two different types of Y-cracks found in the area

Figure A.23 Closely spaced transverse cracks

This pavement showed the first signs of a Y-crack leading to a punch-out (see Figure A.24). However, the majority of failures that were not patched seemed to be caused by closely spaced transverse cracks with intersecting longitudinal cracks, as shown in Figure A.25. Overall the eastbound lane was in poor shape with thirty-three patches in the outside lane alone over the length of the project.

Figure A.24 Two instances where a Y-crack seemed to be developing into a punch-out

Figure A.25 Punchouts forming between closely spaced transverse cracks

Figure A.26 shows the terminal joint at the beginning (left) and the end (right) of the west bound inspection. The joints appeared to be in poor shape with several patches. The westbound lane had many patches of both asphalt and Portland cement. Some of the patches filled with asphalt left an outline that seemed to look like a Y-crack, see Figure A.27, while many of the patches seemed to be caused by closely spaced transverse cracks with longitudinal connecting cracks, see Figure A.28. By observing the westbound lane it was clear that along with the numerous patches, asphalt joint sealant had been applied to many of the transverse cracks along the roadway, see Figure A.29.

Figure A.26 (left) Terminal joint at west bound beginning, (right) terminal joint at west bound end

Figure A.27 Y-shaped patches

Figure A.28 Patches caused by closely spaced transverse cracks

Figure A.29 Transverse cracks sealed with an asphalt joint sealant

While several Y-cracks showed signs of breaking up, Figure A.30 (left), most of the observed distresses appeared to be caused by closely spaced transverse cracks, see Figure A.30 (right). It was also noted that the image in Figure A.30 (right) showed a longitudinal steel splice. The steel appeared to be approximately two inches from the concrete surface.

Figure A.30 (left) Y-crack breaking up, (right) distress caused by close transverse cracking

As mentioned previously, the east bound lane was in poor shape, with thirty-three patches in the outside lane alone; however, the east bound lane was in significantly better shape than the west bound lane, which recorded two-hundred seventy-seven patches in the outside lane alone. One factor that could be helping provide these failures is the pavements thickness. This pavement matches Atoka County for the thinnest CRCP pavement in the state at nine inches.

A.6 Atoka County

A.6.1 Overview

The series of CRC pavements studied in Atoka County lie along US 69, just north of the town Atoka. Several of the CRC pavements have been overlaid either by asphalt or concrete white-topping; therefore, the entire pavement was not available for inspection. Figure A.31 shows the pavements that were a part of the inspection, each square in the figure represents one square mile of area.

The inspection consisted of three CRCP projects. The ODOT project numbers for the sites are F-299(99), F-299(45), and F-299(35). The following sections will discuss

the construction details of each project referring to them as Atoka 1, Atoka 2, and Atoka 3 respectively. The 2011 AADT data shows that the pavements transport 16,300, 14,700, and 14,700 VPD; while the plan-sets show that the pavements were designed to carry 9,000, 10,800, and 7,500 VPD correspondingly.

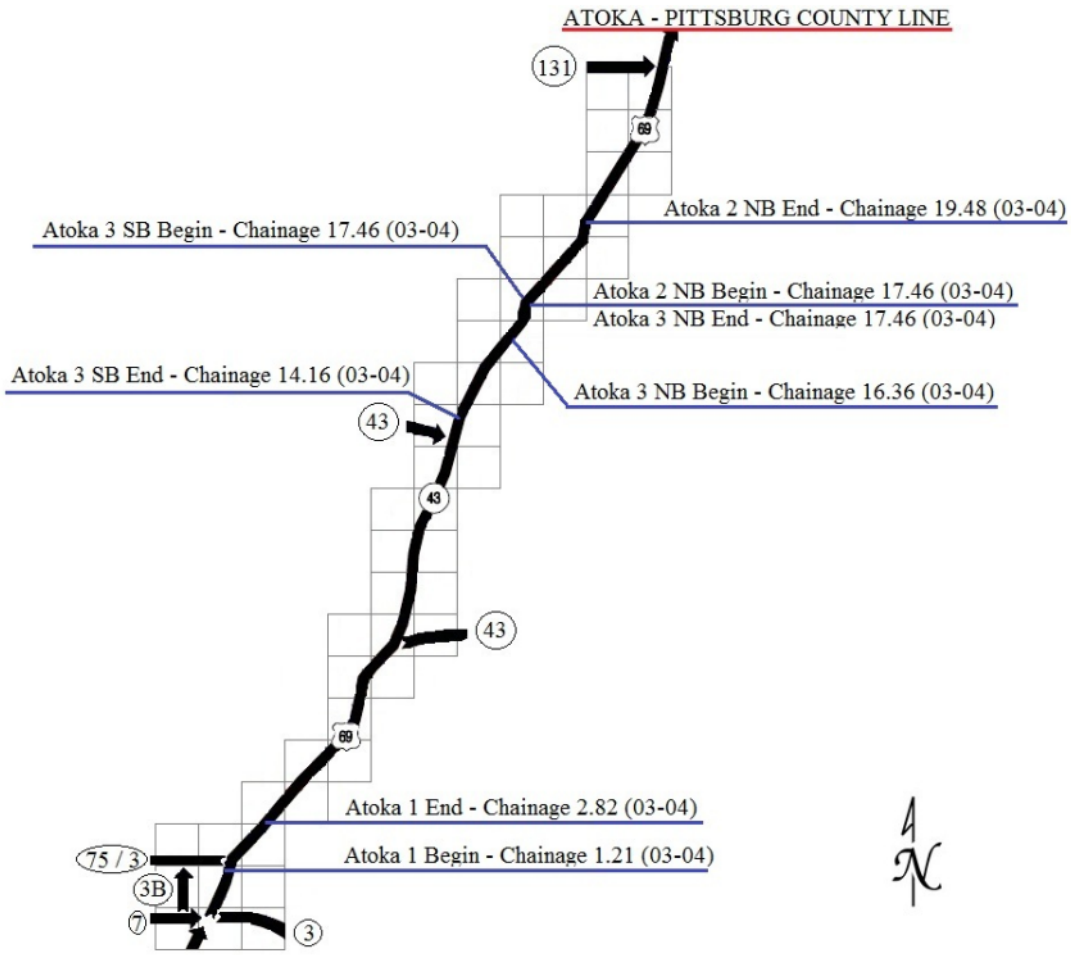

Figure A.31 Layout of the Atoka county CRCP's visited during inspection. The pavements are marked by county name, begin and end points, along with chainage and control section number.

A.6.2 Atoka 1

Atoka 1 was completed in 1989 by Wittwer. The pavement is ten inches thick with 0.61% and 0.07% longitudinal and transverse steel, according to the specifications provided by ODOT. The pavement is sitting on top of three inches of type A AC and twelve inches of aggregate base with jointed plain concrete shoulders.

A visual inspection was performed on July 8, 2011. The inspection of Atoka 1 consisted of 1.25 miles north bound and 1.37 miles in the south bound direction; this is noticeably less than the total project length because the stretch had two bridges. The visual inspection consisted of counting Y-cracks and patches, while photographing subjects of interest. The chainage of each patch and photograph was also noted for future reference. While inspecting this particular pavement another test was also performed; it consisted of measuring the distance between cracks for a random five-hundred foot section.

A.6.3 Atoka 1 Inspection Details

The pavement in the northbound lane inspection contained several patches. Many of these patches were not full lane patches and punchouts had developed near the patch (Figure A.32 right), while some patches showed signs of distress (Figure A.32 left). Most of the w-shaped beams used at terminal joints showed signs of deterioration. Signs of deterioration were spalling of the CRCP, AC patching, and missing sections of the w-shape, see Figures A.33 and A.34.

Figure A.32 Small patch with distress developing close by

Figure A.33 Terminal joints showing signs of spalling

Figure A.34 Terminal Joints with different kinds of distress

The pavement did exhibit Y-cracks; however, the first Y-crack in the northbound lane did not occur until 0.13 miles into the project. Figure A.35 shows a typical Y-crack for the area. It was noted that a few of the Y-cracks appeared to be leading to punchouts, mainly because of longitudinal cracks connecting the two legs of the “Y”, see Figure A.36.

Figure A.35 Typical Y-crack for the area

Figure A.36 Y-cracks leading to punch-out and eventually failure

The southbound lane showed many of the same characteristics as the northbound lane. Several of the w-shaped beams at the terminal joints had deterioration, see Figure A.37. Figure A.38 (left) shows a patch starting to break up and possibly develop into a punch-out; meanwhile, Figure A.38 (right) shows the stretch of roadway in the southbound lane where the crack spacing measurements were taken. Overall, both lanes seemed to be in similar condition, and both recorded the same number of patches; however, the south bound lane contained one-hundred more Y-cracks than the north bound lane.

Figure A.37 Terminal joints showing distress

Figure A. 38 (left) patch showing signs of distress (right) area of road where crack survey was taken.

A.6.4 Atoka 2

Atoka 2 was completed in 1986 by Koss. The pavement is nine inches thick with 0.50% and 0.08% longitudinal and transverse steel respectively, according to the specifications provided by ODOT. The pavement is sitting atop three inches of type C

AC with jointed plain concrete shoulders. Type C AC is equivalent to a super pave S5 mix that has a 3/8 inch NMS.

A visual inspection was performed on July 8, 2011. The inspection of Atoka 2 consisted of 1.37 miles in the northbound lane only; the southbound lane was not CRCP and appeared to be a concrete overlay. The visual inspection consisted of counting Y-cracks and patches per mile, while photographing subjects of interest. The chainage form the beginning of the project to the location of every patch and photograph was also documented for future reference.

A.6.5 Atoka 2 Inspection Detail

Atoka 2 north bound showed wear throughout the length of the pavement. The roadway surface tines had been greatly worn down in most places; this can be seen in Figure A.39. The construction and terminal joints also showed signs of deterioration, mainly spalling of the pavement edge along the joint, as seen in Figure A.40. Several large patches displayed map cracking as seen in Figure A.40 (right); however, these sections had not led to any punch-out or other type of failure. The project recorded four patches over its length, and none of the patches showed any clues as to what may have caused them. The roadway also contained many Y-cracks, with none of them showing signs of developing into punchouts.

Figure A.39 Spalled terminal joint with worn roadway surface

Figure A.40 Spalled terminal joints, with the (right) displaying map-cracking

A.6.6 Atoka 3

Atoka 3 was completed in 1986 by Northern Improvements. The pavement is nine inches thick with 0.50% and 0.08%, longitudinal and transverse steel respectively. The thickness and steel contents were taken from the specifications provided by ODOT. The pavement is sitting atop three inches of type C ac (3/8 Nominal Maximum Aggregate (NMS)), with jointed plain concrete shoulders.

A visual inspection was conducted on July 8, 2011. The inspection of Atoka 3 consisted of 1.03 miles in the northbound lane and 2.15 miles in the south bound lane. The visual inspection consisted of counting Y-crack and patches, while photographing subjects of interest. The chainage of each patch and photograph was also documented for future reference. A crack spacing measurement procedure was also implemented to determine the mean spacing, standard deviation, and coefficient of variation for a five-hundred foot section of pavement in both directions.

A.6.7 Atoka 3 Inspection Details

The northbound lane of Atoka 3 had many patches, especially for the length of roadway inspected. The pavement had twenty-two total patches over a 1.08-mile stretch. The majority of the patches seemed to be caused by closely spaced transverse cracks intersected by longitudinal cracks, as seen in Figures A.41 and A.42. However,

a few of the patches seemed to have been caused by the breakup of Y-cracks. The Y-cracks seemed to have longitudinal cracks intersecting the two legs of the “Y”, as seen in Figure A.43 (left). Several of the patches left no evidence of the cause of the patch, as seen in Figure A.43 (right). It was noted that in Figure A.43 (right) the longitudinal steel was protruding through the patch. Despite the fact that a few of the Y-cracks appeared to have caused failures, the majority of the distress seemed to be the result of closely spaced transverse cracks being intersected by longitudinal cracks, see Figure A.44.

Figure A.41 Patches caused by closely spaced transverse cracks

Figure A.42 More patches cause by closely spaced transverse cracks

Figure A.43 (left) Patch caused by a Y-crack (right) patch with steel protruding through

Figure A.44 Two transverse cracks intersected by a longitudinal crack

The southbound lane appeared to be in worse condition that the northbound lane; it contained more patches per mile and showed promise for future patches. Like the Okfuskee County project, several of the transverse cracks had been sealed with an asphalt crack sealant material. The majority of the visible patches seemed to be caused by transverse cracks being intersected by longitudinal cracks, see Figures A.45 – A.47. Several future and developing punchouts were also noted and appeared to be caused by the same phenomenon, see Figure A.48. The southbound lane displayed several instances where multiple transverse cracks were intersected by longitudinal cracks, see Figure A.49. Despite the majority of the distresses appearing to be caused by transverse cracks being intersected by longitudinal cracks, a few patches seemed to display evidence of a Y-crack causing the patch, see Figure A.50. However, the instances were very miniscule compared to the other cause.

Figure A.45 Transverse cracks intersected by longitudinal cracks

Figure A.46 Transverse cracks intersected by longitudinal cracks

Figure A.47 Transverse cracks intersected by longitudinal cracks

Figure A.48 Two transverse cracks intersected by a longitudinal crack

Figure A.49 Multiple transverse cracks intersected by a longitudinal crack

Figure A.50 Patches that appear to be the result of a failed Y-crack

A.7 Pittsburg County

A.7.1 Overview

The series of CRC pavements studied in Pittsburg County lie along US 69, between the town of McAlester and the McIntosh-Pittsburg County line. Figure A.51 shows the location of each project for the region, where one square represents one square mile of area.

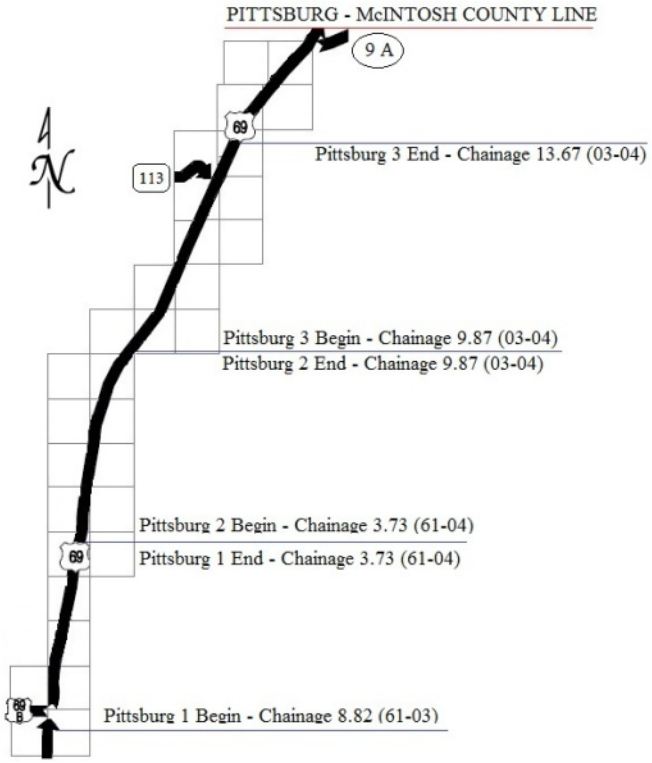

Figure A.51 Layout of the Pittsburg county CRCPs visited during inspection. The pavements are marked by county name, begin and end points, along with chainage and control section number.

Three CRCP projects were inspected in Pittsburg County. The ODOT project numbers for these projects are MAF-186(183), MAF-186(185), and DPIY-204(001). These projects will be referred to as Pittsburg 1, Pittsburg 2, and Pittsburg 3, respectively. According to the 2011 AADT provided by ODOT, Pittsburg 1 and 2 were estimated to handle 16,100 VPD, while Pittsburg 3 was assessed to carry 15,200 VPD; meanwhile, the plan-sets for the projects showed the design ADT to be 20,000 for Pittsburg 1 and 2 and 9,000 for Pittsburg 2.

All three of the Pittsburg County projects have the same characteristics; the only differing factor between the projects is the year of completion, with Pittsburg 1 completed in 1991, Pittsburg 2 completed in 1989, and Pittsburg 3 completed in 1994. Otherwise, the pavements were all constructed by Koss and are ten inches thick, with 0.61% and 0.07% longitudinal and transverse steel respectively. The steel contents and thicknesses were taken from the specifications provided by ODOT. The pavements are supported by four inches of open graded concrete base and twelve inches of stabilized aggregate, with jointed plain concrete shoulders.

A visual inspection for Pittsburg County was conducted over a course of two days with the northbound direction being inspected July 9, 2011 and the southbound direction inspected on July 10, 2011. The visual inspections consisted of counting Y-cracks and patches, while photographing subjects of interest. The chainage of each patch and photograph was also noted for future reference.

A.7.2 Pittsburg 1 Inspection Details

Overall Pittsburg 1 north bound was in good shape, but it showed signs of future deterioration. The terminal joints at the project were in good shape overall, displaying only a small amount of spalling, see Figure A.52. The pavement contained a few distresses (Figure A.53 (left)) that seemed to be random and unrelated to any cracking. It was also noted that many cracks, both Y-cracks and transverse cracks had spalling, see Figure A.53 (right). There were also a few Y-cracks showing signs of beginning to develop into punchouts, see Figure A.53 (right). There were several other places along the pavement where closely spaced transverse cracks were being intersected by longitudinal cracks and beginning to form punchouts, see Figure A.54. The North bound lane also contained a few patches of map-cracking, see Figure A.55. Despite all of this the northbound lane only contained two patches over its four mile length, see Figure A.56.

Figure A.52 Terminal joints at north bound beginning and end

Figure A.53 (Left) Large circular distress, (right) Spalled Y-crack beginning to break up

Figure A.54 Two developing punchouts

Figure A.55 Stretch of pavement showing signs of map-cracking

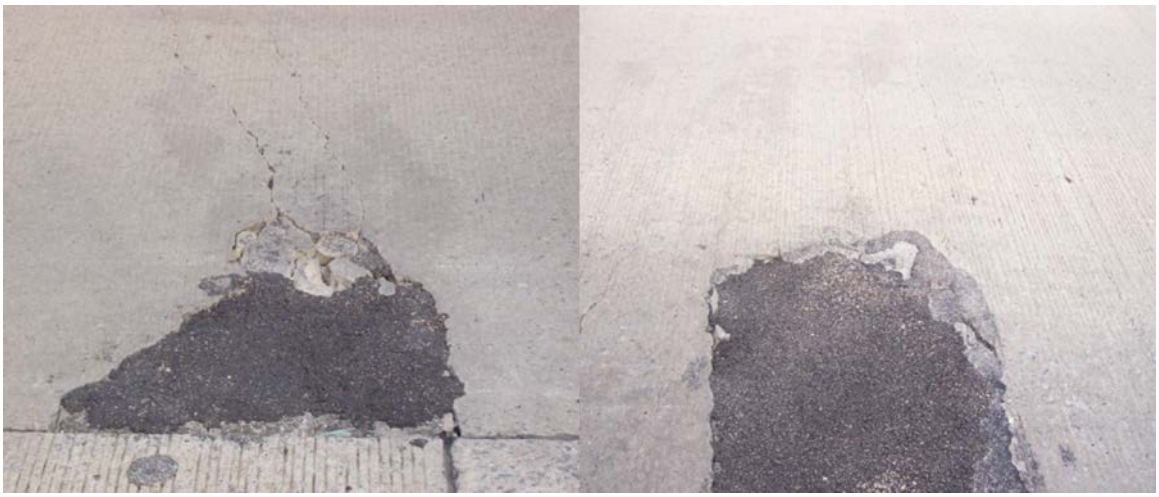

Figure A.56 The two patches in the north bound lane

The northbound lane also contained several places where past testing had been done, see Figure A.57. These testing sites consisted of several cores. Some of the cores had been taken from along the outside edge of the pavement and even in the shoulder. A few cores were also taken out of the roadway, and showed signs of sensors of some type being implemented, see Figure A.58.

Figure A.57 (right) road test sign found beside roadway, (left) one of several large cores taken

Figure A.58 (left) cores taken from shoulder, (right) core with censor wire extending to shoulder

The southbound lane was in a similar condition to the northbound lane. The southbound lane did show more deterioration at the terminal joints, Figure A.59. Like the northbound lane, the southbound lane seemed to have several instances where closely spaced transverse cracks led to distress, see Figure A.60 (left). The south

bound lane also contained a Y-crack beginning to develop into a punch-out, but this was a rare case when compared to the closely spaced transverse cracks leading to distresses, see Figure A.60 (right).

Figure A.59 Terminal joints at the beginning and end of the project

Figure A.60 (left) Two closely spaced transverse cracks, (right) Y-crack developing into a punch-out

Overall both directions of CRCP had very similar characteristics. Both contained a high Y-crack per mile average and a low number of patches, while showing signs of

future deterioration. They were also similar in that the main cause of deterioration seemed to be closely spaced transverse cracks being intersected by longitudinal cracks.

A.7.3 Pittsburg 2 Inspection Details

The northbound lane of Pittsburg 2 was in overall good shape. Figure A.61 shows the terminal joints on each end of the project; both appear to be in good shape, displaying only a minor amount of spalling. The pavement recorded just two patches over its six-mile length, despite the occurrence of Y-cracking. The patches did not leave any evidence of what may have caused them; however, there was one Y-crack that appeared to be developing into a punch-out, see Figure A.62. Even though one Y-crack seemed to be developing into a punch-out, none of the other Y-cracks showed this.

Figure A.61 Terminal joints on each end of the project

Figure A.62 Y-crack developing into a punch-out

The southbound lane of Pittsburg 2 was in worse condition than the northbound lane. Figure A.63 shows the terminal joints at the project beginning and end, which like the north bound lanes, were in good condition, displaying only minor signs of spalling. The southbound lane contained eight patches over its six-mile length, which is four times more than the northbound lane. All of the patches seemed to be the result of closely spaced transverse cracks, see Figures A.64. It was noted during the inspection that the third mile of the project contained a heavy amount of Y-cracking -- two-hundred and eight cracks within the mile. However, this stretch of pavement only contained one patch. Despite the occurrence of patches and Y-cracks, there was no evidence of a Y-crack leading to a punch-out or patch over the six miles of pavement in the southbound direction.

Figure A.63 Terminal joints at the project beginning and end

Figure A.64 Patches formed near closely spaced transverse cracks

A.7.4 Pittsburg 3 Inspection Details

Pittsburg 3 north bound was in good shape as far as patches, recording zero over its 2.66-mile length. However, most of the project contained map-cracking, but no punchouts or patches had developed as a result of the map-cracking. The sections of roadway that did have map-cracking reported slightly lower numbers of Y-cracks. Figure A.65 shows the map-cracking. Figure A.66 shows the w-shaped beams used at

the joints; these joints show signs of spalling, which could possibly be enhanced by the map-cracking.

Figure A.65 Close ups showing map-cracking

Figure A.66 Terminal joints at project beginning and end

Pittsburg 3 south bound displayed many of the same issues as its northbound counterpart. The southbound lane contained map-cracking throughout its entire length, see Figure A.67. Despite having one of the lowest amounts of Y-cracks per mile, the

project did have three patches over its 2.62-mile length. None of the patches seemed to be related to the Y-crack phenomenon, Figure A.68. Figure A.69 shows the terminal joints at the projects beginning and end, both of which show deterioration.

Figure A.67 Map cracking in the south bound lane

Figure A.68 Patches in the southbound lane

Figure A.69 Terminal joints at the beginning and end of the project

Overall the CRCP at Pittsburg 3 appeared to be in good shape, containing only three patches over it 7.28-mile length. However, the presence of map-cracking and close transverse cracking interconnected by longitudinal cracks seems to hint at future deterioration.

A.8 Noble County

A.8.1 Overview

The CRC pavement investigated in Nobles County is located on Interstate 35. The project begins five and a half miles north of Perry Oklahoma and extends north for just over five and a half miles. Figure A.70 shows the location of the pavement with each square in the figure representing one square mile of area. The pavement survey consisted of 5.47 miles in the northbound direction and 5.46 miles of pavement in the south bound direction. The 2011 AADT data provided by ODOT estimated 16,554 VPD for the roadway, while the plan sets showed the 20 year design ADT to be 20,000.

The project was completed in 1988 by Northern Improvements. The CRCP is ten inches thick with 0.61% and 0.11% longitudinal and transverse steel respectively, according to the plan sets provided by ODOT. According to a document provided by

ODOT epoxy coated steel was used in the north bound only. The 0.11% transverse steel gives the pavement the highest transverse reinforcing ratio of all of the pavements observed in the study. The pavement is supported by four inches of econocrete with a method B subbase and has jointed plain concrete shoulders.

A visual inspection was conducted on March 15, 2012. The visual inspection consisted of counting Y-cracks and patches, while photographing subjects of interest along the pavement. The chainage of each patch and photograph was also noted for future reference.

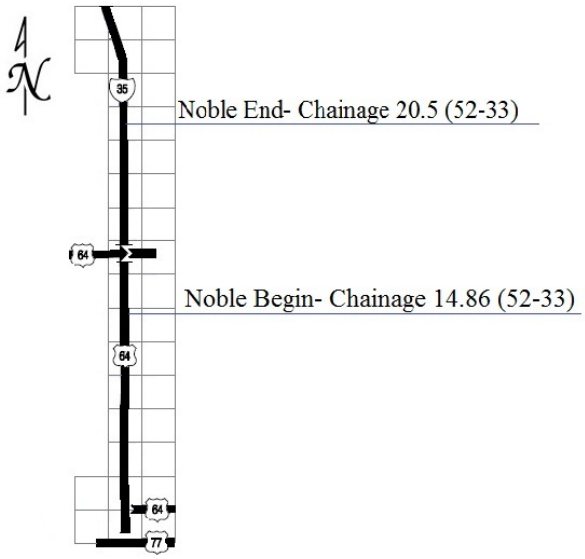

Figure A.70 Layout of the Noble county CRCP visited during inspection. The pavement is marked by county name, begin and end points, along with chainage and control section number.

A.8.2 Inspection Details

The inspection began in the northbound direction. The first mile of pavement had a crack spacing that varied greatly, it ranged from stretches of pavement having 2-3' spacing to stretches that had 10-20' spacing. After the first mile of CRCP the crack spacing seemed to become more regular. The pavement contained Y-cracks, but also

contained many meandering cracks that at first glance appeared to be Y-cracks; however, the meandering cracks stopped just short of a “Y” intersection. Examples of this can be seen below in Figures A.71 and A.72. Most forming punchouts seemed to be developing between closely spaced transverse cracks with intersecting longitudinal cracks, as seen in Figure A.73.

Figure A.71 Meandering cracks with small patches stopping just short of a “Y” intersection

Figure A.72 A transverse crack stopping just short of a “Y” intersection with another transverse crack.

Figure A.73 Punchouts forming between closely spaced transverse cracks

The pavement did have several stretches where short longitudinal cracking was seen, along with some Portland cement patches that contained longitudinal cracks, see Figure A.74. While most of the distress seemed to be from closely spaced transverse cracks or from corner breaks at construction joints or patches, see Figure A.75. A few Y-cracks did show signs of distress, but in all of these cases a longitudinal crack intersected the region isolated by the branching of the crack. In all cases these distresses formed at the edges of the lane. Figures A.76 – A.78 show the cases where a Y-crack seemed to lead to a punch-out.

Figure A.74 Patches with longitudinal cracking

Figure A.75 Patches forming between closely spaced transverse cracks and at construction joints

Figure A.76 Punchouts/ patches forming near Y-cracks

Figure A.77 Punchouts/ patches forming near Y-cracks

Figure A.78 Punchouts/ patch forming near Y-cracks

Overall, the north bound lane was in relatively poor shape, containing 27 patches, some of this could be due to the fact that epoxy coated steel was used in place of black steel, which was used in the south bound lane. Of the 852 Y-cracks observed in the 5.47-mile pavement, only five showed sign of forming a punch-out.

The southbound direction was in slightly better condition than the northbound direction. The southbound direction contained 16 patches. A few of the patches in the south bound direction left clues as to what may have led to their existence. Three of the patches observed occurred at construction joints, see Figure A.79 (left). Meanwhile several of the other patches were small asphalt patches that seemed to be related to some sort of surface distress. The crack spacing in the south bound lane was not as erratic as those of the north bound lane; however, closely spaced transverse cracks leading to punchouts were observed, see Figure A.79 (right). Of the 849 Y-cracks observed in the south bound direction none of them appeared to be developing into a punch-out.

Figure A.79 (Left) Patch at construction joint, (Right) closely spaced transverse cracks with a patch

A.9 Washita County

A.9.1 Overview

The CRC pavement investigated in Washita County is located on Interstate 40. The project begins at the Beckham-Washita County line and extends east for just over three miles. Figure A.80 shows the location of the pavement with each square in the figure representing one square mile of area. The pavement survey consisted of 2.08 miles in the westbound direction and 2.03 miles of pavement in the east bound direction. The 2011 AADT data provided by ODOT estimated 19,567 VPD for the roadway, while the plan sets showed 22,000 as the twenty-year design ADT.

The project was completed in 1992 by Koss. The CRCP is ten inches thick with 0.61% and 0.07% longitudinal and transverse steel respectively, according to the plan sets. The pavement is supported by four inches of open graded concrete base and four inches of aggregate base with jointed plain concrete shoulders.

A visual inspection was conducted on March 17, 2012. The inspection consisted of counting Y-cracks and patches, while photographing subjects of interest along the pavement. The chainage of each patch and photograph was also documented for future reference.

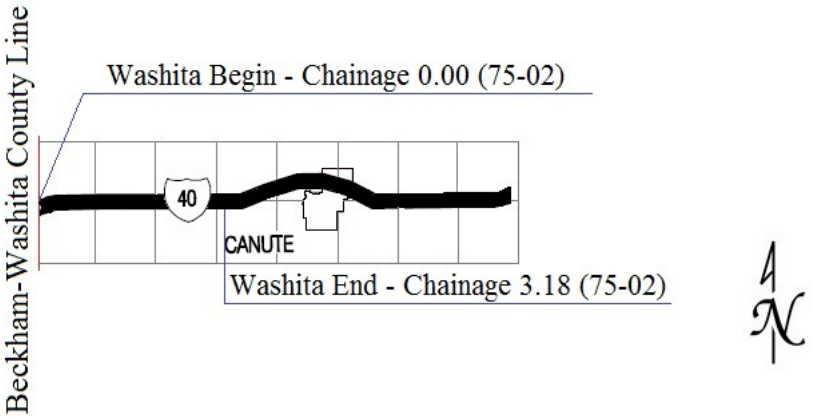

Figure A.80 Layout of the Washita county CRCP visited during inspection. The pavement is marked by county name, begin and end points, along with chainage and control section number.

A.9.2 Inspection Details

The inspection began in the westbound direction. For the first 0.65 mile, until the first construction joint, the pavement contained a lot of longitudinal cracking and certain areas even had map-cracking. The first five hundred feet of the project had the majority of the map-cracking, thereby resulting in eighteen of the twenty one patches observed in the west bound lane. Photographs of what was seen can be seen in Figure A.81. A few of the distresses in the area also appeared to be related to steel placement, see Figure A.82. The roadway contained many transverse cracks that were spaced close together and appeared to be on intersecting paths but stopped approximately 3-6” short of a “Y” intersection, see Figure A.82. Despite having other distress types the pavement did contain 362 Y-cracks over its 2.08-mile length. None of the Y-cracks showed signs of developing into punchouts, despite punchouts and patches located adjacent to the Y-cracks, see Figure A.84.

Figure A.81 Map-cracking showed at or near patches in the roadway

Figure A.82 Roadway patches with exposed steel

Figure A.83 Y-cracks with patches located near them

Figure A.84 Closely spaced, nearly intersecting transverse cracks

The eastbound lane of traffic appeared to be in better condition, containing only eleven patches over its length. The pavement did contain a relatively high number of Y-cracks within the first mile, Figure A.85. However, many of the transverse cracks did not extend entirely across the lane of traffic, with the crack spacing being very irregular with cracks that tended to meander, see Figure A.86. After the first mile of the project the Y-crack count decreased, with many cracks appearing to be Y-cracks at first glance, but at the “Y” point one crack stopped just short. Much like what was seen in the westbound direction, see Figure A.87 (left). During the third mile of the project the Y-crack count picked back up along with the longitudinal cracking, see Figure A.87 (right). Overall, the eastbound lane contained less patches than the westbound lane, with a few of the patches coming at construction joints, and did not exhibit map-cracking. Despite containing 391 Y-cracks over its 2.03 mile length, the pavement did not have any Y-cracks showing signs of distress.

Figure A.85 Typical Y-cracks observed in the inspection

Figure A.86 Transverse cracks not extending entirely across the roadway

Figure A.87 (Left) two transverse cracks nearly connecting (right) longitudinal cracking

A.10 McIntosh County

A.10.1 Overview

The CRC pavement investigated in McIntosh County is located on Interstate 40. The project begins about one mile east of the Highway 150 and Interstate 40 junction and extends west for nearly four and a quarter miles. Figure A.88 shows the location of the pavement with each square in the figure representing one square mile of area. The pavement survey consisted of 4.11 miles in the eastbound direction and 4.12 miles in the west bound direction. The 2011 AADT provided by ODOT estimated 12,000 VPD, while the twenty-year design ADT from the plan sets yielded 21,000 VPD.

The project was completed in 2005 by Duit. The CRCP is a nine-inch thick unbonded overlay with 0.71% and 0.08% longitudinal and transverse steel respectively, according to the plan sets. The unbonded overlay sits atop nine inches of mesh dowel concrete pavement and four inches of fine aggregate bituminous base with Portland cement concrete shoulders. This makes the project the only overlay studied during the investigations.

A visual inspection was conducted on March 18, 2012. The inspection consisted of counting Y-cracks and patches, while photographing all subjects of interest along the

pavement. The chainage of each patch and photograph was also noted for future reference.

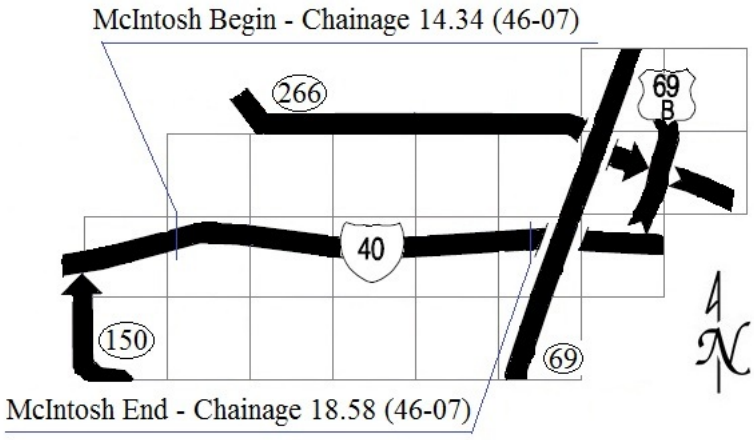

Figure A.88 Layout of the McIntosh County CRCP visited during inspection. The pavement is marked by county name, begin and end points, along with chainage and control section number.

A.10.2 Inspection Details

The inspection began in the eastbound direction. Despite only being seven years old the east bound pavement had seven patches. Two of the seven patches occurred near construction joints, see Figure A.89. The roadway contained unusual cracking patterns not seen in any of the other CRCPs. The pavement had many circular cracks which typically intersected other transverse cracks because of their large radius, see Figures A.90 and A.91. Typically these circular cracks occurred where a cluster of transverse cracks were located as seen in the previous two figures. The pavement did contain a few Y-cracks, see Figure A.92, but the pavement contained much lower Y-crack numbers than any of the other pavements studied in this investigation. The eastbound lane contained a total of 340 Y-cracks over its 4.11-mile length. Despite a low Y-crack count patches were still observed.

Figure A.89 Patches occurring next to construction joints

Figure A.90 Circular cracks intersecting transverse cracks

Figure A.91 A circular crack intersecting multiple transverse cracks

Figure A.92 Typical Y-cracks seen in the East bound direction

The West bound lane of CRCP was in much better condition than the East bound lane. The West bound lane had no patches over its 4.12 mile length; however, a few steel placement issues were observed in the pavement, see Figure A.93. This direction of pavement had 224 Y-cracks over its entire length. When the transverse crack spacing was large (10-15') fewer Y-cracks were seen, but the transverse cracks did tend to meander more. For the most part, Y-cracking was concentrated in areas of closely spaced transverse cracks. However, no Y-cracking related punchouts or patches were observed in either direction. Overall, the roadway showed little wears,

displaying deep tines and small crack widths. While this is good for durability, it made Y-crack observation more difficult.

Figure A.93 Exposed steel on the surface of the pavement

APPENDIX B - HIPERPAVE III DETAILED RESULTS

Table B.1 OK-1 Sub-Variable Averages at 72 Hours

HIPERPAV Input Variables	HIPERPAV Outputs	Data Group Number	Average			
			7:00 A.M.	10:00A.M.	3:00 P.M.	
Construction Time	Crack Spacing Average (ft.)	1	7.73	8.10	10.33	
	Crack Spacing Standard Deviation (ft.)	2	1.76	1.80	2.26	
	Crack Width (in.)	3	0.029	0.029	0.027	
			1/12/1988	7/26/1988	10/22/1988	
Construction Date	Crack Spacing Average (ft.)	4	11.19	6.39	8.55	
	Crack Spacing Standard Deviation (ft.)	5	2.53	1.47	1.81	
	Crack Width (in.)	6	0.024	0.032	0.029	
			None	Single Coat	Double Coat	Plastic Sheeting
Curing Method	Crack Spacing Average (ft.)	7	7.95	8.55	8.60	9.76

HIPERPAV Input Variables	HIPERPAV Outputs	Data Group Number	Average			
	Crack Spacing Standard Deviation (ft.)	8	1.79	1.94	1.89	2.14
	Crack Width (in.)	9	0.030	0.029	0.028	0.027
			AC (Rough)	AC (Smooth)		
Base Material	Crack Spacing Average (ft.)	10	7.41	10.00		
	Crack Spacing Standard Deviation (ft.)	11	1.57	2.30		
	Crack Width (in.)	12	0.026	0.033		
			100 psi	150 psi	200 psi	
Subgrade Support	Crack Spacing Average (ft.)	13	8.67	8.76	8.71	
	Crack Spacing Standard Deviation (ft.)	14	1.94	1.94	1.94	
	Crack Width (in.)	15	0.029	0.028	0.028	

HIPERPAV Input Variables	HIPERPAV Outputs	Data Group Number	Average			
			Siliceous Gravel	Granite	Limestone	
Aggregate Type	Crack Spacing Average (ft.)	16	7.86	8.19	10.10	
	Crack Spacing Standard Deviation (ft.)	17	1.82	1.84	2.16	
	Crack Width (in.)	18	0.029	0.029	0.027	

Table B.2 OK-1 Sub-Variable Averages at 1 Year

HIPERPAV Input Variables	HIPERPAV Outputs	Data Group Number	Average			
			7:00 A.M.	10:0 A.M.	3:00 P.M.	
Construction Time	Crack Spacing Average (ft.)	1	5.16	5.17	5.27	
	Crack Spacing Standard Deviation (ft.)	2	1.76	1.77	1.87	
	Crack Width (in.)	3	0.056	0.056	0.054	
			1/12/1988	7/26/1988	10/22/1988	

HIPERPAV Input Variables	HIPERPAV Outputs	Data Group Number	Average			
Construction Date	Crack Spacing Average (ft.)	4	6.3	4.58	4.72	
	Crack Spacing Standard Deviation (ft.)	5	2.27	1.48	1.66	
	Crack Width (in.)	6	0.046	0.067	0.052	
			None	Single Coat	Double Coat	Plastic Sheeting
Curing Method	Crack Spacing Average (ft.)	7	5.13	5.23	5.23	5.21
	Crack Spacing Standard Deviation (ft.)	8	1.75	1.81	1.81	1.84
	Crack Width (in.)	9	0.056	0.055	0.055	0.054
			AC (Rough)	AC (Smooth)		
Base Material	Crack Spacing Average (ft.)	10	4.56	5.83		
	Crack Spacing Standard Deviation (ft.)	11	1.46	2.15		
	Crack Width (in.)	12	0.048	0.061		
			100 psi	150 psi	200 psi	
Subgrade Support	Crack Spacing Average (ft.)	13	5.19	5.21	5.19	

HIPERPAV Input Variables	HIPERPAV Outputs	Data Group Number	Average			
	Crack Spacing Standard Deviation (ft.)	14	1.80	1.80	1.80	
	Crack Width (in.)	15	0.055	0.055	0.055	
			Siliceous Gravel	Granite	Limestone	
Aggregate Type	Crack Spacing Average (ft.)	16	5.07	5.18	5.35	
	Crack Spacing Standard Deviation (ft.)	17	1.73	1.79	1.89	
	Crack Width (in.)	18	0.057	0.055	0.053	

Table B.3 OK-2 Sub-Variable Averages at 72 Hours

HIPERPAV Input Variables	HIPERPAV Outputs	Data Group Number	Average			
			7:00 A.M.	10:00A.M.	3:00 P.M.	
Construction Time	Crack Spacing Average (ft.)	1	5.85	6.16	7.79	

HIPERPAV Input Variables	HIPERPAV Outputs	Data Group Number	Average			
	Crack Spacing Standard Deviation (ft.)	2	1.41	1.49	1.79	
	Crack Width (in.)	3	0.023	0.023	0.024	
			1/12/1987	7/26/1987	10/22/1987	
	Crack Spacing Average (ft.)	4	9.37	4.40	6.03	
Construction Date	Crack Spacing Standard Deviation (ft.)	5	2.13	1.11	1.46	
	Crack Width (in.)	6	0.021	0.024	0.025	
			None	Single Coat	Double Coat	Plastic Sheeting
	Crack Spacing Average (ft.)	7	5.98	6.61	6.73	7.08
Curing Method	Crack Spacing Standard Deviation (ft.)	8	1.42	1.57	1.60	1.67
	Crack Width (in.)	9	0.024	0.023	0.023	0.024

HIPERPAV Input Variables	HIPERPAV Outputs	Data Group Number	Average		
			AC (Rough)	AC (Smooth)	
Base Material	Crack Spacing Average (ft.)	10	5.81	7.39	
	Crack Spacing Standard Deviation (ft.)	11	1.28	1.86	
	Crack Width (in.)	12	0.021	0.026	
			100 psi	150 psi	200 psi
Subgrade Support	Crack Spacing Average (ft.)	13	6.59	6.61	6.60
	Crack Spacing Standard Deviation (ft.)	14	1.57	1.56	1.56
	Crack Width (in.)	15	0.023	0.023	0.023
			Siliceous Gravel	Granite	Limestone
Aggregate Type	Crack Spacing Average (ft.)	16	5.95	6.20	7.64

HIPERPAV Input Variables	HIPERPAV Outputs	Data Group Number	Average			
	Crack Spacing Standard Deviation (ft.)	17	1.40	1.50	1.80	
	Crack Width (in.)	18	0.023	0.023	0.024	

Table B.4 OK-2 Sub-Variable Averages at 1 Year

HIPERPAV Input Variables	HIPERPAV Outputs	Data Group Number	Average			
			7:00 A.M.	10:00A.M.	3:00 P.M.	
Construction Time	Crack Spacing Average (ft.)	1	4.08	4.15	4.25	
	Crack Spacing Standard Deviation (ft.)	2	1.39	1.42	1.54	
	Crack Width (in.)	3	0.047	0.048	0.046	
			1/12/1987	7/26/1987	10/22/1987	
Construction Date	Crack Spacing Average (ft.)	4	4.79	3.75	3.95	

HIPERPAV Input Variables	HIPERPAV Outputs	Data Group Number	Average			
	Crack Spacing Standard Deviation (ft.)	5	1.86	1.13	1.36	
	Crack Width (in.)	6	0.038	0.057	0.046	
			None	Single Coat	Double Coat	Plastic Sheeting
	Crack Spacing Average (ft.)	7	4.06	4.19	4.19	4.22
Curing Method	Crack Spacing Standard Deviation (ft.)	8	1.37	1.46	1.47	1.49
	Crack Width (in.)	9	0.048	0.047	0.047	0.047
			AC (Rough)	AC (Smooth)		
	Crack Spacing Average (ft.)	10	3.80	4.53		
Base Material	Crack Spacing Standard Deviation (ft.)	11	1.19	1.71		
	Crack Width (in.)	12	0.043	0.051		

HIPERPAV Input Variables	HIPERPAV Outputs	Data Group Number	Average		
			100 psi	150 psi	200 psi
Subgrade Support	Crack Spacing Average (ft.)	13	4.16	4.16	4.17
	Crack Spacing Standard Deviation (ft.)	14	1.45	1.45	1.45
	Crack Width (in.)	15	0.047	0.047	0.047
			Siliceous Gravel	Granite	Limestone
Aggregate Type	Crack Spacing Average (ft.)	16	4.06	4.15	4.29
	Crack Spacing Standard Deviation (ft.)	17	1.38	1.43	1.53
	Crack Width (in.)	18	0.048	0.047	0.046

Table B.5 OK-3 Sub-Variable Averages at 72 Hours

HIPERPAV Input Variables	HIPERPAV Outputs	Data Group Number	Average			
			7:00 A.M.	10:00A.M.	3:00 P.M.	
Construction Time	Crack Spacing Average (ft.)	1	6.25	6.51	8.54	
	Crack Spacing Standard Deviation (ft.)	2	1.50	1.58	1.92	
	Crack Width (in.)	3	0.025	0.026	0.027	
			1/12/1989	7/26/1988	10/22/1988	
Construction Date	Crack Spacing Average (ft.)	4	9.20	5.15	6.95	
	Crack Spacing Standard Deviation (ft.)	5	2.11	1.28	1.62	
	Crack Width (in.)	6	0.021	0.028	0.029	
			None	Single Coat	Double Coat	Plastic Sheeting
Curing Method	Crack Spacing Average (ft.)	7	6.32	7.01	6.98	8.10

HIPERPAV Input Variables	HIPERPAV Outputs	Data Group Number	Average			
	Crack Spacing Standard Deviation (ft.)	8	1.51	1.64	1.66	1.86
	Crack Width (in.)	9	0.026	0.025	0.025	0.028
			AC (Rough)	AC (Smooth)		
Base Material	Crack Spacing Average (ft.)	10	6.34	7.87		
	Crack Spacing Standard Deviation (ft.)	11	1.41	1.92		
	Crack Width (in.)	12	0.023	0.028		
			100 psi	200 psi	300 psi	
Subgrade Support	Crack Spacing Average (ft.)	13	7.09	7.10	7.11	
	Crack Spacing Standard Deviation (ft.)	14	1.67	1.67	1.67	
	Crack Width (in.)	15	0.026	0.026	0.026	

HIPERPAV Input Variables	HIPERPAV Outputs	Data Group Number	Average			
			Siliceous Gravel	Granite	Limestone	
Aggregate Type	Crack Spacing Average (ft.)	16	6.38	6.81	8.12	
	Crack Spacing Standard Deviation (ft.)	17	1.50	1.64	1.86	
	Crack Width (in.)	18	0.026	0.026	0.026	

Table B.6 OK-3 Sub-Variable Averages at 1 Year

HIPERPAV Input Variables	HIPERPAV Outputs	Data Group Number	Average			
			7:00 A.M.	10:00A.M.	3:00 P.M.	
Construction Time	Crack Spacing Average (ft.)	1	4.56	4.59	4.70	
	Crack Spacing Standard Deviation (ft.)	2	1.53	1.57	1.70	
	Crack Width (in.)	3	0.052	0.052	0.051	

HIPERPAV Input Variables	HIPERPAV Outputs	Data Group Number	Average			
			1/12/1989	7/26/1988	10/22/1988	
Construction Date	Crack Spacing Average (ft.)	4	5.39	4.16	4.30	
	Crack Spacing Standard Deviation (ft.)	5	2.03	1.27	1.51	
	Crack Width (in.)	6	0.041	0.064	0.050	
			None	Single Coat	Double Coat	Plastic Sheeting
Curing Method	Crack Spacing Average (ft.)	7	4.54	4.64	4.66	4.62
	Crack Spacing Standard Deviation (ft.)	8	1.52	1.60	1.62	1.65
	Crack Width (in.)	9	0.052	0.051	0.051	0.052
			AC (Rough)	AC (Smooth)		
Base Material	Crack Spacing Average (ft.)	10	4.17	5.06		

HIPERPAV Input Variables	HIPERPAV Outputs	Data Group Number	Average		
	Crack Spacing Standard Deviation (ft.)	11	1.31	1.89	
	Crack Width (in.)	12	0.047	0.056	
			100 psi	200 psi	300 psi
	Crack Spacing Average (ft.)	13	4.62	4.61	4.62
Subgrade Support	Crack Spacing Standard Deviation (ft.)	14	1.60	1.60	1.60
	Crack Width (in.)	15	0.052	0.052	0.052
			Siliceous Gravel	Granite	Limestone
	Crack Spacing Average (ft.)	16	4.52	4.59	4.73
Aggregate Type	Crack Spacing Standard Deviation (ft.)	17	1.53	1.57	1.71
	Crack Width (in.)	18	0.053	0.052	0.050

Table B.7 OK-4 Sub-Variable Averages at 72 Hours

HIPERPAV Input Variables	HIPERPAV Outputs	Data Group Number	Average			
			7:00 A.M.	10:00A.M.	3:00 P.M.	
Construction Time	Crack Spacing Average (ft.)	1	5.95	6.23	7.74	
	Crack Spacing Standard Deviation (ft.)	2	1.45	1.51	1.80	
	Crack Width (in.)	3	0.023	0.024	0.025	
			1/12/1985	7/26/1984	10/22/1984	
Construction Date	Crack Spacing Average (ft.)	4	9.82	4.20	5.90	
	Crack Spacing Standard Deviation (ft.)	5	2.27	1.06	1.43	
	Crack Width (in.)	6	0.023	0.024	0.025	
			None	Single Coat	Double Coat	Plastic Sheeting
Curing Method	Crack Spacing Average (ft.)	7	6.07	6.69	6.87	6.93

HIPERPAV Input Variables	HIPERPAV Outputs	Data Group Number	Average			
	Crack Spacing Standard Deviation (ft.)	8	1.46	1.60	1.66	1.63
	Crack Width (in.)	9	0.024	0.024	0.023	0.024
			AC (Rough)	AC (Smooth)		
Base Material	Crack Spacing Average (ft.)	10	5.81	7.48		
	Crack Spacing Standard Deviation (ft.)	11	1.29	1.88		
	Crack Width (in.)	12	0.022	0.026		
			100 psi	150 psi	200 psi	
Subgrade Support	Crack Spacing Average (ft.)	13	6.65	6.65	6.63	
	Crack Spacing Standard Deviation (ft.)	14	1.59	1.59	1.59	
	Crack Width (in.)	15	0.024	0.024	0.024	

HIPERPAV Input Variables	HIPERPAV Outputs	Data Group Number	Average			
			Siliceous Gravel	Granite	Limestone	
Aggregate Type	Crack Spacing Average (ft.)	16	6.01	6.31	7.60	
	Crack Spacing Standard Deviation (ft.)	17	1.46	1.52	1.78	
	Crack Width (in.)	18	0.024	0.024	0.024	

Table B.8 OK-4 Sub-Variable Averages at 1 Year

HIPERPAV Input Variables	HIPERPAV Outputs	Data Group Number	Average			
			7:00 A.M.	10:00 A.M.	3:00 P.M.	
Construction Time	Crack Spacing Average (ft.)	1	4.07	4.11	4.25	
	Crack Spacing Standard Deviation (ft.)	2	1.37	1.39	1.53	
	Crack Width (in.)	3	0.048	0.048	0.047	

HIPERPAV Input Variables	HIPERPAV Outputs	Data Group Number	Average			
			1/12/1985	7/26/1984	10/22/1984	
Construction Date	Crack Spacing Average (ft.)	4	4.79	3.69	3.94	
	Crack Spacing Standard Deviation (ft.)	5	1.85	1.08	1.35	
	Crack Width (in.)	6	0.038	0.058	0.047	
			None	Single Coat	Double Coat	Plastic Sheeting
Curing Method	Crack Spacing Average (ft.)	7	4.04	4.17	4.16	4.19
	Crack Spacing Standard Deviation (ft.)	8	1.35	1.44	1.46	1.47
	Crack Width (in.)	9	0.048	0.048	0.047	0.048
			AC (Rough)	AC (Smooth)		
Base Material	Crack Spacing Average (ft.)	10	3.79	4.49		
	Crack Spacing Standard Deviation (ft.)	11	1.17	1.69		
	Crack Width (in.)	12	0.044	0.052		
			100 psi	150 psi	200 psi	

HIPERPAV Input Variables	HIPERPAV Outputs	Data Group Number	Average		
Subgrade Support	Crack Spacing Average (ft.)	13	4.14	4.14	4.14
	Crack Spacing Standard Deviation (ft.)	14	1.43	1.43	1.43
	Crack Width (in.)	15	0.048	0.048	0.048
			Siliceous Gravel	Granite	Limestone
Aggregate Type	Crack Spacing Average (ft.)	16	4.03	4.12	4.27
	Crack Spacing Standard Deviation (ft.)	17	1.36	1.41	1.52
	Crack Width (in.)	18	0.049	0.048	0.047

Table B.9 OK-5 Sub-Variable Averages at 72 Hours

HIPERPAV Input Variables	HIPERPAV Outputs	Data Group Number	Average		
			7:00 A.M.	10:00A.M.	3:00 P.M.
Construction Time	Crack Spacing Average (ft.)	1	4.90	5.16	6.56

HIPERPAV Input Variables	HIPERPAV Outputs	Data Group Number	Average			
	Crack Spacing Standard Deviation (ft.)	2	1.11	1.18	1.47	
	Crack Width (in.)	3	0.017	0.018	0.015	
			1/12/1990	7/26/1989	10/22/1989	
	Crack Spacing Average (ft.)	4	7.69	3.94	4.97	
Construction Date	Crack Spacing Standard Deviation (ft.)	5	1.67	0.95	1.14	
	Crack Width (in.)	6	0.016	0.018	0.016	
			None	Single Coat	Double Coat	Plastic Sheeting
	Crack Spacing Average (ft.)	7	5.11	5.51	5.67	5.86
Curing Method	Crack Spacing Standard Deviation (ft.)	8	1.17	1.25	1.28	1.31
	Crack Width (in.)	9	0.018	0.017	0.017	0.018

HIPERPAV Input Variables	HIPERPAV Outputs	Data Group Number	Average		
			CSB (CRS =15 psi)	CSB (CRS =10 psi)	
Base Material	Crack Spacing Average (ft.)	10	5.43	5.64	
	Crack Spacing Standard Deviation (ft.)	11	1.23	1.28	
	Crack Width (in.)	12	0.017	0.018	
			200 psi	250 psi	300 psi
Subgrade Support	Crack Spacing Average (ft.)	13	5.54	5.52	5.55
	Crack Spacing Standard Deviation (ft.)	14	1.25	1.26	1.25
	Crack Width (in.)	15	0.018	0.017	0.017
			Siliceous Gravel	Granite	Limestone
Aggregate Type	Crack Spacing Average (ft.)	16	4.92	5.65	6.04

HIPERPAV Input Variables	HIPERPAV Outputs	Data Group Number	Average		
	Crack Spacing Standard Deviation (ft.)	17	1.09	1.27	1.40
	Crack Width (in.)	18	0.017	0.015	0.018

Table B.10 OK-5 Sub-Variable Averages at 1 Year

HIPERPAV Input Variables	HIPERPAV Outputs	Data Group Number	Average		
			7:00 A.M.	10:00A.M.	3:00 P.M.
Construction Time	Crack Spacing Average (ft.)	1	3.59	3.67	3.77
	Crack Spacing Standard Deviation (ft.)	2	1.08	1.12	1.23
	Crack Width (in.)	3	0.038	0.039	0.038
			1/12/1990	7/26/1989	10/22/1989
Construction Date	Crack Spacing Average (ft.)	4	4.05	3.40	3.59

HIPERPAV Input Variables	HIPERPAV Outputs	Data Group Number	Average			
	Crack Spacing Standard Deviation (ft.)	5	1.40	0.95	1.09	
	Crack Width (in.)	6	0.029	0.046	0.039	
			None	Single Coat	Double Coat	Plastic Sheeting
	Crack Spacing Average (ft.)	7	3.62	3.69	3.70	3.70
Curing Method	Crack Spacing Standard Deviation (ft.)	8	1.12	1.15	1.16	1.16
	Crack Width (in.)	9	0.039	0.038	0.038	0.038
			CSB (CRS =15 psi)	CSB (CRS =10 psi)		
	Crack Spacing Average (ft.)	10	3.64	3.72		
Base Material	Crack Spacing Standard Deviation (ft.)	11	1.12	1.17		
	Crack Width	12	0.038	0.039		

HIPERPAV Input Variables	HIPERPAV Outputs	Data Group Number	Average		
	(in.)				
			200 psi	250 psi	300 psi
Subgrade Support	Crack Spacing Average (ft.)	13	3.68	3.67	3.68
	Crack Spacing Standard Deviation (ft.)	14	1.14	1.15	1.14
	Crack Width (in.)	15	0.038	0.038	0.038
			Siliceous Gravel	Granite	Limestone
Aggregate Type	Crack Spacing Average (ft.)	16	3.50	3.68	3.85
	Crack Spacing Standard Deviation (ft.)	17	1.05	1.14	1.25
	Crack Width (in.)	18	0.038	0.038	0.039

APPENDIX C - STATISTICAL INVESTIGATION OF HIPERPAVE III

Table C.1 OK-1 Inferences from Matched Pairs at 72 Hours

Data Group Number	Statistical Inputs			*t* value Test Statistic	Critical Value	Is there a statistical difference?
	đ	s_d	n			
1	2.59	1.41	213*	26.8	±2.600	Yes
2	0.49	0.052	213*	13.7	±2.600	Yes
3	0.001	0.002	213*	7.0	±2.600	Yes
4	-4.80	2.01	216	-35.0	±2.600	Yes
5	-1.05	0.55	216	-28.3	±2.600	Yes
6	0.009	0.003	216	37.6	±2.600	Yes
7	1.81	1.45	159*	15.8	±2.611	Yes
8	0.35	0.51	159*	8.7	±2.611	Yes
9	0.001	0.003	159*	4.8	±2.611	Yes
10	2.55	1.56	321*	29.2	±2.591	Yes
11	0.72	0.53	321*	24.3	±2.591	Yes
12	0.008	0.003	321*	50.9	±2.591	Yes
13	0.04	0.52	215*	1.2	±2.600	No
14	0.00	0.06	215*	0.2	±2.600	No
15	0.000	0.001	215*	0.3	±2.600	No
16	2.24	1.40	213*	23.3	±2.600	Yes
17	0.33	0.50	213*	9.5	±2.600	Yes
18	0.000	0.002	213*	3.1	±2.600	Yes

* Some values in these data groups were extremely high or low and were ignored in the sub-variable averages and inferences from matched pairs.

Table C.2 OK-1 Inferences from Matched Pairs at 1 Year

Data Group Number	Statistical Inputs			*t* value Test Statistic	Critical Value	Is there a statistical difference?
	đ	s_d	n			
1	0.11	0.22	216	7.5	±2.600	Yes
2	0.10	0.011	216	13.7	±2.600	Yes
3	-0.002	0.002	216	-12.7	±2.600	Yes
4	-1.72	0.45	216	-56.8	±2.600	Yes
5	-0.79	0.18	216	-64.8	±2.600	Yes
6	0.021	0.004	216	69.0	±2.600	Yes
7	0.08	0.19	162	5.3	±2.611	Yes
8	0.09	0.12	162	9.1	±2.611	Yes
9	-0.002	0.003	162	-8.2	±2.611	Yes
10	1.27	0.40	324	56.7	±2.591	Yes
11	0.69	0.16	324	76.3	±2.591	Yes
12	0.013	0.003	324	84.0	±2.591	Yes
13	0.00	0.20	216	0.3	±2.600	No
14	0.00	0.04	216	-0.9	±2.600	No
15	0.000	0.002	216	-1.1	±2.600	No
16	0.28	0.28	216	15.1	±2.600	Yes
17	0.16	0.12	216	19.1	±2.600	Yes
18	-0.004	0.004	216	-16.6	±2.600	Yes

Table C.3 OK-2 Inferences from Matched Pairs at 72 Hours

Data Group Number	Statistical Inputs			*t* value		Is there a statistical difference?
	đ	s_d	n	Test Statistic	Critical Value	
1	1.94	0.81	216	35.1	±2.600	Yes
2	0.38	0.25	216	22.5	±2.600	Yes
3	0.001	0.002	216	13.3	±2.600	Yes
4	-4.97	1.56	216	-46.9	±2.600	Yes
5	-1.02	0.42	216	-35.7	±2.600	Yes
6	0.003	0.002	216	21.1	±2.600	Yes
7	1.10	0.63	162	22.3	±2.611	Yes
8	0.25	0.19	162	16.1	±2.611	Yes
9	0.001	0.002	162	5.4	±2.611	Yes
10	1.57	1.13	324	25.1	±2.591	Yes
11	0.58	0.33	324	31.8	±2.591	Yes
12	0.005	0.002	324	52.3	±2.591	Yes
13	0.01	0.27	216	0.3	±2.600	No
14	-0.01	0.05	216	-2.0	±2.600	No
15	0.000	0.001	216	0.0	±2.600	No
16	1.69	1.25	216	19.8	±2.600	Yes
17	0.40	0.32	216	18.7	±2.600	Yes
18	0.001	0.002	216	6.8	±2.600	Yes

Table C.4 OK-2 Inferences from Matched Pairs at 1 Year

Data Group Number	Statistical Inputs			*t* value		Is there a statistical difference?
	đ	s_d	n	Test Statistic	Critical Value	
1	0.17	0.26	216	9.4	±2.600	Yes
2	0.15	0.15	216	14.4	±2.600	Yes
3	-0.001	0.004	216	-2.3	±2.600	No
4	-1.04	0.33	216	-46.0	±2.600	Yes
5	-0.73	0.24	216	-45.0	±2.600	Yes
6	0.020	0.003	216	105.9	±2.600	Yes
7	0.16	0.22	162	8.9	±2.611	Yes
8	0.11	0.11	162	13.5	±2.611	Yes
9	0.000	0.003	162	-1.8	±2.611	No
10	0.74	0.25	324	53.9	±2.591	Yes
11	0.52	0.16	324	57.2	±2.591	Yes
12	0.008	0.002	324	68.6	±2.591	Yes
13	0.01	0.14	216	0.8	±2.600	No
14	0.00	0.04	216	-0.8	±2.600	No
15	0.000	0.001	216	0.7	±2.600	No
16	0.23	0.22	216	15.3	±2.600	Yes
17	0.15	0.09	216	24.0	±2.600	Yes
18	-0.003	0.003	216	-13.5	±2.600	Yes

Table C.5 OK-3 Inferences from Matched Pairs at 72 Hours

Data Group Number	Statistical Inputs			*t* value		Is there a statistical difference?
	đ	s_d	n	Test Statistic	Critical Value	
1	2.30	1.10	216	30.6	±2.600	Yes
2	0.43	0.40	216	15.6	±2.600	Yes
3	0.002	0.002	216	11.3	±2.600	Yes
4	-4.04	1.87	216	-31.7	±2.600	Yes
5	-0.83	0.45	216	-26.9	±2.600	Yes
6	0.007	0.004	216	29.0	±2.600	Yes
7	1.77	1.39	162	16.2	±2.611	Yes
8	0.35	0.40	162	11.3	±2.611	Yes
9	0.002	0.004	162	7.9	±2.611	Yes
10	1.53	1.44	324	19.2	±2.591	Yes
11	0.51	0.45	324	20.3	±2.591	Yes
12	0.005	0.003	324	32.5	±2.591	Yes
13	0.02	0.29	216	1.1	±2.600	No
14	0.00	0.05	216	0.0	±2.600	No
15	0.000	0.001	216	1.0	±2.600	No
16	1.74	1.25	216	20.4	±2.600	Yes
17	0.36	0.39	216	13.5	±2.600	Yes
18	0.001	0.002	216	5.9	±2.600	Yes

Table C.6 OK-3 Inferences from Matched Pairs at 1 Year

Data Group Number	Statistical Inputs			*t* value		Is there a statistical difference?
	đ	s_d	n	Test Statistic	Critical Value	
1	0.15	0.23	216	9.3	±2.600	Yes
2	0.17	0.18	216	14.3	±2.600	Yes
3	-0.001	0.003	216	-7.2	±2.600	Yes
4	-1.23	0.31	216	-58.3	±2.600	Yes
5	-0.76	0.16	216	-68.5	±2.600	Yes
6	0.023	0.003	216	100.6	±2.600	Yes
7	0.09	0.21	162	5.3	±2.611	Yes
8	0.13	0.14	162	12.0	±2.611	Yes
9	-0.00	0.003	162	-3.9	±2.611	Yes
10	0.89	0.29	324	55.9	±2.591	Yes
11	0.58	0.16	324	66.7	±2.591	Yes
12	0.009	0.002	324	71.9	±2.591	Yes
13	0.00	0.15	216	-0.4	±2.600	No
14	0.00	0.04	216	-0.1	±2.600	No
15	0.000	0.002	216	0.1	±2.600	No
16	0.21	0.24	216	12.8	±2.600	Yes
17	0.18	0.15	216	18.4	±2.600	Yes
18	-0.003	0.003	216	-16.2	±2.600	Yes

Table C.7 OK-4 Inferences from Matched Pairs at 72 Hours

Data Group Number	Statistical Inputs			*t* value		Is there a statistical difference?
	đ	s_d	n	Test Statistic	Critical Value	
1	1.80	0.79	216	33.6	±2.600	Yes
2	0.35	0.23	216	23.1	±2.600	Yes
3	0.001	0.002	216	11.9	±2.600	Yes
4	-5.61	1.64	216	-50.2	±2.600	Yes
5	-1.21	0.41	216	-43.3	±2.600	Yes
6	0.002	0.002	216	13.7	±2.600	Yes
7	0.86	0.67	162	16.5	±2.611	Yes
8	0.18	0.20	162	11.0	±2.611	Yes
9	0.000	0.001	162	2.1	±2.611	No
10	1.67	1.27	324	23.7	±2.591	Yes
11	0.59	0.34	324	30.8	±2.591	Yes
12	0.005	0.002	324	52.0	±2.591	Yes
13	-0.03	0.37	216	-1.1	±2.600	No
14	0.00	0.05	216	0.0	±2.600	No
15	0.000	0.001	216	-1.0	±2.600	No
16	1.59	1.16	216	20.1	±2.600	Yes
17	0.32	0.27	216	17.5	±2.600	Yes
18	0.001	0.001	216	6.4	±2.600	Yes

Table C.8 OK-4 Inferences from Matched Pairs at 1 Year

Data Group Number	Statistical Inputs			*t* value		Is there a statistical difference?
	đ	s_d	n	Test Statistic	Critical Value	
1	0.18	0.29	216	8.8	±2.600	Yes
2	0.15	0.15	216	14.5	±2.600	Yes
3	0.000	0.004	216	-0.6	±2.600	No
4	-1.10	0.38	216	-43.2	±2.600	Yes
5	-0.76	0.25	216	-45.6	±2.600	Yes
6	0.020	0.003	216	91.2	±2.600	Yes
7	0.15	0.26	162	7.1	±2.611	Yes
8	0.11	0.10	162	14.3	±2.611	Yes
9	-0.001	0.004	162	-1.8	±2.611	No
10	0.71	0.25	324	51.3	±2.591	Yes
11	0.52	0.17	324	54.0	±2.591	Yes
12	0.008	0.002	324	71.2	±2.591	Yes
13	0.00	0.13	216	-0.1	±2.600	No
14	0.00	0.03	216	-0.9	±2.600	No
15	0.000	0.001	216	0.3	±2.600	No
16	0.24	0.25	216	14.0	±2.600	Yes
17	0.15	0.09	216	26.0	±2.600	Yes
18	-0.002	0.003	216	-10.3	±2.600	Yes

Table C.9 OK-5 Inferences from Matched Pairs at 72 Hours

Data Group Number	Statistical Inputs			*t* value		Is there a statistical difference?
	đ	s_d	n	Test Statistic	Critical Value	
1	1.65	0.69	213*	34.8	±2.600	Yes
2	0.35	0.30	213*	17.0	±2.600	Yes
3	0.001	0.001	213*	8.4	±2.600	Yes
4	-3.75	1.04	216	-52.9	±2.600	Yes
5	-0.72	0.37	216	-28.6	±2.600	Yes
6	0.002	0.002	216	22.0	±2.600	Yes
7	0.74	0.54	159*	17.4	±2.611	Yes
8	0.14	0.29	159*	6.1	±2.611	Yes
9	0.000	0.001	159*	2.3	±2.611	No
10	0.21	1.19	321*	3.2	±2.591	Yes
11	0.04	0.36	321*	2.1	±2.591	No
12	0.000	0.001	321*	6.1	±2.591	Yes
13	0.01	0.30	215*	0.3	±2.600	No
14	0.00	0.06	215*	-0.5	±2.600	No
15	0.000	0.001	215*	-0.6	±2.600	No
16	1.12	1.24	216	13.3	±2.600	Yes
17	0.31	0.39	216	11.8	±2.600	Yes
18	0.001	0.001	216	13.6	±2.600	Yes

* Some values in these data groups were extremely high or low and were ignored in the sub-variable averages and inferences from matched pairs.

Table C.10 OK-5 Inferences from Matched Pairs at 1 Year

Data Group Number	Statistical Inputs			*t* value		Is there a statistical difference?
	đ	s_d	n	Test Statistic	Critical Value	
1	0.18	0.27	216	9.7	±2.600	Yes
2	0.15	0.17	216	12.4	±2.600	Yes
3	0.000	0.003	216	-0.9	±2.600	No
4	-0.66	0.25	216	-38.4	±2.600	Yes
5	-0.45	0.18	216	-36.0	±2.600	Yes
6	0.017	0.003	216	98.2	±2.600	Yes
7	0.08	0.18	162	6.0	±2.611	Yes
8	0.05	0.14	162	4.1	±2.611	Yes
9	0.000	0.002	162	-2.4	±2.611	No
10	0.08	0.20	324	7.5	±2.591	Yes
11	0.04	0.12	324	6.3	±2.591	Yes
12	0.001	0.004	324	3.5	±2.591	Yes
13	-0.01	0.13	216	-0.7	±2.600	No
14	0.00	0.03	216	-0.8	±2.600	No
15	0.000	0.001	216	-0.5	±2.600	No
16	0.35	0.17	216	30.4	±2.600	Yes
17	0.20	0.13	216	22.2	±2.600	Yes
18	0.001	0.002	216	10.6	±2.600	Yes